UNIVERSITÉ LAVAL

Characterization and Surface Modification of Rubber from Recycled Tires

Thèse

Huan Liang

Doctorat en Chimie

Philosophiae doctor (Ph. D.)

Québec, Canada

Characterization and Surface Modification of Rubber from Recycled Tires

Thèse

Huan Liang

Sous la direction de :

Josée Brisson, directrice de recherche

Résumé

Les pneus en fin de cycle de vie soulèvent de graves problèmes environnementaux. Ils doivent être éliminés ou recyclés. En raison de leur structure réticulée, les pneus ne fondent pas ni ne se dissolvent. Ils sont généralement broyés en poudre (caoutchouc de pneu broyé, abrévié GTR). Ensuite, ces poudres sont mélangées avec une matrice (asphalte ou polymère thermoplastique) pour réutilisation.

L'industrie du recyclage se heurte à deux problèmes principaux. En premier lieu, le contrôle de technique qualité est difficile à cause du manque de solubilité de la poudre et de moyens limités pour ces petites industries. Il est nécessaire de trouver des méthodes rapides et à faible coût pour améliorer la caractérisation des GTR. Dans le présent travail, nous avons mis l'accent sur l'utilisation de ces deux techniques et sur la spectrométrie de fluorescence-X (XRF), comme il y a des rapports dans la littérature démontrant que ceux-ci peuvent être utilisés, respectivement, pour déterminer la densité de réticulation, la composition en monomères et la composition élémentaire.

Un deuxième problème est la faible adhérence entre la plupart des polymères et les GTR. Ceci résulte en un manque de résistance mécanique et une tendance à l'effritement des pièces fabriquées. Certaines études se concentrent sur l'ajout de monomère et d'initiateur au GTR, afin de faire une polymérisation in-situ de chaînes greffées sur la surface. Cependant, le poids moléculaire des greffons est inconnu et il est impossible de vérifier si celui-ci est supérieur au poids moléculaire d'enchevêtrement des chaînes. Des réactions photochimiques ont été utilisées pour greffer des chaînes polymériques terminées par un groupement thiol de poids moléculaire connu en utilisant les liaisons doubles présentes à la surface de GTR. La spectrométrie de photoélectrons induits par rayons X (XPS) et la spectroscopie infrarouge à transformée de Fourier (FTIR) ont été utilisées pour détecter les changements de surface et vérifier si le greffage a bien eu lieu. Finalement, la mesure des propriétés mécaniques a été utilisée pour évaluer l'effet du greffage avec les échantillons de GTR greffé mélangés à du polystyrène commercial.

Abstract

End of life tires raise severe environmental problems and must be disposed of or recycled. Due to their cross-linked structure, they do not melt or dissolve, and are usually ground into a powder (ground tire rubber or GTR) and mixed with a matrix (asphalt or a thermoplastic polymer) for reuse.

The recycling industry encounters two main problems. First, quality control is difficult due to the lack of solubility of the powder and to the limited technical means of these small industries. Rapid and low-cost methods are needed to improve characterization of GTR. This work focused on the use of these two techniques and of X-ray fluorescence spectrometry (XRF), as there are reports in the literature showing than these may be used, respectively, to determine cross-link density, monomer and elemental composition.

The second problem is the poor adhesion between most polymers and GTR, resulting in parts that lack mechanical strength and tend to crumble. Some studies focus on adding monomer and initiator to GTR and doing in-situ polymerization of graft chains onto the surface. However, molecular weight of grafts is unknown and it is not possible to verify if the molecular weight is above the chain entanglement molecular weight. Photochemical reactions were used to graft thiol-terminated polymer chains of known molecular weight by using free carbon double bonds that exist on the GTR surface. X-ray photoelectron spectroscopy (XPS) and Fourier transform infrared spectroscopy (FTIR) were used to detect the surface changes and graft degree. Mechanical properties measurement was used to monitor the treated samples blends with polystyrene matrix.

Table of Contents

List of Tables

List of Figures

Abbreviations

AAm	Acrylamide
AAc	Acrylic acid
AIBN	Azobisisobutyronitrile
AN	Acrylonitrile
AMPS	2-acrylamido-2-methylpropanesulfonic acid
BMI	m-phenyl bismaleimide
BPO	Dibenzoyl peroxide
DBTC	S,S-Dibenzyl trithiocarbonate
DP275B	1,1-bis(tert-butylperoxyl) cyclohexane
EPDM	Ethylene-Propylene diene monomer
GMA	Glycidyl methacrylate
GTR	Ground tire rubber
HDPE	High-density polyethylene
HIPS	High impact Polystyrene
LDPE	Low-density polyethylene
MAA	Methacrylic acid
NR	Natural rubber
PE	Polyethylene
PET	Polyethylene terephthalate
PGMA	Poly(glycidyl methacrylate)
phr	Parts per hundred of rubber
PP	Polypropylene
SBR	Styrene-butadiene rubber
TEMPO	2,2,6,6-Tetramethylpiperidin-1-yl)oxyl
TPE	Thermoplastic elastomer
TPV	Thermoplastic vulcanizate
WGR	Waste Ground Rubber

Symbols

M_c	Average molecular weight between two cross-linking points
ρ	Cross-linking density (mol/cm^3)
ρ_p	Density of the non-cross-linked polymer
ρ_s	Density of solvent
V_s	Fraction volume of solvent
Tg	Glass transition temperature
χ	Interactions between polymer and solvent
ΔH_m	Melting enthalpy
V_m	Molar volume of the solvent
E’	Storage modulus
S	Swelling index

To those who have the same goal
in their professional career:

«The roots of education are bitter,
but the fruit is sweet»

Aristotle

Acknowledgments

I would like to say thank you very much to all persons who were involved in my projects and have encouraged me to progress during my Ph.D. studies.

First and foremost, I would like to gratefully and sincerely thank Prof. Josée Brisson for her inspiring, patient and kind guidance in my project. My knowledge about polymers, which grew from zero to understanding, and then engaging in this research in this field, is in my opinion inseparable from the countless explanations and demonstrations under her strong background. Much more, during discussions with her, I learned how to become an independent thinker. I am sure I could not have completed this Ph.D. research without her help. For everything you have done for me, Prof. Josée Brisson, thank you very much.

As well, I would like to express my warm thanks to Prof. Denis Rodrigue for his friendly advices and continuous support to my project.

I also would like to thank Prof. Jean-François Morin for allowing me to perform thiol-ene click reactions in his laboratory.

The assistance of Mrs Plesu (TGA), Mr. Audet (solid-state NMR), Mr. Groleau (AAS and ICP-OES), Mr. Paquet-Mercier (FTIR) and Mr. Bi (XRD) from the Department of chemistry, Université Laval, Mr. Macsiniuc (advice on sample preparation), Mr. Giroux (mechanical properties measurement) and Mr. Adnot (XPS) from the Department of chemical engineering, Université Laval, is also gratefully acknowledged.

All members of the group of Prof. Brisson, Abdel, Jean-Michel, François, Adrien and Simon, are also given my warmest thanks. Especially Adrien, thanks for the valuable discussions with regards to our projects. I would also like to acknowledge the summer students, Jean-Michel and Jacob, for the help in sample preparation and instrumental measurement in my projects.

To my friends at Laval University, warm thanks for all of you for your company during these years of Ph.D. studies. Because of you guys, these four years of my life were not boring, but richly colorful. For my friends in China, I appreciate your encouragement and support.

I wish to acknowledge the financial support of the Natural Sciences and Engineering Research Council of Canada (NSERC), Centre Québécois sur les Matériaux Fonctionnels (CQMF) and Centre de Recherche sur les Matériaux Avancés (CERMA). As well, I benefitted from a scholarship from the China Scholarship Council (CSC), and thankfully acknowledge this support.

Finally, and most importantly, I would like to say thank you very much to my family, especially my parents, for their faith in me and allowing me to be as ambitious as I wanted. It was under their watchful eye that I attained so much drive and an ability to tackle challenges head on. Also, thanks to my two sisters and my nephew and niece, they gave me much strength to pursue my studies. I am also thankful to my relatives, my uncles and aunts, for supporting me over these years.

Foreword

This Ph.D. dissertation is based on three journal papers and consists of five chapters:

Chapter 1

In the first chapter, a general introduction on end of life tires, thermoplastic elastomers and recycled thermoplastics is presented. Characterization and modification of ground tire rubber are discussed by reviewing the literature. Following this, the objectives of this thesis are established.

In the following three chapters, the collected data and characterized properties of the samples based on the experimental work are reported in the form of published, accepted or in-preparation journal articles for which the initial version of the manuscript was written by myself (first author).

Chapter 2

Huan Liang, Jean-Michel Hardy, Denis Rodrigue and Josée Brisson, "**EPDM Recycled Rubber Powder Characterization: Thermal and Thermogravimetric Analysis**", Rubber Chemistry and Technology, 87(3), 538-556(2014). DOI: 10.5254/rct.14.87988

In this chapter, analysis of standard samples of ethylene-propylene diene monomer (EPDM) with varying cross-link densities and carbon black contents, as well as recycled EPDM waste ground rubber, have been performed to improve characterization. The various characterization methods were carried out for quality control in the field of waste ground tire rubber recycling. Detailed chemical compositional analysis was investigated by the inductively coupled plasma optical emission spectrometry, atomic absorption spectrometry and elemental (CHNS) analysis. The thermogravimetric analysis (TGA) can be used not only for rubber composition determination, but also as a quick way to determine the cross-link density. It overcomes the difficulties encountered with the swelling method for powder and is much more rapid to perform. The melting enthalpy in the differential scanning calorimetry (DSC) can be related to the ratio of ethylene/propylene in the EPDM rubber.

In this part, Jean-Michel Hardy has made a noteworthy contributed to sample preparation by performing condition optimization, and has also performed partial preliminary characterization of some of the standards samples.

Chapter 3

Huan Liang, Denis Rodrigue and Josée Brisson, "**Characterization of Recycled SBR Ground Tire Rubber: Combining X-Ray fluorescence, Differential Scanning Calorimetry and Dynamical Thermal Analysis for Quality Control**", Journal of Applied Polymer Science, published online 132 (2015). DOI: 10.1002/app.42692

This chapter investigates another type of GTR sample, based on styrene butadiene rubber (SBR). Likewise, standard samples and ground tire rubber (GTR) recycled samples were used to provide additional information for quality control. Rubber elemental analysis was done using inductively coupled plasma optical emission spectrometry, atomic absorption spectrometry and elemental (CHNS) analysis. Solid-state proton NMR and thermogravimetric analysis (TGA) were also performed for the measurement of styrene/butadiene ratio, and were in good agreement for standard samples, but showed important differences in the case of ground tire rubber samples. It was shown that major metal content can be quickly determined by the X-ray fluorescence (XRF) spectrometry. Differential scanning calorimetry (DSC) was used to detect changes in rubber composition. Both DSC and XRF can be quick and easily available methods for quality control of SBR-based GTR samples.

Chapter 4

Huan Liang, Jacob Dion Gagné, Adrien Faye, Denis Rodrigue and Josée Brisson "**On the Use of the Thiol-ene Click Reaction to Modify the Surface of Ground Tire Rubber: Grafting of Polystyrene and Characterization of a Modified GTR/Polystyrene Blend**" in preparation.

In this chapter, the thiol-ene click reaction was used to modify the GTR surface through grafting of known molecular weight polystyrene. Various techniques were used to characterize the initial and grafted GTR. FTIR and XPS were employed to detect the surface changes (variations in aromatic ring and double bond content), and verify the success of grafting. TGA results in nitrogen indicated a slight enhancement in thermal stability of

grafted GTR, and the grafted efficiency, whereas results in air were used to evaluate semi-quantitatively the quantity of grafted PS. A value of 12 ±3 % was obtained. A standard deviation larger by a factor of three as compared to that of GTR composition indicates a heterogeneity of treated GTR. After the grafting reaction, composites of initial GTR and grafted GTR with recycled polystyrene matrix were prepared in a ratio of 50/50. Dynamic mechanical thermal analysis (DMTA) results show an important increase in storage modulus and Young's moduli as compared to initial GTR/PS50.

Chapter 5

The final chapter presents the general conclusion based on the work performed, then following suggestions for prospective works are presented.

In addition to the above mentioned articles, more results obtained from this thesis were also presented in the following conference presentations:

H. Liang, J-M. Hardy and J. Brisson, "**Characterization of Rubber from Recycled Tires**", 35th Canadian High Polymer Forum (CHPF), Gananoque, Canada, P5 (14-17 August 2012).

H. Liang, D. Rodrigue and J. Brisson, "**Efficient Characterization Methods of Waste Ground Rubber Powder (WGR) For Industrial Quality Control**", 36th Canadian High Polymer Forum (CHPF), Gananoque, Canada, O12 (5-7 August 2014).

Chapter 1: Introduction

1.1 End of life tires

In the world, more than 550 million road vehicles are in everyday use. Annually, due to safety reasons, 1.3 billion end of life tires are dismantled from these vehicles. At the end of 2003, in the US alone, it is estimated that approximately 290 million scrap tires were generated[1].

Table 1.1 The composition of a tire[2,3] (manufactural recipes)

Ingredients	Passenger car tire, (w/w %)	Truck tire, (w/w %)	OTR tire, (w/w %)
Rubbers/Elastomers (natural)	16	30	31
Rubbers/Elastomers (synthetic)	31	15	16
Carbon black	21.5	22	22
Metal	16.5	25	12
Textile	5.5	-	10
Zinc oxide	1	2	2
Sulfur	1	1	1
Additives	7.5	5	6
Carbon-based materials, total	74	67	76

Tires are complicate objects consisting of many different parts, each with a specific formulation, and include natural or synthetic polymers, carbon black, steel, dispersed oils,

sulfur for vulcanization or cross-linking, organic and inorganic additives, and even glass. Table 1.1 and Figure 1.1 illustrate representative formulation recipes for production of different types (passenger cars, trucks and off the road (OTR) applications, such as construction vehicles) of tire and different tire parts, respectively.

Different types of vehicle tires are made up of numerous different rubber compounds, as Table 1.1 shows, in different proportions, natural rubber being less used for in passenger car tires than in truck and OTR tires.

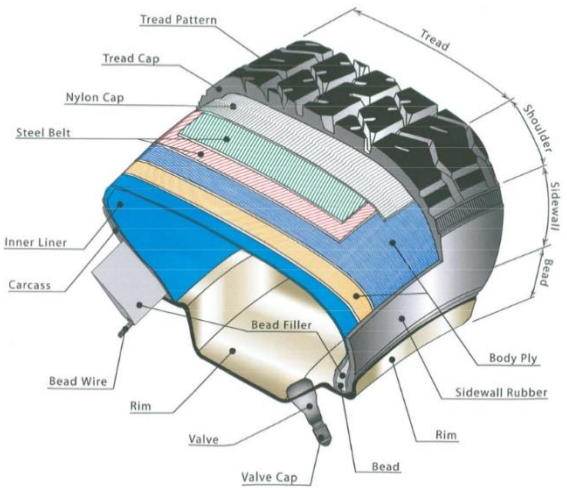

Fig. 1.1 The structure of a tire[3]

Tire rubber recycling is an important concern. At first, natural rubber was used for tire production. Today, many more polymers are synthesized for tire manufacture, such as ethylene-propylene-diene monomer rubber (EPDM), styrene-butadiene rubber (SBR) or acrylonitrile butadiene rubber (NBR). Ethylene-propylene-diene monomer rubber (EPDM) shows the best resistance against oxidation and UV-light, which means it shows good aging resistance. For this reason, it is used for tire sidewalls, as this part is load-bearing and requires good toughness[4]. Styrene-butadiene rubber (SBR), on the other hand, has good abrasion resistance and is used for tire tread fabrication in tire soles. [5]

Normally, the rubber used in tires needs to retain its shape or stable structure, which requires vulcanization or cross-linking, which in turn influences the physical properties, such as

A)

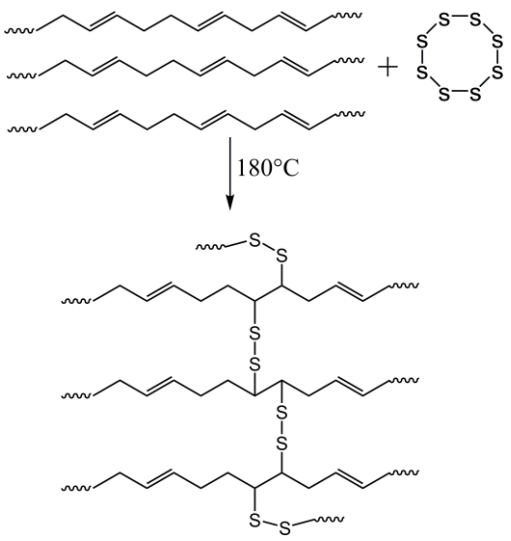

B)

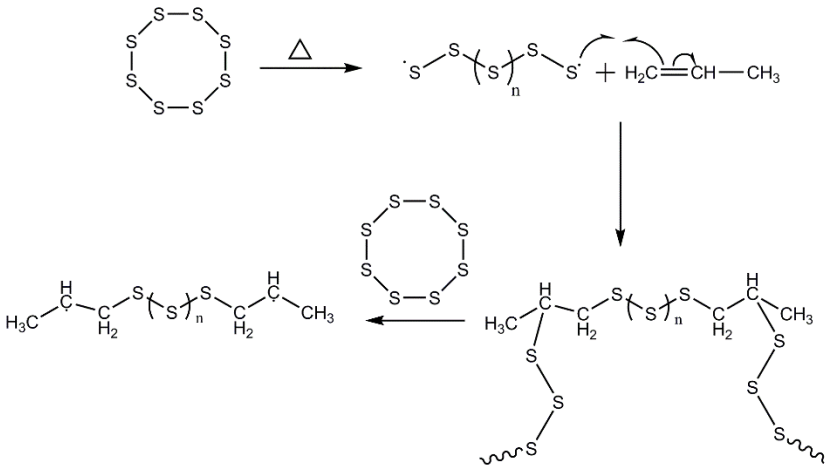

Fig. 1.2 Schematic illustration of cross-links which may be produced by vulcanization A)by destruction of a double bond [6]; B) possible mechanism of vulcanization by destruction of a double bond

A)

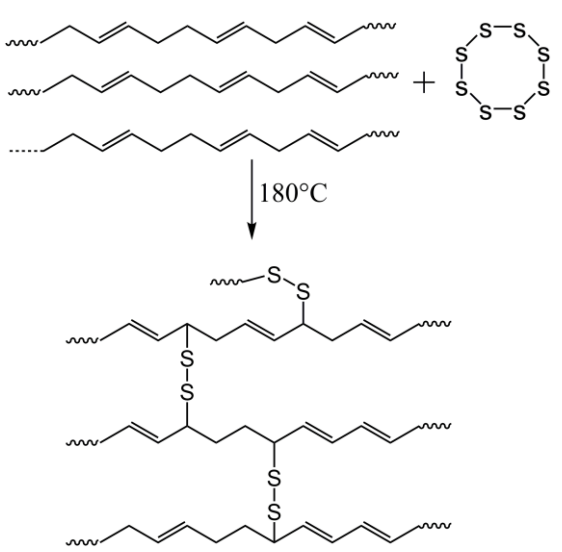

B)

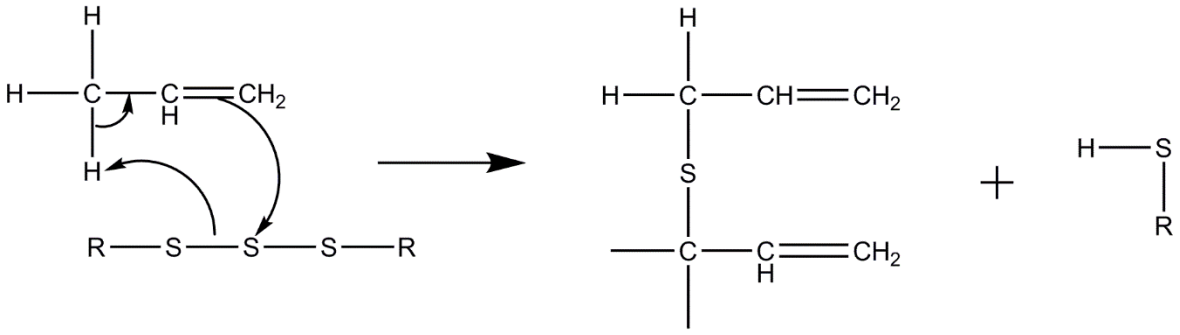

Fig. 1.3 Schematic illustration of cross-links which may be produced by vulcanization A) by replacement of the C-H bond by a C-S bond [7]; B) possible mechanism of vulcanization by replacement of the C-H bond by a C-S bond

solubility, of polymers. Meanwhile, cross-link density (define as ρ), which represents the number of cross-links in the vulcanized volume unit, is an important parameter in quality control of tires both during manufacture and for end of life tires recycling.

Two different types of cross-links exist, physical cross-links, also called chain entanglements, or chemical cross-links. The terms vulcanization and curing, with regard to tires, are associated with the formation of sulfur-associated chemical cross-links. The exact mechanism and resulting chemical effect of cross-linking with sulfur is still the object of

debates. Figure 1.2 A, b and 1.3 A, B are two proposed types of sulfur crosslinks, one in which the double bond is destroyed in favor of two C-S bonds, and the second where the C-H bond in alpha of the double bond is cleaved and replaced by a C-S bond. In addition, rubber sulfur bridges vary: mono-, di- and polysulfide bonds exist, which means that the sulfur content cannot reflect simply the cross-link density of tire rubber.

1.2 The problem of end of life tire disposal

End of life tires, due to their cross-linked structure, do not melt or dissolve, as well, they are not biodegradable. How to dispose of them is a hot topic and a great challenge worldwide.

Historically, end of life tires were to be placed in landfills, or stockpiled and dumped, in which case they provided breeding grounds for mosquitoes and rodents. These practice are now mostly illegal, but still occur in some undeveloped countries[8]. This represents a missed opportunity to gain benefits from recovery and reuse of tires, is not cost-effective or environment friendly way.

In addition, tires are composed of approximately 75 % hydrocarbon, which are highly caloric materials. For example, passenger car tires have a calorific value of approximately 30.2 MJ/kg, which is more than that of hard coal and comparable to the calorific value of coke. Having this in mind, end of life tires are used as an alternative fuel in cement works or power plants in many countries. However, since the end of life tires can easily burn, we still face a real possibility of tire dump fires, which lead to harmful gas emission, such as carbon dioxide (CO_2) and sulfur dioxide (SO_2), that cause important health problem, acid rains and a greenhouse effect, and which are therefore extremely polluting.[9]

1.3 Tire recycling

Due to their complicated cross-linked structure, rubbers are chemically inert. This is a double-edged sword: it is highly desirable for practical applications, but makes it difficult to recycle them. But we need to dispose of them appropriately, so that they will not endanger the environment.

End of life tire are, in fact, an important secondary material, and can be used, after proper treatment, as raw material in the rubber industry, for civil constructions, for sport facilities, or as a filling materials in residential or business buildings, etc.

End of life tires are disposed or recycled in the U.S.A as indicated in Figure 1.4, as reported in a 2014 US survey[1]. We can clearly see that energy recovery accounts for approximately 45% of all recycling methods, which contributes to air pollution even under controlled combustion conditions.

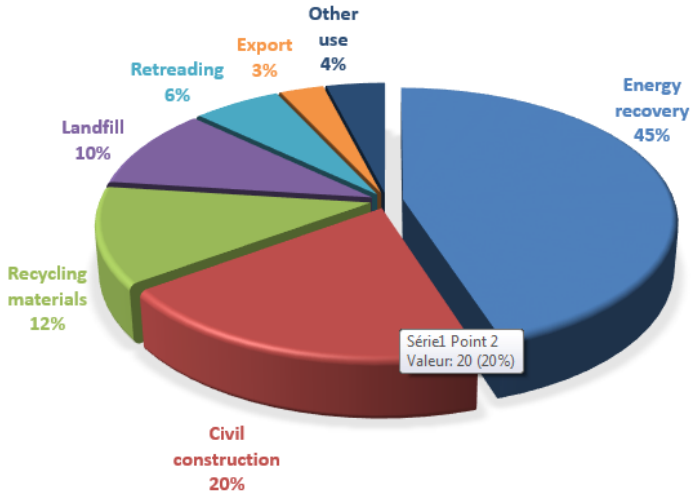

Fig. 1.4 The proportion of various used tire disposal methods in the USA

1.3.1 Crumb rubber modified asphalt

Civil construction applications is a growing market for end of life tires. Recycled rubber has been included in a wide range of highway uses in recent year[10]. End of life tires are mechanically shred to small sizes, resulting in crumb rubber, and then added to asphalt, which allows significant cost reduction and asphalt property improvements. An ASTM standard method (ASTM D6270-98) has even been published to help the industry extend crumb rubber applications[11].

In road pavement, high quality asphalt can be obtained from virgin asphalt blended with crumb rubber at elevated temperature. The crumb rubber derived from end of life tires is an effective additive, and can modify the properties of asphalt binders[12]. The interaction between the asphalt and crumb rubber must be carefully considered. This will seriously affect the quality of road pavement, resulting in safety and economic problems. Therefore, much research is done for improvement of the interaction between crumb rubber and asphalt.

Research of Mashaan and co-worker shows that physical, rheological properties and pavement deformation or rutting resistance of rubberized bitumen depend on the content of crumb rubber, but is not affected by blending time. Relatively higher rubber content will have potential to resist rutting deformation, as well as enhancing traffic loading which occurs in road pavement[13,14].

Okur and co-workers studied asphalt concrete modified with different crumb rubber of different sizes and chemical composition, and found that particle size affects the shear modulus and damping ratio. This means that rubber-modified asphalt concrete can mitigate vibrations generated from traffic loading and results in a reduction of damage from cyclic straining. This will effectively prolong the sustainability of road pavement[15].

End of life tires can therefore be widely used in civil construction as an asphalt modifier. In this way, we can not only reduce the cost of materials, but also consume a large quantity of end of life tires.

1.3.2 Pyrolysis

Pyrolysis is also an important recycling technique in engineering. It can produce alternative energy from end of life tires. Pyrolysis involves thermal degradation at high temperature (200 – 900 °C) in the absence of air, under vacuum or atmospheric pressure.

Juma and co-workers pyrolysed scrap tires from 250 °C to around 550 °C, and obtained around 40 w/w % solid residue, 50 w/w % liquid fraction and 10 w/w % gas fraction as the temperature increasing. Detailed analysis of the three products was reported: the solide residue consisted in carbon black and inorganic matter, derived liquids consisted in a variety of aromatic molecules, and gas included H_2, H_2S, CO, CO_2, CH_4, and other light

hydrocarbons. Finally, they also found that after combustion of scrap tires, lots of pollutants, such as SO_2, NO_x, CO or PAHs, were emitted and pollutes the environment when compared to pyrolysis [16]

Scatolim Rombaldo and co-workers investigated different operating condition for pyrolysis of scrap tires to produce fuel oil and activated carbon. They found that the properties of activated carbons obtained from pyrolysis of scrap tires were similar to that of commercial products, and that the surface area exceeding 200 m^2/g. They also discovered that surface area changes with processing temperature, and at higher temperatures larger surface area are obtained.[17]

Osayi and co-workers used pyrolysis to produce biocrude, of which around 55 w/w % was obtained from end of life tires using a pyrolysis temperature range of 250 °C to 550°C, which is the same range as reported by Juma et al. Through analysis, they found that the biocrude was composed not only of aromatics, but also of aliphatic hydrocarbons or hydroxyl compounds. [18]

Pyrolysis is a good method to reuse end of life tires, it can produce useful products for the industry. It is also an environmentally friendly way to reuse end of life tires. However, there are still a lot of studies needed to improve the liquid fraction or biocrude yield, and to reduce the cost.

1.3.3 Crumb rubber modification

Ground tire rubber can be modified by physical or chemical methods, and some functional groups can be grafted on the surface of ground tire rubber, which results in changes in the properties of ground tire rubber. These two methods are based on the presence of double bonds on the surface of ground tire rubber. As it is known, tires are made using natural and synthetic rubber, and in both cases, double bonds are present and involved in cross-linking reactions. However, not all double bonds are consumed, and remaining ones can be used for chemical reactions. Furthermore, during mechanical grinding, some double bonds are also generated[19]. Surface-modified crumb rubber can be used directly in some applications, but is also investigated to improve GTR blends with thermoplastics for various applications.

Whether physical or chemical methods are used for ground tire rubber modification, as a result, these will lead to the chemical changes on the ground tire rubber surface. Therefore, the term "physical methods" may be a little ambiguous. In order to modify the surface of ground tire rubber, ozone[20], plasma[21,22] and irradiation[23] treatments have been explored. It is known that, even in air, irradiation of organic systems results in oxidation manifested by the appearance of hydroperoxy, peroxy, carbonyl and hydroxyl groups[24]. The presence of these groups, to some extent, favors interaction of the treated ground tire rubber with polar polymers, such as poly(methyl methacrylate) (PMMA) or poly(vinyl alcohol) (PVA).

Chlorination is considered as an easy way to polarize the ground tire rubber surface, and chlorinated ground tire rubber can be used as a filler for polyvinylchloride (PVC), resulting in cost reduction and improving properties[25]. Ground tire rubber has also been oxidized using HNO_3, H_2O_2 and $HClO_4$ solutions, which resulted in improving interaction with HDPE[26] and natural rubber (NR)[27].

As it is well known, these physical methods are difficult to perform due to high temperature or voltages needed. As well, the reactions are hard to control, and use of oxidizing chemicals is hazardous.

With regards to chemical methods, small chemical groups are not the only species which can be grafted onto ground tire rubber, and polymer chains can also be covalently bound onto the surface. Chemical methods to modify ground tire rubber are convenient to control and graft the desired target groups, ones which have been selected for their compatibility with the selected application. In addition, modified ground tire rubber can be blended with recycled thermoplastics. In this way, we can recycle both end of life tires and used thermoplastics, such as polyethylene, polypropylene or polystyrene, for new use.

Aggour and his co-worker used 2-acrylamido-2-methylpropanesulfonic acid (AMPS) to modify ground tires through a grafting process involving free radical reactions[28]. After modification and characterization, particle size and crystallinity of the modified rubber increased. The obtained rubber is a candidate for future applications of soil and water treatment as an ion exchange resin.

Abdel-Bary and co-workers employed γ-irradiation to initiate grafting and polymerization of various vinyl monomers such as acrylamide (AAm), acrylic acid (AAc) or acrylonitrile (AN) onto rubber powder, and concluded that the acrylamide could be grafted in high graft yield, and that the resulting products are efficient as ion exchanger for both copper and lead ions[29]. Tolstov and his co-workers also used γ-irradiation initiation to graft maleic acid and acrylamide onto ground tire rubber. The corresponding treated ground tire rubber was then used in thermoplastic elastomer formulations. As a consequence, the maleic acid grafted groups reacted with amine ($-NH_2$) functional groups present at the surface of thermoplastic elastomers used. An important enhancing of interactions between the treated ground tire rubber and the thermoplastic elastomer resulted in tremendous increases in mechanical properties[30].

Bhowmick and co-workers used dicumyl peroxide initiation at 160 °C in the presence of maleic anhydride to produce maleated ground tire rubber. Blending modified rubber and a thermoplastic (acrylated high-density polyethylene) at a ratio 60/40, resulted in a significant improvement in physical properties, and the blends expressed good reprocessability, like thermoplastic elastomers[31].

Furthermore, the synthesis of the polymer chains covalently bound to the surface of ground tire rubber was also drawn much attention for surface modification. Initiators, such as dibenzoyl peroxide (BPO), azobisisobutyronitrile (AIBN), or 2,2,6,6-tetramethylpiperidin-1-yl)oxyl (TEMPO) will form free radicals at a certain temperature to initiate polymerization at the surface. Therefore, the resulting polymer chains will be attached to the surface of ground tire rubber. This should result in an improvement of adhesion between ground tire rubber itself or ground tire rubber and thermoplastics, due to the chain entanglement of these polymers. This improvement should normally depend on the grafting degree and on the molecular weight of these grafted polymer chains.

Coiai et al. prepared polystyrene grafted onto a GTR surface with a free radical reaction. They demonstrated that reactive double bonds are present on the surface of ground tire rubber and may act as “anchoring” sites for styrene grafting. The grafting efficiency can be as high as 45 % when using dibenzoyl peroxide (BPO) as an initiator, whereas lower values are

obtained using azobisisobutyronitrile (AIBN), due to the different H-abstraction capability of the two mentioned initiator[32,33]. A similar approach was followed by Zhang and his group, and the results indicate that an excellent grafting efficiency, approximately 89 %, was achieved. Through grafting, thermal stability was improved as compared to the ungrafted samples[34].

Normally, polymerization initiated by BPO and AIBN is highly reactive and not easy to control, and the use of TEMPO, a temperature mediated stable radical, has some definite advantages. Earlier in 1999, Shimada and co-workers used TEMPO to control polymerization after initiation by BPO, and successfully grafted polystyrene onto commercially available polypropylene. Through the controlling of TEMPO, the polystyrene had a narrow polydispersity, which confirmed that stable free radical polymerization can be used for graft polymerization. [35,36]

Daniel and co-workers grafted polystyrene onto the surface of waste natural rubber by the TEMPO-mediated radical polymerization process. They used microprobe Raman mapping to better monitor grafting distribution and concentration of PS on the NR surface which was related to the grafting time. Unfortunately, they did not use mechanical properties for comparing changes before and after treatment.[37]

Yu and co-workers employed TEMPO to graft polystyrene onto waste cis –1,4 polybutadiene. They investigated different ratio of TEMPO/initiator and showed that changes in this ratio strongly affected the mechanical properties of the final modified material.[38]

TEMPO mediated grafting polymerization as therefore be proven to be useful for surface modification of rubbers, but has not been used for ground tire rubber.

Compared to the γ-irradiation or peroxide initiation, ultra-violet (UV) grafting is an interesting surface modification approach which is safer and simple to the chemists. A photoinitiator is decomposed by UV light, hydrogen atoms are abstracted from the rubber (i.e. ground tire rubber), and a radical is generated on the surface. In this way, radical polymerization can be initiated fast, and the monomers are directly grown on the ground tire

rubber particle surface, so that time-consuming diffusion of the initiator is omitted. Even though photoinitiated grafting has already been applied to improve properties of ground tire rubber[39-41], many factors such as solvent selection, photoinitiator, UV-irradiation time and monomers remain to be optimized. Further, this reaction process can be easily controlled via changes in UV radiation intensity[42-44].

Poly(glycidyl methacrylate) (PGMA) has been grafted onto the surface of vulcanized styrene-butadiene rubber (SBR) via UV irradiation by Shanmugharaj and co-workers[39], using benzophenone as an initiator. They found that the graft ratio, to some extent, depends on the duration of UV irradiation. Carbon black has been shown to significantly reduce irradiation absorbance. The grafted SBR can further react with nylon-6 for recycling. Shanmugharaj and co-workers also studied GTR grafting in the presence of allylamine, with the same initiator and UV irradiation condition. Blends of the modified GTR with recycled polypropylene (PP) showed improved tensile strength and elongation at break, which is attributed to entanglement between chains present at the GTR surface and the PP chains[23,40].

Du and co-workers attempted to incorporate m-phenyl bismaleimide (BMI) onto WGR obtained by a cryogenic procedure by UV irradiation. Resulting blends with natural rubber showed good physical properties at a 85/15 (w/w %) ratio [41].

Fuhrmann and Karger-Kocsis functionalized glycidyl methacrylate (GMA) and methacrylic acid (MAA), two monomers, onto the ground tire rubber particles via photochemically induced grafting reaction. When the amount of carbon black is less than 15 % in the ground tire rubber, the grafting reaction proceeds well[45,46].

1.4 Thermoplastic recycling using crumb rubber

Day to day, thermoplastic consumption is very enormous, which also causes environmental problems. Compared to end of life tires, thermoplastics such as HDPE, LDPE, PP or polystyrene (PS) are easy to melt and remold due to the absence of a stable reticulated structure present in rubbers. Possibilities for commercial re-use are however often limited. As they cannot be reused for food applications due to the danger of contamination (which

explains in great part why PS recycling is so limited), and are often of various colors, resulting in an unsightly brown color of the final material. The possibility of blending some of these with GTR is attractive, as GTR will impart a more uniform, black color and should yield rubbery materials, thus opening new applications for the resulting material.

GTR can be modified by various methods, as shown by the review of the literature reported in the preceding section. Once treated, good interactions can exist between GTR and thermoplastics or thermoplastic elastomers due to specific interactions or to chain entanglement between chains present at the modified rubber surface and thermoplastic polymer chains. These lead to good mechanical properties, and in this way, not only can we reuse end of life tires, but also used thermoplastics.

In a work of Lopez-Cuesta et al., ground tire rubber powders experienced oxidation treatments by potassium permanganate solutions (wet process) or γ-irradiation (in air, dry process), and were then blended with maleic anhydride grafted polyethylene (MA-g-PE), and the results showed improvement in mechanical properties as compared to non-treated blends[47].

La Mantia and co-workers employed recycled polyethylene pellets mixed with ground tire rubber powders, then fed these into an industrial twin screw extruder to produce composites. Through mechanical performance evaluation, the results show that at a relatively low GTR concentration and under proper thermal conditions, composites with fairly good properties can be obtained. However, a high processing temperature can lead to partial carbonization of ground tire rubber powders [48].

Ground tire rubber powders were functionalized with allylamine and benzoyl peroxide, characterization showed that the surface energy of the functionalized rubber powder seems to increase. Physical properties of functionalized rubber/maleic anhydride grafted polypropylene blends were improved due to an enhancement in chemical interaction between the GTR and the PP phases. This technique is amenable to large-scale process[49]. Likewise, Lee and co-workers also studied allylamine grafted onto the ground tire rubber surface, then blended with polypropylene modified by maleic anhydride, and the mechanical performance improved due to an increase in interfacial interaction through chemical reaction[50].

Isayev and co-worker directly blended ground tire rubber powder with commercial polypropylene under various ultrasonic treatment conditions, and composites were then prepared by a twin screw extruder. Mechanical properties showed improvements as compared to untreated composite samples[51].

Polystyrene (PS) is particularly troublesome for recycling due to the two following reasons. First of all, PS density is similar to that of other thermoplastics, but as many PS applications use it as a foam, density of the PS recycled parts are much lower by a factor approximately of 10, which raises the transportation and storage cost per gram as compared to other thermoplastics. Moreover, PS is used mainly in food vessel applications (utensil, plates, etc.), which have high purity requirements and therefore are incompatible with the use of recycled material. Based on these two factors, polystyrene is mainly recycled as an energy source, which is not economic. To increase the number of potential applications for recycled PS, its impact properties must be improved. It is therefore a good candidate for blending with modified ground tire rubber powder.

In 1988, Papaspyrides and co-workers used dissolution in solvents such as benzene or toluene, to recycle polystyrene. Reprecipitation, filtering and dispersion were used to recycle polystyrene in large scale, and it was found that recycling in this way caused no important change in properties of the products[52].

Santana and co-worker studies have shown that, when incorporating GTR into post-consumed PP or high impact polystyrene (HIPS), the particle size of filler (ground tire rubber) affects the void content in the obtained composites, possibly due to higher surface area of ground tire rubber or to rheological properties. The SEM characterization results indicated that differences exist in the composite fracture structure after tensile tests, which were dependent on the nature of the matrix (ductile for PP and fragile fracture for HIPS). Good interfacial interactions existed for HIPS as compared to the PP matrix. However, mechanical performances with these two matrices, decreased because of the weak interfacial adhesion between composites components[53].

In a recent work by Veilleux and Rodrigue, SBR/PS blends were obtained by twin-screw extrusion for a wide range of SBR concentrations (0 to 62 %). Blends revealed good

mechanical properties. A solvent treatment was used and improved remarkably the quality and mechanical properties of blends [54].

1.5 Quality control of crumb rubber

As is introduced previously, the reticulated structure of end of life tires leads to insoluble and unmeltable material. End of life tires are therefore mechanically grinded to obtain GTR powder in micro dimensions. However, the resulting powder is challenging to characterize: on top of being insoluble and unmeltable, particle size is small, and it shows a large inhomogeneity in particle size and chemical composition, due to the use of various type of tires, such as summer tires, winter tires, truck tires or passenger tires. The conventional characterization methods for rubbers often have to be modified, due to the small particle size, and are much more time-consuming. Therefore, this brings several quality control problems for the GTR industry, such determination of as cross-linking density, monomer composition in rubber, carbon black and inorganic filler content.

1.5.1 Cross-linking density

In the end of life tires, a very important characterization parameter is cross-linking density, which largely influences mechanical properties.

As it is known, tire rubber is vulcanized or cured with sulfur, and the traditional characterization technique for the resulting insoluble reticulated network is an equilibrium swelling experiment, which allows determination of the cross-link density.

Based on a work by Frenkel, a preliminary criterion of equilibrium was recognized to express the chain configuration entropy on the basis of rough calculations of the swelling limit for vulcanized rubber. Then he realized that entropies attained from the ideal solution laws were not unsound[55]. Continuing this line of thought, Flory and co-worker, on the basis of research from Frenkel, found that the activity of the solvent can be expressed as a function of its concentration in the swollen network and of the degree of cross-linking[56,57]. The equilibrium swollen equation (1.1) was then simply described as the following:

$$M_c = \frac{V_m \rho_p \left[(V_s / 2) - V_s^{1/2} \right]}{\ln(1 - V_s) + V_s + \chi V_s^2} \quad (1.1)$$

where M_c is the average molecular weight between two cross-linking points; V_m represents the molar volume of the selected solvent; ρ_p is the density of the non-cross-linked polymer; V_s is the fraction volume of solvent; χ represents the interactions between polymer and solvent.

The detailed calculation procedure will be expressed here to better understand equation (1). One piece of determined size (usually around 1 mm x 5 mm) of rubber is cut and weighed, then put in toluene solvent for 72 hours to achieve equilibrium swelling. The excess solvent is then removed without touching the swollen rubber, then the weight can be measured and the swelling index (S) can be calculated using the following equation (1.2):

$$S = \frac{Mass\ of\ swollen\ rubber}{Mass\ of\ unswollen\ rubber} \quad (1.2)$$

Then V_s can be obtained according to the next equation (1.3):

$$V_s = \frac{1}{1 + (S - 1)(\rho_p / \rho_s)} \quad (1.3)$$

In the equation, ρ_s is the density of selected solvent.

Based on equations (1.1), (1.2) and (1.3), the cross-linking density ρ (mol/cm^3) can be calculated by the equation (1.4):

$$\rho\left(mol / cm^3\right) = \frac{2}{M_c} \quad (1.4)$$

The ASTM D6814 method published for measurement of cross-link density of rubbers. In the case of ground tire rubber, Rodrigue and co-worker modified slightly this technique. They performed it on a powder, and measured the density of the powder using a gas pycnometer at room temperature, using toluene as the solvent [58].

This conventional swelling equilibrium methods are time-consumed, normally 72 hours or more, and difficulties related to removal of solvent from the sample surface are much greater for GTR powder due to the higher surface area. Rubbers' cross-link density can also be established from mechanical property measurements and rheological measurements on rubber pieces, [59,60] but these cannot be performed on a power. Further, this method is difficult; to apply to GTR powder due to the small particle size. Alternate methods to characterize this parameter are therefore needed for GTR.

Solid state nuclear magnetic resonance (NMR) is a powerful instrument for characterizing insoluble samples, and is also useful to investigate cross-linking density of rubbers. During the vulcanization process, a certain amount of chemical cross-links are formed and, as a consequence, the degree of freedom of the molecules decreases. It is well established that the change of molecular mobility can be monitored indirectly by NMR relaxation measurements[61].

Blümich and co-workers adopted the NMR-MOUSE (mobile universal surface explore) cross-linking density measurement in elastomers with transverse relaxation measurement. This surface sensitive method can be done well in inhomogeneous magnetic fields, rather than homogeneous fields[62].

Filip and Aluas, based on a systematic numerical analysis, were able to accurately reproduce all the characteristic features of the cross-polarization curves measured on such materials. This is particularly important for investigating cross-linking density of blends of great technological potential, like thermoplastic elastomers (EPDM/PP)[63].

By the proton NMR T_2 relaxation experiments, Litvinov opened new possibilities for selective characterization of molecular mobility in different phases of thermoplastic vulcanizates (TPVs), of network density, which means cross-linking density in the rubbery phase of EPDM/PP TPVs and of the molecular heterogeneity of different phases[64]. The NMR method for cross-linking density measurement has several important advantages, in comparison with most conventional methods such as swelling or stress-strain measurements: it is a non-destructive technique, and can be used on powders, which is impossible for any conventional cross-linking determination method. However, no investigation of GTR samples have been reported using this technique, and even if it was found applicable to GTR

powders, NMR is industrially not attractive at the moment, due to the high cost and maintenance requirements of solid-state NMR instruments.

Differential scanning calorimetry may also give insights on the cross-linking density. Zattera and co-workers observed that there is a tendency toward lower glass transition temperature Tg values in thermograms of GTR samples without paraffinic oil (which is often used in tire formulations during processing), as well as an increase in the range of this transition, with an increase in the exposure time of the samples to radiation, attributed to an increase in the chain mobility related to the rupture of covalent bonds, such as C-S and S-S[65]. Glass transition temperature are known to be influenced by cross-linking density due to the restriction of chain movement that cross-links induce.

However, GTR samples are complex, as they do not vary only in cross-link density, but also in monomer composition and crystallinity, which also affect Tg. Thus, investigations on real samples are necessary to determine which factors dominate in GTR samples, and therefore whether DSC can be used for cross-link density estimations of GTR samples.

One overlooked possible method of investigation of cross-link density is thermogravimetric analysis (TGA). In this technique, the weight of a sample is closely monitored as temperature is increased. Mass loss due to degradation is observed, and can be correlated to thermal stability. However, the sulfur loss in TGA degradation could be related to the cross-link density of GTR sample. It is therefore worthwhile to investigate the use of this technique and verify whether it is amenable quantitatively or semi-quantitatively to cross-link density determination.

1.5.2 Monomer composition

Monomer composition of a rubber is another parameter which can determine, to some extent, the properties of samples. We will review here the main existing techniques that can be applied to monomer composition analysis.

As it is known, NMR itself is a powerful tool for structure analysis for solid or liquid materials. Different monomers have structures that lead to different NMR peaks in terms of intensities and chemical shifts. NMR can also be used to quantity each monomer by

determining peak intensities. Solid-state proton NMR of SBR, NR and BR mixtures-based GTR was investigated by Koval'akova and co-worker, and the spectra display three dominant peak groups. The first peak at 2 ppm is assigned to aliphatic protons (methyl, methylene and unsaturated methine) and come both from natural rubber and SBR, the second at 5 ppm is assigned to protons on unsaturated carbon atoms such as cis-1,4-isoprene units from natural rubber and uncross-link double bonds from SBR and the third at 7 ppm is related to aromatic rings from SBR. Peak intensities can be used to estimate the relative proportions of each rubber in SBR-based blends [66]. Another work was done by Zhang and Li, which used solid-state NMR to detect changes in existing double bonds in SBR before and after grafting. This confirms that solid-state NMR is useful for quantitative determination of the relative composition of monomers in real GTR samples[67].

DSC, an important thermal technique for polymer materials, give information on glass and melt transitions related to the chain movement or crystallinity in polymer samples. Bhattacharjee and co-workers studied the EPDM with various ethylene content by the DSC technique, and found that as the ethylene content increases in EPDM, the melt transition increases greatly in the range of 54 % to 68 % (w/w %). Similar conclusions were reached by Ver Strate and co-workers for different contents of ethylene in EPDM block copolymers by determining crystallinity measured by DSC, and comparing to the value results from X-ray diffraction [68].This indicates that information on the ethylene content can be gained with this technique by the calculation of the thermal melt enthalpy.

Therefore, the use of DSC to determine monomer composition will be investigated to determine if quantification is possible.

TGA has been used for determining the styrene-butadiene ratio in SBR by Castaldi and Kwon. They observed a two-stage degradation in the rubber phase which was attributed to degradation of aliphatic units from the butadiene and styrene, and aromatic units from styrene, respectively. This is related to the relative stability of these two types of chemical groups. Their results were in good agreement with the values from the recipe used for BR manufacture, which indicates a possible use for semi-quantitative determination of the styrene/butadiene ratio[69]. This method has however never been used on GTR samples.

1.5.3 Carbon Black

Carbon black is used in various formulations with different rubber types to customize the performance properties of tires. It is a good reinforcement material, and has the function of increasing strength, abrasion resistance and UV protection. At present, as the fuel price is increasing and demand for carbon black also increases for tire manufactures, quality control for carbon black is attracting attention due to the increasing use of carbon black from recycled sources.

Various techniques can be used to detect the content of carbon black inside ground tire rubber, such as the ASTM methods of TGA and pyrolysis.

TGA is a routine carbon black analytical method for rubber, described in ASTM D6370-99. The ground tire rubber, under air atmosphere, will usually thermally degrade in various steps corresponding to organics and carbon black, non-degradable material such as inorganics making up the residual parts. Several authors report using this methods to determine the quantity of carbon black in the case of ground tire rubber or waste rubber.[70-74] This method is proven, simple, affordable and fast for quantification of carbon black in quality control procedures for the industry.

Furthermore, another feasible way to calculate the carbon black content is pyrolytic analysis, for which a standard method (ASTM D5805-14) has also been proposed. This method can give the carbon black content in GTR through an inert or vacuum pyrolysis test.

Additionally, pyrolysis can also be used for production of carbon black or pyrolytic oil.[75-77] In all, this method is a good quality control technique, and as well a good strategy to produce carbon black or fuel from tires.

1.5.4 Inorganics

The inorganics in the ground tire rubber exist as fillers (SiO_2, $CaCO_3$) or vulcanization accelerators (ZnO). In TGA, after combustion in oxygen atmosphere, they remain as ash, so the amount of these elements can be known. Specific quantities of each of these fillers must be determined by other methods, such as ICP-OES and XRF, and alternative methods for industrial quality control while these elements quantification is an important issue.

Aguado and co-workers performed ICP analysis to investigate the metal composition in granulated waste tire rubber, and observed that the zinc content is much higher than other inorganic elements. Silica content was also measured. [78] Arockiasamy and co-workers used energy-dispersive x-ray spectroscopy to successfully measure the elemental content in tire residues after thermal treatment. [73]

1.6 Project Objectives

Each year, due to the greatly increasing car consummation, an increasing number of end of life car tires are discarded. Due to their non-biodegradability, insolubility and sulfur content, they are not only hard to reuse, but also cannot be burned directly as a fuel source, so that their reuse is an important challenge which modern societies face. A great number of end of life tires are accumulated, a phenomenon called "black pollution", which will lead to serious environmental or healthy problems. Nowadays, a growing number of people and organism work on disposal of end of life tires. At the moment, steels are first removed from end of life tires, then the remaining rubber parts will be ground into various size of powders. These powders can be directly used in the road pavement with asphalt, or can be blended with other thermoplastics for production of new objects. As interactions between ground rubber and thermoplastics is often poor, mechanical properties are also low, which limits possible uses. An interesting strategy is to modify first the powdered rubber surface, using physical and chemical methods, to improve interactions. In this way, properties of new ground rubber based products can be improved.

In addition, used thermoplastics such as polyethylene, polypropylene and polystyrene, are also generated is large quantities by modern societies. Reuse of both ground tire rubber and these post-consumption thermoplastics would make economic sense and help to solve an important environmental problem. This is especially true for polystyrene, for which the main uses are food containers and packaging. Due to health concerns, recycled PS cannot be used in food applications, which severely limits possible post-recycling applications. Adding rubber particles would impart better impact resistance, and may open up new markets for this recycling of this thermoplastic. In order to do this, improvements in interfacial interactions,

which will lead to improvements in mechanical properties are needed. Meanwhile, this will help us to solve the problems.

Quality control of ground tire rubber or manufacturing of new products from treated ground tire rubber is attracting much attention from the industry. With regard to the ground tire rubber, properties strongly depend on physico-chemical characteristics, such as cross-link density, metal content, carbon black content or monomer composition. As well, characterization methods for the surface of the modified powders can help select and improve chemical treatments for specific applications.

In this project, two types of ground tire rubber were obtained from an industrial facility and investigated, ethylene-propylene diene monomer (EPDM) and styrene-butadiene rubber (SBR) with different processing conditions and various powder sizes. These two ground rubbers are common synthetic rubber in tire manufacture, and are used for sidewall and tire tread, respectively.

In order to achieve the aims of recycling and reusing, we have divided the research project as follow:

1) To enhance the understanding of rubber powder material through laboratory testing, various methods, including TGA, DSC, NMR, FTIR, ICP-OES, AAS and CHNS analysis were used. Results are compared with those of standard samples, which were prepared by using pure EPDM and SBR rubber blended with carbon black, cross-link agent, glass fibers or accelerator. In this way, the standard samples serve as benchmarks to verify the analysis possibilities of these methods, whereas industrial samples are studied next, in order to verify the applicability for real industrial samples, for which compositions are more complex, homogeneity is low and contamination may be an issue. Therefore, through the use of these experimental methods, we aimed at obtaining more information for quality control of industrial rubber powder.

2) On the surface of the rubber powder, existing double bonds can be used for chemical modifications. In the present work, we aimed at grafting polymer chains of a known molecular weight. Reactions with thiol terminated polystyrene were selected to graft thermoplastic chains onto the surface of ground tire rubber. Then, XPS and FTIR will be

used to detect the surface changes of initial and grafted GTR. TGA can be also used to investigate the thermal stability and rough grafting efficiency for grafted GTR.

3) In order to assess if this type of treatment is effective to enhance interactions between rubber particles and a thermoplastic, composites were prepared with initial GTR or grafted GTR composites and the same thermoplastic as the chains which were grafted, polystyrene. This was done using a ground rubber with low chemical affinity for polystyrene, EPDM and not SBR, as SBR contains styrene domains. Investigation of mechanical properties for those composites were performed by dynamic mechanical thermal analysis (DMTA). This is an indirect method for interphase interaction assessment, as improvements will lead to increases in mechanical properties.

Finally, this research work focuses on environmental friendly and low-cost methods to improve characteristics of rubber.

Chapter 2: EPDM Recycled Rubber Powder Characterization: Thermal and Thermogravimetric Analysis

Huan Liang, Jean-Michel Hardy, Denis Rodrigue and Josée Brisson, Rubber Chemistry and Technology, 87(3), 538-556(2014). DOI: 10.5254/rct.14.87988

Résumé

Des recherches sur le caoutchouc éthylène-propylène-diène (EPDM) avec des densités de réticulation et un contenu de noir de carbone variables, ainsi que sur des poudres d'EPDM recyclées à partir de pneus usés (WGR), ont été effectuées afin d'améliorer les méthodes de caractérisation. Le but est de fournir des méthodes de contrôle de qualité supplémentaires dans le domaine du recyclage de caoutchouc, car le WGR est transformé et réutilisé sous forme de tapis de caoutchouc principalement pour des applications de terrains de jeu, en agriculture, pour le sport et dans les automobiles. La spectrométrie d'émission optique plasma à couplage inductif, la spectrométrie d'absorption atomique et des analyses élémentaire (CHNS) ont été utilisées pour déterminer le contenu d'éléments chimiques divers. L'analyse thermogravimétrique (ATG) a été utilisée pour déterminer la quantité de noir de carbone et de matériel inorganique dans les échantillons. La perte massique à 400 °C a été liée à la densité de réticulation. L'ATG couplée avec la spectrométrie de masse a permis de déterminer que cette perte massique correspond à la perte de SO_2, puisque les liaisons de réticulation sont détruites au cours du chauffage. Les points de fusion et les températures de transition vitreuse qui sont déterminés par calorimétrie différentielle à balayage sont principalement proportionnels au rapport massique d'éthylène/propylène.

Abstract

Investigations on ethylene–propylene–diene rubber (EPDM) with varying cross-link densities and carbon black contents, as well as commercial EPDM waste ground rubber (WGR), have been performed to improve characterization. The aim is to provide additional quality-control methods in the field of rubber recycling, as WGR is transformed and reused in the form of rubber mats mainly for playground, agricultural, sport, and automobile applications. Inductively coupled plasma optical emission spectrometry, atomic absorption spectrometry, and elemental (CHNS) analyses were used to determine the content of various chemical elements. Thermogravimetric analysis (TGA) was used to determine the amount of carbon black and inorganic material in the sample. Mass loss at 400 °C was related to cross-link density. TGA coupled with mass spectrometry showed that this mass loss corresponds to the loss of SO_2 as cross-links are destroyed during heating. Melt point and glass transition temperatures determined by differential scanning calorimetry are mainly proportional to the ethylene/propylene weight ratio.

2.1 Introduction

Cross-linked rubbery materials, including ethylene–propylene–diene rubber (EPDM), are found in a wide range of applications.[1–4] A large volume of waste rubber is generated each year,[5] and its costly disposal is an important environmental concern. Significant efforts are made to reuse rubber. Waste rubber is ground into powders, resulting in waste ground rubber (WGR), that can be revitalized when combined with thermoplastic polymers.[6–11] WGR is currently recycled mostly as molded rubber mats or linings for varied uses, including playgrounds, agricultural applications, golf and other sports, construction material, blasting equipment, and protective automobile parts.

Characterization of rubber is well established. It includes determination of cross-linking density (ρ) through swelling experiments,[12,13] nuclear magnetic resonance (NMR) measurements of relaxation time[14–16] or mechanical properties,[17,18] glass transition temperature and melting point determinations by differential scanning calorimetry (DSC),[19–21] compositional analysis by chemical or thermogravimetric analysis (TGA),[22,23] and analysis of functional groups at the surface.[24,25] The benchmark technique to measure cross-link density, swelling measurements, is time-consuming, and alternative methods for rapid estimation of the cross-link density are always sought.

WGR samples present additional characterization challenges. Due to their granulometric composition, mechanical properties and swelling of WGR are very difficult to measure. Rubber composition and cross-link density vary from batch to batch and even within each batch and are strongly affected by thermomechanical history. Macsiniuc et al.[9] have shown that, within a given batch, the size of the powdered rubber also influences the properties of post-recycling parts. Therefore, there is a need for fast, low-cost quality-control characterization methods.

In a previous study by our group on thermomechanical regeneration of WGR,[9] commercial WGR samples collected at a recycling facility were mechanically sieved to separate them by powder size and then subjected to thermomechanical treatments in an internal batch mixer at various temperatures and rotor speeds. Cross-link density was measured before and after treatment by swelling experiments following the approach

proposed by Flory and Rehner.[12] These time-consuming measurements were performed on a large number of particles, and difficulties related to removal of surface solvent limited precision and increased measurement time. An alternative method is clearly needed for quality control, and the present study investigates methods that can be used to characterize such EPDM WGR samples, along with benchmark standards to do so.

Furthermore, WGR samples are often inhomogeneous and include various additives, the nature and quantity of which may have significant impact on their properties. The present investigation therefore focuses on rapid and cost-effective methods to analyze EPDM, including challenging samples such as WGR. Chemical analysis was performed on WGR samples by various techniques, including inductively coupled plasma optical emission spectrometry (ICP-OES), atomic absorption spectrometry (AAS), and elemental (CHNS) analysis, whereas swelling measurements to determine cross-link densities were reported previously.[12,13] Two methods amenable to routine measurements were investigated in this context: TGA and the thermal method DSC. TGA is already used for determination of carbon black and fillers (ash) in rubber (ASTM D6370), and DSC is widely available and does not require long sample preparation. Solid-state NMR, previously proposed to quantify cross-link density in rubbers,[9] was also investigated to determine to what extent this method is applicable to EPDM WGR samples.

To determine the effect of specific variables (i.e., variations in cross-link density, quantity of carbon black, and presence of glass used as filler), standard EPDM samples were prepared and analyzed. EPDM prepolymers were cross-linked in the presence of known additives. As the prepared standards were in the form of rubber films and not powders, characterization by standard swelling methods was straightforward. Results for these standard samples will be used to gain a better understanding of the effects of carbon black and of changes in cross-link degree and ethylene/ propylene weight ratio (E/P) on properties measured in the present work. Finally, possible characterization techniques for WGR in an industrial environment are discussed.

2.2 Experimental

2.2.1 Preparation of Rubber Standards

In a 100 mL beaker with a magnetic bar, 2 g of an EPDM prepolymer [Royalene 580HT containing a 53/47 E/P and 2.7 w/w % ethylene norbornene (ENB), Royalene 556 with 71/29 E/P and 4.5 w/w % ENB and Royalene 539 EPDM containing 74/26 E/P and 4.6 w/w % ENB], kindly supplied by Lion Copolymer Inc. (Geismar, LA, USA), was dissolved in 30 mL of toluene, heated to 60 °C to favor dissolution, and stirred until complete dissolution was achieved. In a 50 mL Erlenmeyer flask, 10 mg of tetramethylthiuram disulfide, 40 mg of stearic acid dissolved in 1 mL of toluene, and 100 mg of ZnO were introduced. This accelerator solution was heated at 50 °C until complete dissolution was achieved and then was added to the EPDM solution, after which active carbon black (CC N991, Cancarb Limited Inc., Medicine Hat, AB, Canada) was added in quantities varying from 0.60 to 1.40 g, corresponding to 30–70 parts per hundred of rubber (phr). In one sample, milled glass fibers (731ED, fiber diameter 10 lm, Owens Corning, Huntingdon, PA, USA) was also added at a concentration of 28 phr, corresponding to 17 w/w %. Finally, the cross-linking agent, an aliquot corresponding to 0.05–2 phr of a 1.0 mL S_2Cl_2 solution in 10 mL of toluene, was added using a syringe, while stirring. The mixture was poured rapidly into stainless steel molds that had been sprayed with PEI 35838 ORAPI Northern-Cape silicon releasing agent (15 cm^2 x 15 cm^2 plates having four 0.2 cm deep, 4 cm wide depressions). Solutions were allowed to dry in the molds for around 2 h at room temperature in a hood. Once dry, films were removed from the mold, and the mold was cleaned using ethyl acetate. Mold surfaces were then treated with the silicon releasing agent, and rubber samples were reinserted in the mold, covered with a silicon-treated plate, and placed for 30 min in a Carver press preheated to 180 °C.

Standard samples of cross-linked EPDM having a 53/47 E/P, without carbon black, are abbreviated CDX-Y, where CD indicates a series of samples with the same E/P but different cross- link densities, X is the weight ratio of ethylene, and Y is the cross-link density (ρ) of the sample. A series of samples were also prepared from the 53/47 E/P prepolymer with varying proportions of carbon black, but with as constant as possible cross-link densities. These are

Table 2.1 Proportions Used in the Preparation of Standard EPDM Samples

Component	Mass used, g	Composition, phr
EPDM	2	100
Stearic acid	0.04	2
TMTD	0.01	0.5
ZnO	0.1	5
S_2Cl_2	0.04 to 0.2	2 to 10
Carbon black	0.00 to 1.4	0 to 70
Milled glass fibers	0.00 and 0.55	0 and 28

abbreviated CB-Z, where CB refers to the presence of carbon black and Z is the amount (in percentage) of carbon black added to the sample with respect to EPDM alone. The addition of "+G" indicates the presence of milled glass fibers in the rubber. Quantities used are summarized in Table 2.1, and a more detailed description appears in the Supplemental Material.

2.2.2 Industrial WGR Sample Selection and Preparation

Industrial EPDM WGR samples were provided by Recyclage Granutech Inc. (Plessisville, QC, Canada). These samples mostly came from truck and oversized tire parts and tire flaps that were ground and blended and were mainly composed of various EPDM vulcanized rubbers. Four samples were chosen at random from standard batches prepared by this industrial site, and they correspond to four different random sampling days. This sampling technique was chosen to provide samples representative of WGR composition variations that can be found in the industry. Before use, they were submitted to thermomechanical regeneration using a Haake Büchler Rheomix internal mixer, as described in detail in ref 9.

Processing conditions used for each waste rubber sample are reported in Table 2.2 (WGR average particle size, processing temperature, and speed), along with previously measured cross-link densities. Abbreviations used in the present text (WGR- A to WGR-D) are also introduced in Table 2.2.[9] Samples were submitted to an extraction procedure using acetone under reflux for 24 h to remove low-molecular-weight molecules used or produced during processing. Cross-link densities were previously measured by swelling in toluene and acetone, as described in ref 9. For all analyses reported, three portions of the initial samples were selected at random, prepared separately, and measured. Standard deviations are reported to estimate the error, along with detection limit for quantitative analysis techniques.

2.2.3 Cross-link Density Measurements

Cross-link density ρ of the rubber standards was measured by using modified versions of ASTM D3616 swelling method. For standard rubbers, samples (1 mm x 5 mm) were cut from the rubber films, weighted accurately and submerged in toluene. Samples were allowed to swell for 72 hours at room temperature protected from light. After 72 hours, excess solvent was removed using a pipette without touching the swollen gel pieces. Each gel piece was then lightly dabbed with absorbent paper and immediately weighted accurately. For commercial WGR samples, measurements were performed using a modified version of ASTM D6814, and described in a previous paper by Macsiniuc *et al.*[58]. Cross-link densities of EPDM varies with ENB percentages, quantify of sulfur used during vulcanization and effectiveness of the vulcanization procedure. Expected maximum cross-link densities were calculated, following Averko et al.[79], as 14 to 72 $\times 10^{-5}$ mol/cm^3 for ENB weight percentages of 2 to 10 w/w %, commonly found in commercial EPDM. In the EPDM source used here, cross-link densities are low, indicating low ENB percentage and/or vulcanization degrees. Although swelling measurements result in overall cross-link densities, as the cross-linking procedure used in the tire automobile industry is mostly vulcanization or sulfur cross-linking, and as WGR samples studied were from this source, as most industrial WGR, it is proposed that these values represent sulfur cross-link densities. The thermomechanical regeneration process to which these WGR samples were subjected also affects cross-link density, as reported previously.[58]

Table 2.2 Characteristics of Various WGR Samples Used in this Work

WGR Sample	Average Powder Particle Size, μm	Processing Temperature,°C	Processing Speed, rpm	Cross-Link Density ρ, 10^{-5} mol/cm^3
	± 10	± 5		± 0.5
WGR-A	125	220	40	3.3
WGR-B	125	220	120	2.5
WGR-C	710	180	40	5.5
WGR-D	1,000	220	120	8.1

Note: Cross-link density values were previously calculated from swelling measurements.[58]

2.2.4 Atomic Absorption Spectrometry (AAS)

Sample preparation prior to analysis included calcination at 650 °C for 2 hours in a muffle oven, after which the temperature was raised to 700 °C overnight. Residuals were transferred to a plastic volumetric vial and dissolved in 1 mL hydrofluoric acid. Deionized water (HPLC grade) was added to raise the volume to 50 mL. Standard solutions of 5 to 100 ppm were prepared by dilution from an assurance grade standard silicon solution (10,000 mg/L in H_2O /4.0 % F^- purchased from Spex CertiPrep Inc.). A Perkin Elmer 3110 atomic absorption spectrometer was used with a nitrous oxide (35 mL/min)-acetylene (43 mL/min) flame at the 251.6 nm spectral line position, optimized according to the manufacturer's recommendations.

2.2.5 Inductively Coupled Plasma Optical Emission Spectrometry (ICP-OES)

Inductively coupled plasma optical emission spectrometry (ICP-OES) (Optima 3000, Perkin Elmer) was performed using a radio frequency power of 1300 W, and gas flows for plasma at 15 L/min, for auxiliary gas at 0.5 L/min, for nebulizer at 0.8 L/min, and for the mobile

phase at 1.5 mL/min. Around 50 mg samples were placed in a ceramic holder and then burnt in a muffle furnace at 750 °C for 3 h. Next, using deionized water and 10 mL nitric acid, residuals were solubilized and quantitatively diluted to 100 mL with deionized water prior to measurements.

2.2.6 CHNS Elemental Analysis

CHNS elemental analysis was performed on an organic elemental analyzer (Flash 2000, Thermo Scientific). Cystine, used as a standard sample, was put in a universal soft tin container (100pc, outside diameter = 5 mm, height = 8 mm, volume = 157 μL), which also served as a blank sample. Around 0.5 mg of each sample was encapsulated in the same type of container.

2.2.7 Differential Scanning Calorimetry (DSC)

Differential scanning calorimetry (DSC) characterization was performed using a DSC823e (Mettler Toledo Company) apparatus with a liquid nitrogen cooling accessory. Approximately 15 mg of sample was inserted in an aluminum pan, and DSC measurements were performed by heating from –100 °C to 100 °C at 20 °C/min under a nitrogen atmosphere, holding the sample at this temperature for 5 minutes and then cooling back to -100 °C at 20 °C/min. A second heating scan was then performed under the same conditions, and is the one reported in all cases. Crystallinity is estimated using the enthalpy value of the melting peak, a constant interval of 30 to 60 °C being used in all cases.

2.2.8 Solid-State ^{1}H NMR Spectroscopy

Solid-state ^{1}H NMR spectra of EPDM samples were recorded on a 400 MHz solid-state NMR spectrometer (Bruker Biospin Ltd). Samples (cut into small pieces for rubber films, prepared as described above for WGR) were packed in 4 mm sample tubes and spun at 10 kHz at the magic angle.

2.2.9 Thermogravimetric Analysis (TGA) and Thermogravimetry Analysis Coupled with Mass Spectrometry (TGA-MS)

Thermogravimetric analysis (TGA) was performed using a TGA/SDTA 851e (Mettler Toledo Company) apparatus. One to two mg of samples was put in a ceramic pan, and measurements were performed by heating from 50 °C to 900 °C at 20 °C/min, either under nitrogen or air atmosphere. A thermogravimetric analyzer using a diamond TG/DTA (Perkin Elmer Co.) coupled with a MS GSD 301 T3 (Pfeiffer Vacuum Thermostar) mass spectrometer (TGA-MS) was used to analyze gases evolving during degradation. Analysis was performed on 16 mg samples in an air atmosphere with a flow rate of 100 mL/min measured by a Bronkhorst gas mass-flow meter over the 22-920 °C temperature range at 20 °C/min.

2.3 Results and Discussion

2.3.1 Preliminary Analysis of WGR by ICP-OES, AAS and CHNS Analysis

Commercially available EPDM composition varies with respect to proportions of ethylene, propylene and diene, the latter typically being a dicyclopentadiene, an ethylidene norbornene or a 1,4-hexadiene. Many combinations can be found in WGR, depending on the origin of the recycled products. Furthermore, relative proportion of carbon black, proportion and nature of additives, and cross-link density vary in WGR depending on the recycled rubber characteristics. These in turn cause important variations in properties of parts made with WGR, hence the need for effective quality control measurements. In the present work, it was chosen to use EPDM standards prepared in the laboratory and for which composition, EPDM type as well as cross-link densities could be controlled to establish characterization benchmarks. However, the use of standard samples may not be representative of industrially relevant samples, which are often contaminated with metals, other rubbers or various impurities. Therefore, a few representative commercial WGR samples were selected to provide additional validation that the methods were robust enough to be used with industrial WGR samples. These were not prepared using a specific grade of EPDM nor by controlling in any way the material used or the treatment the samples were submitted to. Instead, samples

were gathered at the same industrial site, using the same reclaimed rubber sorting strategy. Sampling was undertaken four different, statistically chosen production days. Therefore, these are believed to represent normal variations that can be found on a given industrial production site. As samples chosen in this way resulted in material with ill-defined properties, WGR samples were investigated in more depth than expected for quality control purposes, in order to gain a better understanding of the samples studied here. Chemical composition was investigated mainly using three different techniques. Atomic absorption spectrometry, inductively coupled plasma optical emission spectrometry (ICP-OES) and elemental analysis were used. Results are reported as percentages of the initial WGR in Table 2.3, along with the sum of all metals measured, noted as Metals (total).

The two most important metals found are calcium and zinc. Calcium ranges from 4.00 to 6.15 %. It is often added as a filler in the form of $CaCO_3$, or can also be used as a processing aid in the form of calcium fatty acid salts.[80] The use of CaO as a cure activator in concentrations ranging from 2 % to 8 % has also been reported, although commercial use is infrequent.[81,82] Zn percentages are smaller, varying from 1.43 to 1.73 %. Its most probable source is zinc oxide, which is used as a catalyst/activator.[83] All other elements measured (Cd, Cr, Cu, Fe, Mg, Mn, Na, Ni, P, Ti) could not be detected above the detection limit of the method (0.01 %), except for aluminum, which samples WGR-C and D contained 1.02 % and comparison purposes with other techniques, Table 2.3 also reports the sum of calcium, silicon, zinc and aluminum, (expressed as $CaCO_3$, SiO_2, ZnO and Al_2O_3). No correlation was expected when comparing cross-link density and percentages of Zn, since although used as comparison purposes with other techniques, Table 2.3 also reports the sum of calcium, silicon, zinc and aluminum, (expressed as $CaCO_3$, SiO_2, ZnO and Al_2O_3). No correlation was expected when comparing cross-link density and percentages of Zn, since although used as an accelerator, zinc is not part of the cross-links per se. Samples with lower cross-link densities (WGR-A and WGR-B) however, have higher percentages of calcium, which may be related to the specific formulations used in the WGR studied. Determination of the

Table 2.3 Concentration of Elements in w/w % of Initial WGR as Determined by ICP-OES, AAS (Si expressed as SiO2) and CHNS Elemental Analysis (Sulfur)

	Standard deviation	Detection Limit	WGR-A	WGR-B	WGR-C	WGR-D
Residual mass[a]	0.2	-	20	18	17	18
Residual mass[b]	2	-	20	19	21	23
Al	0.02	0.04	0.00	0.00	1.02	0.75
P	0.01	0.01	0.00	0.00	0.00	0.00
Ca	0.07	0.02	6.15	5.62	4.00	4.85
Ti	0.01	0.01	0.00	0.00	0.00	0.00
Cd	0.01	0.01	0.00	0.00	0.00	0.00
Cr	0.01	0.01	0.00	0.00	0.00	0.00
Cu	0.01	0.01	0.00	0.00	0.00	0.00
Fe	0.01	0.01	0.00	0.00	0.00	0.00
Mg	0.01	0.01	0.00	0.00	0.00	0.00
Mn	0.01	0.01	0.00	0.00	0.00	0.00
Na	0.01	0.01	0.00	0.00	0.00	0.00
Ni	0.01	0.01	0.00	0.00	0.00	0.00
Zn	0.20	0.04	1.73	1.59	1.43	1.74
Metals(total)	-	-	7.97	7.30	6.43	7.34
$CaCO_3$ +ZnO+ SiO_2 + Al_2O_3	-	-	19.9	18.2	16.0	18.0
SiO_2	0.02	0.03	2.70	2.18	1.87	1.82
S	0.1	0.001	0.4	0.1	0.4	0.1

[a] As determined from calcination prior to spectrometry measurements
[b] As determined from TGA analysis

quantity of calcium may therefore be useful for quality control purposes, although an alternate, faster method, such as X-ray fluorescence spectrometry, would be preferable.

Silicon is present as SiO_2 filler in some formulations, but quantities are not related to cross-link density. Industrially, cross-linking of rubber is performed by vulcanization using sulfur, and therefore sulfur determination was performed by elemental analysis. Sulfur concentrations are small in WGR, varying from 0.1 to 0.4 %, in agreement with the low cross-link density of these samples, but no clear correlation can be observed between quantity of sulfur and cross-link density, which is probably related to the use of excess sulfur during rubber vulcanisation, to the variable number of sulfur atoms in each cross-links or to the presence of sulfur in the carbon black that the WGR samples studied here contain.

2.3.2 Solid-state ^{1}H NMR Spectroscopy

NMR is a powerful technique to investigate the chemical structure of insoluble material. For EPDM rubbers, NMR can be used to quantify the ethylene/propylene ratio, and has been proposed as a means to investigate cross-link density through the relative intensity of the diene peak, the relative width of the ethylene peak[31] and the measurement of the spin-spin T_2 relaxation time.[32-37] However, the limited availability of solid-state NMR instruments outside regional facilities limits the use of this technique as a routine industrial quality control method. Further, as shown by chemical analysis of WGR samples in the present work, paramagnetic metals (calcium and aluminum) are present in WGR samples in large quantities, and will therfore also contribute to peak broadening. In order to assess to what extent this effect would limit the usefulness of NMR for the study of commercial WGR samples, Figure 2.1 reports NMR spectra of representative samples studied in this work (additional NMR spectra are reported in Supplementary material).

For EPDM samples prepared in our laboratory, peak width is limited, and a good resolution is noted. Spectra comprise two main peaks at 0.95 and 1.38 ppm, corresponding respectively to methyl groups from propylene units and methylene hydrogen atoms from ethylene and propylene units. Around 3.0 ppm can also be seen a small peak indicating the presence of residual diene units in the rubber, as this sample was not fully cross-linked. Peak width for these laboratory prepared samples correlate with the cross-link density measured by the swelling approach. Addition of carbon black (sample 50CB) and glass (sample 50CB+G)

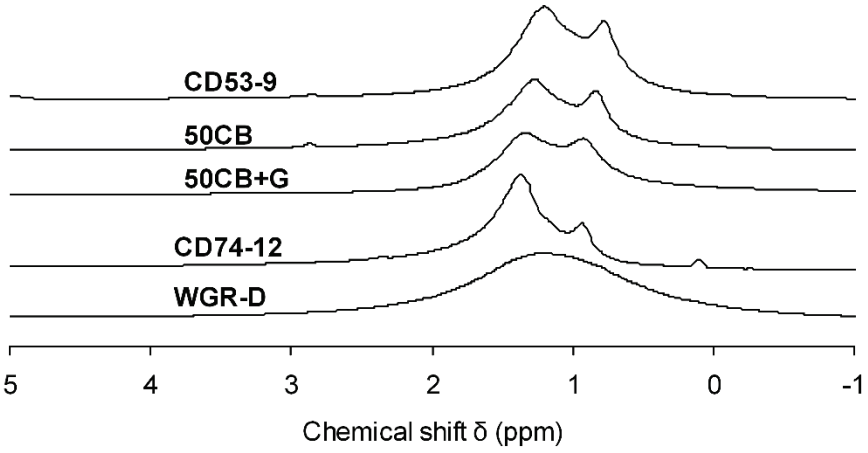

Fig. 2.1 Solid-state ^{1}H NMR spectra of representative samples

does not lead to a significant increase in peak width, and changes in E/P weight ratio (CD53-9 has a 53/47 ratio and CD74-12 has a 74/26 ratio), which also changes crystallinity, has a small effect.

Unfortunately, as seen in Figure 2.1 for a representative sample, WGR samples present severe line broadening, well above that expected from their cross-link density alone. This is attributed to the presence of important quantities of calcium and aluminum paramagnetic atoms, as shown by ICP-OES measurements. Magnetic impurities such as iron may also be present in trace amounts due to the sample processing conditions, and could also contribute to peak broadening. Therefore, a single, very wide peak centered near 1.0 ppm is observed, and spectra cannot be used to determine the relative proportion of ethylene and propylene in industrial WGR samples. Further, peak broadening due to magnetic and paramagnetic effect is larger than that expected for cross-link density variations, and this technique therefore cannot be used to investigate changes in cross-link density of industrial WGR samples. Attempts to measure Fourier transform infrared (FTIR) spectra in transmission or reflection mode all resulted in poor quality spectra (not shown), in which it was virtually impossible to assign with certainty any vibration. No valid information could be obtained from this technique on WGR samples, which is attributed to the presence of various additives such as carbon black or silicates.

It is concluded that, although spectroscopic techniques such as NMR or FTIR are powerful to investigate the nature and quantity of cross-links in rubbers, as well as the chemical composition of the EPDM rubber chains, for industrial samples such as WGR, they are not useful. For NMR, this is due to the line broadening effect of paramagnetic species present in important concentrations. Other approaches must therefore be found to gain insights on these two factors for WGR samples.

2.3.3 Thermogravimetric Analysis (TGA)

Thermogravimetric analysis (TGA), which is routinely used for rubber characterization, was performed next. Although it is not a classical composition analysis technique, TGA is used in ASTM D6370-99 and E1131-08 methods to quantify carbon black and ash (filler) in rubbers and non-organic solids in liquids and solids. Curatives (such as excess sulfur), organic accelerators, emulsifiers and antioxidants (often designated as highly volatile matter) are lost below 300 °C, and oils and plasticizers are typically lost between 300 and 350 °C, although less volatile oils can degrade at higher temperatures.[70]

EPDM itself is reported to loose mass between 480-550 °C. Under nitrogen, degradation stops at this point, but in air, oxidation of carbon black to carbon dioxide occurs between 520 and 575 °C. The remaining ash is composed of various inorganic compounds.

Typical TGA degradation curves in air of standard EPDM samples with varying proportions of carbon black are shown in Figure 2.2A, and with varying cross-link density in Figure 2.2B. Degradation of neat EPDM (abbreviated 0CB) starts around 300 °C and ends around 540 °C, as reported in the literature.[70,84] Carbon black degrades next and forms carbon dioxide between 600 and 700 °C.[40] As expected, the curve does not go to zero and residual ash remains, which is composed mainly of inorganics such as ZnO, $CaCO_3$, SiO_2 and Al_2O_3.

A)

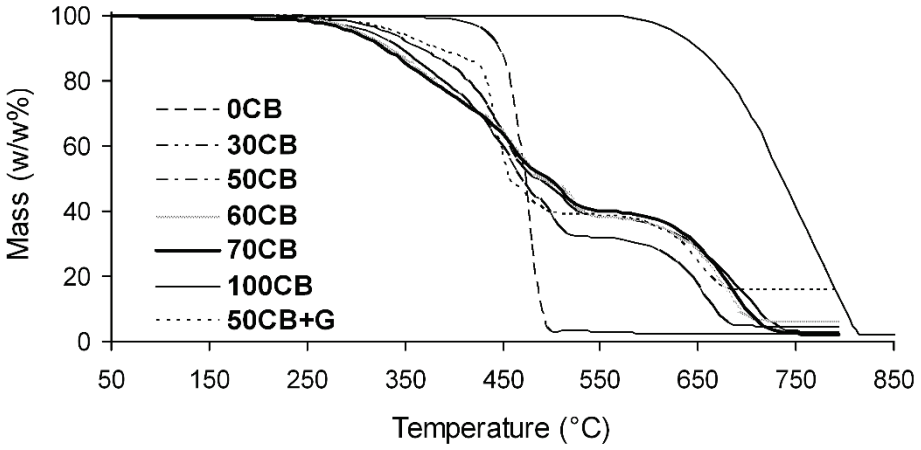
100
80
60
40
20
0
Mass (w/w%)
0CB
30CB
50CB
60CB
70CB
100CB
50CB+G
50
150
250
350
450
550
650
750
850
Temperature (°C)

B)

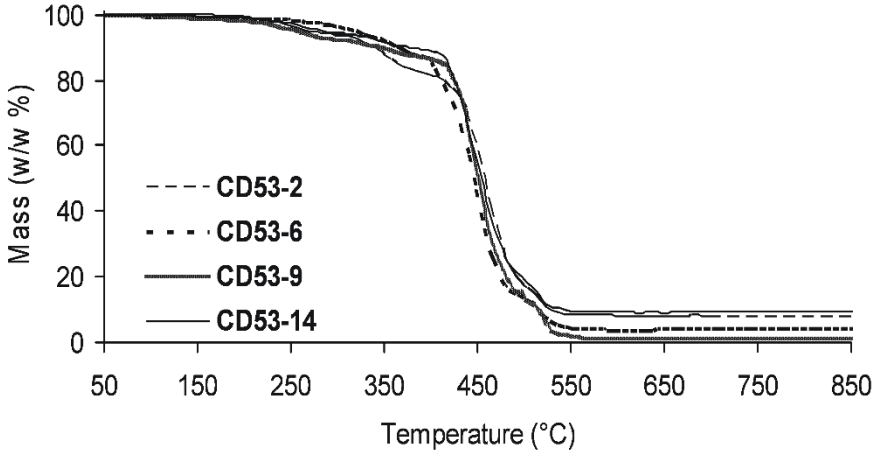
100
80
60
40
20
0
Mass (w/w %)
CD53-2
CD53-6
CD53-9
CD53-14
50
150
250
350
450
550
650
750
850
Temperature (°C)

C)

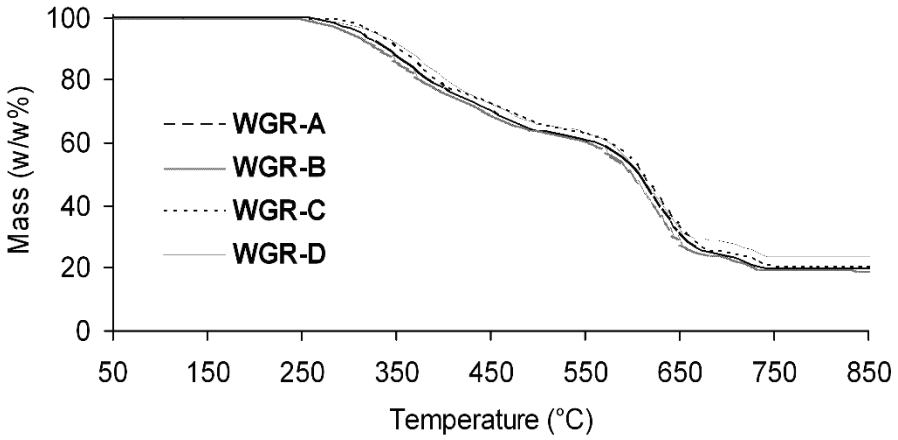

D)

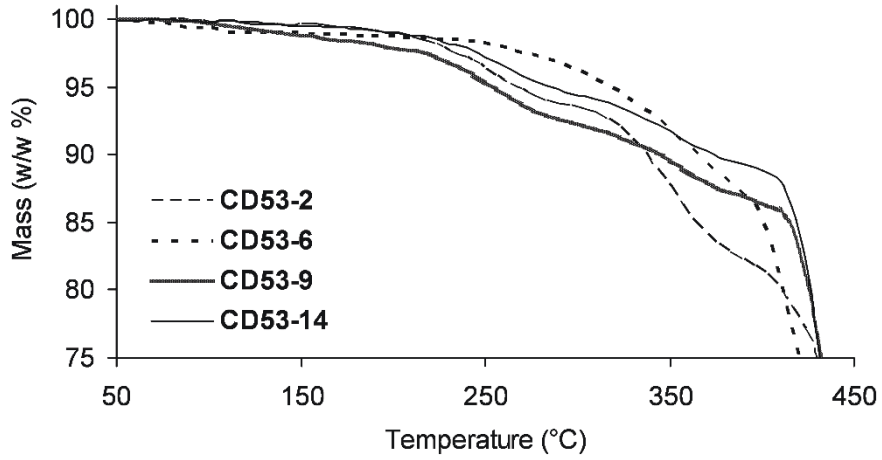

Fig. 2.2 TGA, in air, of EPDM and WGR samples: A) CB standard samples (similar ρ, different carbon black and glass content); B) CD53 standard samples (no carbon black, different cross-link densities); C) WGR samples; D) Enlargement of curve (b)

EPDM percentage is determined from the mass loss at the plateau between EPDM and carbon black degradation, or 1st mass loss and carbon black from the difference between EPDM and residual inorganic percentage or 2nd mass loss and residual percentages. These are reported in Table 2.4. A good fit is observed, as expected, between the percentage of carbon black used to prepare standard samples and 2nd TGA mass loss. Residual ash percentage also fits, within experimental error, with the inorganics used to prepare the standard samples (ZnO and SiO_2), as these do not degrade thermally. This accounts for 2-5 w/w % of mass loss, with the exception of sample 50CB+G which contains milled glass, and therefore shows a much higher residual percentage of 16 w/w %.

Degradation curves of WGR samples are reported in Figure 2.2C. No degradation occurs below 250 °C, contrary to other EPDM samples reported in the literature[70], in which smaller molecular weight molecules are used as modifiers degrade. In the WGR sample preparation procedure used in this work, extraction by Soxhlet removed most low molecular weight molecules, which explains this observation. The first degradation step is therefore attributed to EPDM, and its onset may be slightly shifted depending on EPDM composition, higher quantities of ethylene being known to degrade at slightly higher temperatures, which may also be related to crystallinity of higher ethylene compositions. [41]

Quantification of EPDM, carbon black and inorganics for WGR are reported in Table 2.5. The main difference as compared to standard EPDM samples is the presence of an important residual mass. This residual mass (varying from 19 to 23 w/w %) fits, within experimental error, with the sum of $CaCO_3$, ZnO, SiO_2 and Al_2O_3 as determined from calcination prior to ICP-EOS and flame spectrometry measurements, as reported in Table 2.3.

Table 2.4 TGA Degradation Temperatures and Relative Mass Loss Percentages for Standard samples

	Onset $T_{degr\ 1,}$ °C	Mid-point $T_{degr\ 1,}$ °C	1st Mass Loss, w/w %	EPDM Used, w/w % *	Onset $T_{degr\ 2,}$ °C	Mid-point $T_{degr\ 2,}$ °C	2nd Mass Loss, w/w %	Carbon Black Used, w/w %	Residual Mass, w/w %	ZnO + SiO_2 Used, w/w %
0CB	300	475	98	95	-	-	-	0	2	5
30CB	248	462	68	74	556	658	28	22	4	4
50CB	247	457	62	65	551	699	35	32	3	3
60CB	249	468	62	61	563	673	32	36	6	3
70CB	214	463	60	57	556	684	38	40	2	3
100CB	-	-	-	0	565	771	100	100	0	0
50 CB+G	215	444	58	55	597	654	26	27	16	18
CD53-2	300	461	92	95	-	-	-	0	8	5
CD53-6	285	453	97	95	-	-	-	0	3	5
CD53-9	282	446	93	95	-	-	-	0	7	5
CD53-14	294	461	92	95	-	-	-	0	8	5
CD71-1	275	451	95	95	-	-	-	0	5	5
CD71-4	283	445	92	95	-	-	-	0	8	5
CD71-7	280	454	93	95	-	-	-	0	7	5
CD71-8	280	457	92	95	-	-	-	0	8	5
CD71-11	300	459	93	95	-	-	-	0	7	5

It has been reported that the presence of cross-links[42] and higher percentages of ethylene in the polymer[41] can increase thermal stability of EPDM. The effect of cross-links was therefore verified using standard samples, in the hope of determining whether this technique could be used to provide information on cross-link density in commercial WGR samples, instead of having to rely on the time-consuming swelling technique. An enlargement of the degradation curves of standard samples with varying cross-link densities is presented in Figure 2.2D. In the 350 to 400 °C range, samples with higher cross-link densities showed higher degradation. Plots of mass loss between 350 and 400 °C were therefore drawn with respect to cross-link density. In all cases, a linear relationship appeared to exist, and the best correlation coefficient was found at 400 °C, as reported in Figure 2.3A for standard and WGR samples. However, for the samples studied, three different linear relationships were observed. For the WGR rubber samples and for the standard samples containing an E/P ratio of 53/47, degradation

Table 2.5 TGA Degradation Temperatures and Relative Mass Loss Percentage for WGR Samples

Sample	Onset $T_{degr\ 1,}$ °C	Midpoint $T_{degr\ 1,}$ °C	1st Mass Loss, w/w %	Onset $T_{degr\ 2,}$ °C	Midpoint $T_{degr\ 2,}$ °C	2nd Mass Loss, w/w %	Residual Mass, w/w %
WGR-A	296	363	37	584	631	43	20
WGR-B	287	360	37	580	627	44	19
WGR-C	321	383	36	589	648	43	21
WGR-D	320	394	35	580	634	42	23

decreased with increasing cross-link density, as observed previously by Gamlin et al.[41] Curves were parallel, and for a given cross-link density, degradation is lower for WGR samples (resulting in a smaller y-intercept). In order to verify whether this could be due to the presence of carbon black, as samples prepared with varying cross-link densities did not contain any, degradation at 400 °C is plotted as a function of carbon black content for

standard samples containing either no carbon black or carbon black in the range expected for commercial WGR samples. As seen in Figure 2.3B, degradation is constant, within experimental error, for carbon black percentages from 30 to 70 % carbon, but when carbon black is absent, a significant decrease in degradation occurs. Therefore, the presence of carbon black could explain the observed difference in behaviour between WGR samples and standard samples with a 53/47 E/P ratio.

The third curve, for samples with a higher percentage of ethylene (E/P ratio of 71/29), without carbon black, is very different from the first two. The absolute value of the slope is smaller, the relative degradation at low cross-link density, as expression by the y-intercept of the curve, is also smaller, and the sign of the slope has changed, indicating that degradation is increasing instead of decreasing with increasing cross-link density. This clearly indicates that the degradation behaviour is not controlled by the same factor in this case, as will be discussed later in this article. TGA may therefore be useful to investigate the cross-link density of EPDM WGR samples. It will however be essential to prepare calibration curves from samples with similar ethylene proportion and carbon black content, and this estimation should be considered semi-quantitative due to the effect of the variations in ethylene content on thermal degradation. Nevertheless, this method is faster and less time-consuming than the

a)

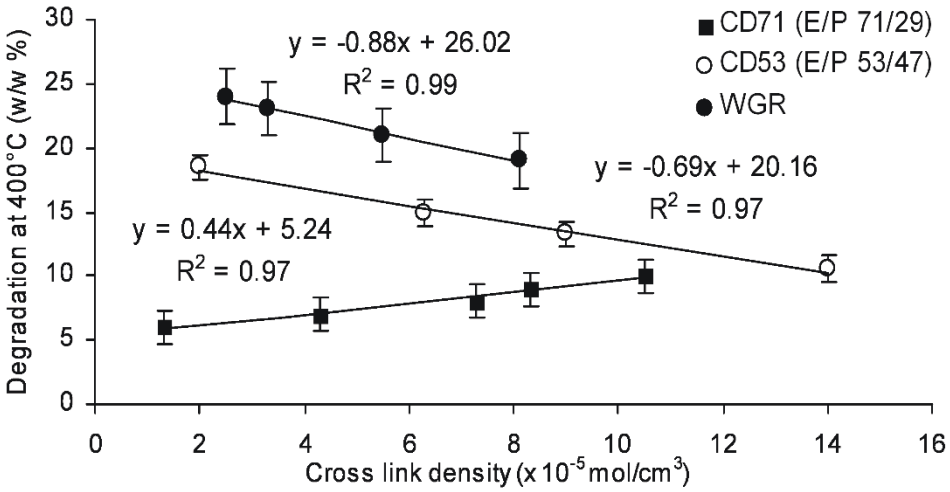

b)

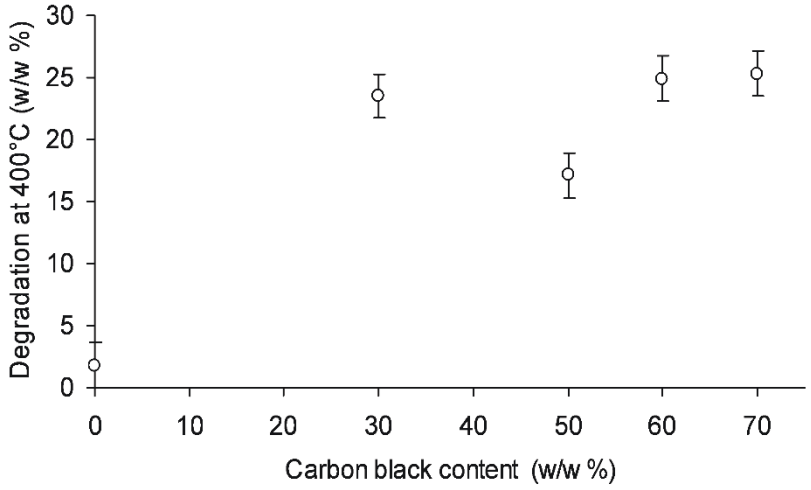

Fig. 2.3 TGA degradation at 400 °C A) for standard EPDM samples having two different E/P ratios and for WGR samples as a function of cross-link density; B) for standard E/P 53/47 samples as a function of carbon black content (CB series)

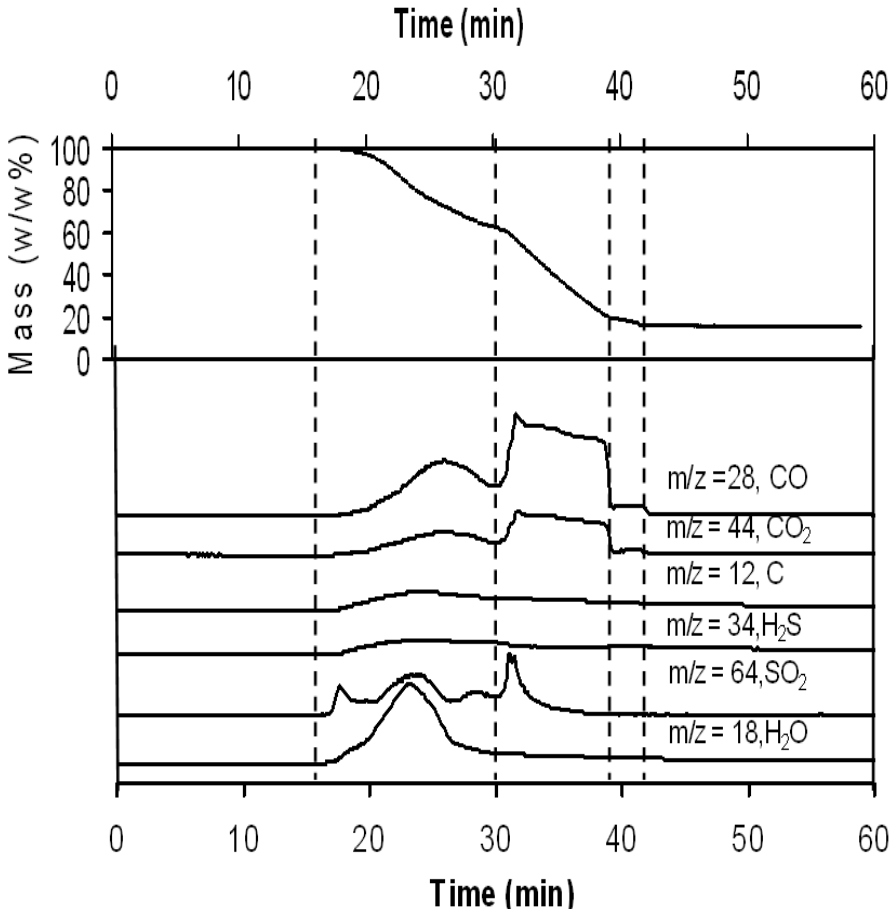

Fig. 2.4 TGA-MS results for a typical EPDM waste ground rubber (WGR-D)

standard swelling measurements, especially for WGR samples, and could be useful for in-house quality control.

In order to determine why EPDM resistance to thermal degradation varies with cross-link density, analysis of gas evolving during the thermal degradation of the polymers were studied by TGA-MS. A typical plot of the most important fragments detected is shown in Figure 2.4. As seen in this figure, the first important masses detected were of m/z = 64, corresponding to the onset of SO_2 loss, therefore indicating that sulfur bridges are most probably among the first groups to be thermally degraded, in agreement with the expected lower bond energy for S-S bonds.[43-45] Loss of SO_2 occurs as a series of more or less sharp peaks, spanning the complete temperature range for EPDM degradation, indicating that a series of positions may be attacked successively, possibly due to the length of sulfur bridges (2, 3, 4 or more atoms).

Since SO_2 is the first gas to evolve, it can be proposed that cross-links are first attacked by oxygen, providing a temporary protection to polymer chains themselves, perhaps by limiting its diffusion.

Water is lost by the samples almost simultaneously, but evolves on a shorter temperature scale. This may indicate that the mechanism for SO_2 formation involves attack of the hydrogen atoms on the polymer chain next to the sulfur bridge. This is followed by the detection of CO_2 and CO, indicating that degradation of the polymer chains is occurring. After 30 minutes (around 600 °C), a second peak appears for CO_2 and CO, which corresponds to oxidation of carbon black. As the quantity of CO_2 increases sharply at this time, a last sharp SO_2 peak is observed, in agreement with the presence of sulfur within the carbon black, this sulfur being less accessible to oxygen than the sulfur present in cross-links, due to a lower oxygen permeability of carbon black as compared to EPDM rubber. Sulfur in carbon black will therefore degrade mostly once carbon black itself starts to degrade.

These observations explain the observed correlation between mass loss and cross-link density at 400 °C in TGA. In this region, degradation is related to the preferential attack of sulfur bridges, and is therefore proportional to the number of cross-links and/or their availability to oxygen through diffusion in samples. The fact that degradation can be higher or lower with increasing cross-link density is attributed to changes in oxygen diffusion, which will be affected by two main factors: cross-link density itself and crystallinity, which both decrease oxygen diffusion. When crystallinity is high, such as in the case of the CD71 samples, crystallinity dominates diffusion, and degradation is small at low cross-link density (the y-intercept of the curve is small), as seen in Figure 2.3A. Crystallinity is constant for CD71 samples (which will be confirmed by DSC data reported in the following section), and as diffusion is crystallinity-controlled, an increase in cross-link density does not change noticeably oxygen diffusion, but will result in an increase in available C-S and S-S bonds, and therefore as cross-link density increases, so does the mass loss or percentage of degradation. The slope of the degradation curve is therefore positive.

When crystallinity is low (WGR) or absent (CD53), and when cross-link density is small, oxygen diffusion is more rapid, resulting in higher degradation (and in a high value of the y-intercept). As cross-link density increases, diffusion speed decreases due to these cross-links,

and so does degradation, oxygen being less available in spite of the presence of more S-S bonds in the sample. The slope of the degradation curve is now negative.

The increase in degradation in presence of carbon black, as noted in Figure 2.3A, could be likewise related to a higher porosity and therefore higher oxygen diffusion in carbon black-containing rubbers. It is not related to degradation of sulfur found within carbon black, as this only becomes accessible to oxygen and mostly degrades when carbon black itself degrades, at a much higher temperature (around 550 °C), and therefore does not cause significant errors in the estimation of the cross-link density, contrarily to total sulfur concentrations, as measured by elemental analysis, and which were found not to correlate to cross-link density. The choice of temperature is important: if a lower temperature is chosen, degradation may not affect all cross-links. On the other hand, when the temperature is too high, polymer chains degrade and emit CO_2 or CO, thus contributing to the observed percentage of mass loss, and linearity between mass percentage and cross-link density is lost. Peroxide-cured EPDM, which have not been studied in the present work, has chemically different cross-links and may therefore not present the same tendency.

Thermogravimetric techniques offer the advantage of being sensitive to cross-links, carbon black and metals in completely different temperature ranges, and therefore evaluation of each can be made without interference, which is a definite asset in the case of commercial rubber products, which often have complex formulations.

2.3.4 Thermal Analysis by Differential Scanning Calorimetry

Two different phenomena are mainly studied in DSC, glass and melt transitions. The glass transition temperature (T_g) is correlated to chain mobility and therefore is affected by cross-link density.[85] However, in the case of EPDM, T_g is also strongly affected by changes in the ethylene content.[81,86] The melt endotherm, on the other hand, is characterized by the melt temperature T_m and the melt enthalpy ΔH_m, which is related to crystallinity and is mainly a function of EPDM comonomer composition.[81] Therefore, DSC could yield qualitative information on both cross-link density and relative amount of ethylene in the EPDM polymer used, and is therefore potentially complementary to TGA. This is of particular interest in the

case of WGR samples, as FTIR spectra that are taken by reflection mode are of poor quality, and as NMR measurements do not allow to measure the quantity of ethylene due to peak enlargements, as mentioned earlier.

In the present work, erasing any prior thermal history is necessary prior to analyzing the samples, since processing conditions, which are different from sample to sample, affect EPDM crystallinity. Only the second heating scan, for which changes in melt transitions reflect structural differences alone, is reported and discussed here. WGR sample endotherms are reported in Figure 2.5. The same transitions were observed for all standard samples, in the presence or not of carbon black (see Supplementary material for endotherms). The first transition, observed near -40 °C, is a change in heat capacity corresponding to the glass transition. For WGR, and for standard samples with higher E/P ratios, this transition is followed by an exothermic peak which is attributed to the melting transition of ethylene crystals when high enough concentrations (typically above 50 w/w %) of ethylene are present. This endotherm is typically broad, due to variations in the ethylene distribution. [87]

The melt transition will be discussed first, as it is known to mainly be a function of the ethylene to propylene (E/P) ratio, whereas T_g may depend on both this ratio and cross-link density. When present (standard samples with a E/P ratio of 53/47 showed no noticeable melt transition), the melting point can be characterized by the melting temperature, reported as midpoint in Table 2.6 and by the area under the peak, corresponding to the melting enthalpy. A further difficulty is the fact that the baseline for standard samples is not straight, as can be seen in Figure 2.5, and therefore it is difficult to determine at which positions to measure the melt enthalpy, in the present case, values of -30 °C to 60 °C were chosen, as these yielded enthalpy values comparable to those reported by Ver Strate and Wilchinsky[48]. Peak position changes slightly, but as the width of the transition is very large, this change is not significant. Of more interest are the changes in melt enthalpy. For comparison purposes, melt enthalpy per gram of polymer is also reported for WGR samples, in order to remove the effect of carbon black and inorganic fillers present. An estimation of the E/P composition of WGR samples can be obtained by comparing the observed melt enthalpies to those reported by Ver Strate and Wilchinsky.[68] Values observed in the present study correspond to those of samples having an E/P ratio of 66/34. This estimation is however semi-quantitative, as shown by the comparison with results reported by Ver Strate and Wilchinsky in Table 2.6, since

percentages of norbornene and possibly cross-link density also affect, although to a lesser degree, the melt enthalpy.

A)

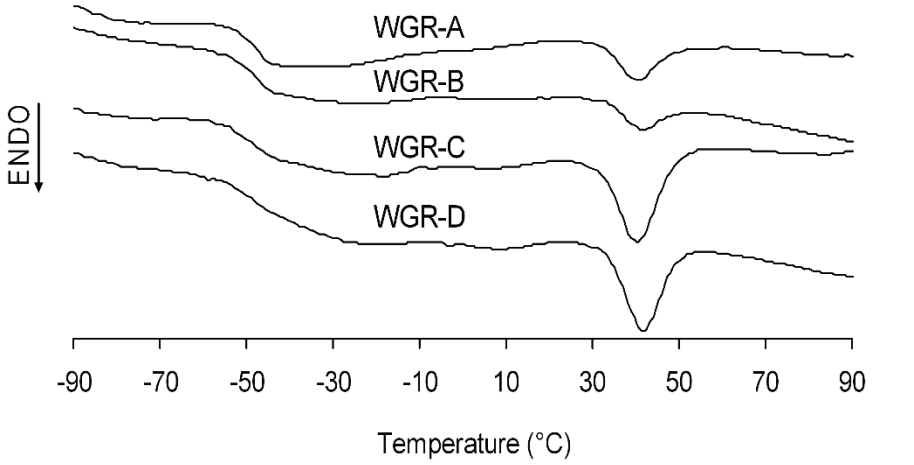

B)

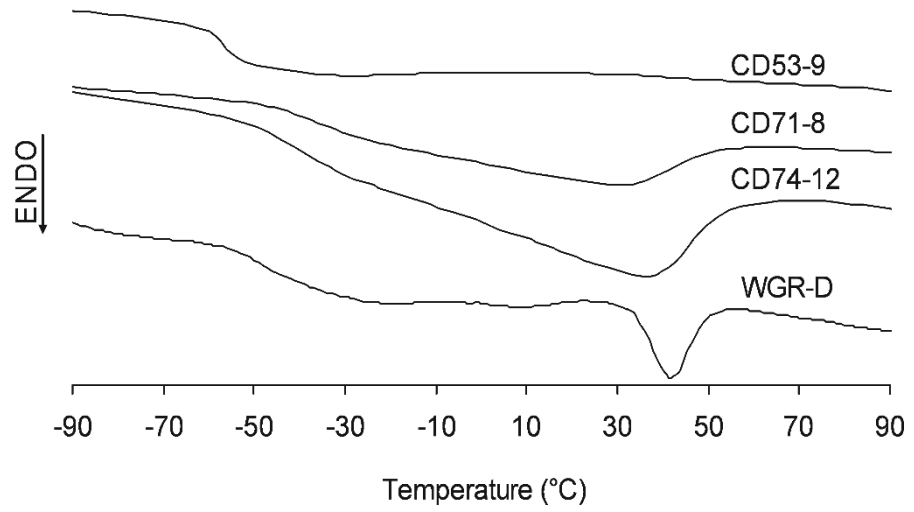

Fig. 2.5 Differential scanning calorimetry endotherms of selected samples: a) comparison of WGR samples; b) comparison between a representative WGR sample and standard EPDM samples with varying E/P ratios

Table 2.6 Characteristics of the Melting Peak Observed in EPDM WGR Samples During the Second DSC Scan

Sample	Midpoint T_m,°C	ΔH_m, J/g	ΔH_m, J/g of polymer[a]	ΔH_m (Ver Strate and Wilchinsky[48], same E/P ratio), J/g
CD71-1	32	17	16.7	
CD71-4	32	16	16	
CD71-7	31	16	16	16
CD71-8	33	16	16	
CD71-11	30	16	16	
CD74-12	38	20	20	20
WGR-A	40	1.1	3	-
WGR-B	41	0.6	2	-
WGR-C	42	1.6	5	-
WGR-D	42	2.2	7	-

[a] As calculated using the percentage of polymer in the samples as determined by TGA measurements

Glass transition temperatures were compared next. These appear in Table 2.7, which also reports glass transition width and cross-link density. Glass transition can vary with many factors, as it is a function not of chain regularity, such as in the case of crystallinity, but of long-range movements, which are affected by flexibility of the repeat unit or units found in the rubber chains, as well as cross-links and physical constraints such as those imposed by the crystal phase or by particles acting as reinforcement.[88]

For standard samples prepared with the 53/47 EPDM prepolymer and varying quantities of cross-linking agent (S_2Cl_2), and therefore with varying cross-link density, as observed in Table 2.7, no notable changes in T_g were observed, indicating that cross-linking has little or

Table 2.7 DSC-Determined Tg Values and Cross-Link Density ρ for Standard and WGR Samples

Sample	T_g		T_g Width	ρ , 10^{-5} mol/cm^3
	Onset, °C	Midpoint, °C	$T_g^{endpoint}$-T_g^{onset}, °C	
EPDM standard samples (E/P 53/47) with carbon black				
0CB	-56	-52	7	37
30CB	-57	-52	8	31
50CB	-56	-52	7	50
60CB	-57	-53	7	59
70CB	-56	-53	6	35
50CB+G	-56	-52	8	54
EPDM standard samples (E/P 53/47, 71/29 and 74/26) without carbon black				
CD53-14	-56	-50	12	14
CD53-9	-61	-55	11	8.6
CD53-6	-61	-55	11	6.3
CD-2	-55	-51	8	1.7
CD71-1	-46	-38	18	1.3
CD71-4	-47	-38	19	4.3
CD71-7	-47	-39	18	7.3
CD71-8	-47	-39	21	8.3
CD71-11	-47	-39	21	10.5
CD74-12	-50	-42	19	12
WGR Samples				
WGR-A	-53	-48	9	3.3
WGR-B	-50	-46	7	2.5
WGR-C	-50	-46	8	5.5
WGR-D	-56	-47	19	8.1

no effect on the glass transition of EPDM in the cross-link density range studied here, which corresponded to that observed for the WGR samples. This may be related to the low cross-link densities observed for these samples, and highly cross-linked samples may behave differently. Changes in carbon black concentrations were also investigated, and these could cause physical constraint and affect T_g. As seen in Table 2.7, again, no noticeable changes were found with changes in the ratio of carbon black. This clearly indicates that, for this rubber and this carbon black source, for up to 70 w/w % carbon black and in the cross-link density range studied, cross-link density and presence of carbon black will only affect marginally T_g.

Bhattacharjee et al. showed that T_g varies with EPDM composition, more specifically with ethylene content and, to a lower degree, with ethylene norbornene (ENB) content.[81] For WGR samples, as seen in Figure 2.5 and reported in Table 2.7, random variations of up to 5 °C for onset and midpoint T_g were observed for the same E/P composition (E/P 53/47), therefore indicating that estimation of EPDM composition using T_g cannot be very precise. Nevertheless, midpoint T_g values from -60 to -40 °C have been reported with increasing ethylene composition.[81,86] An approximate estimation of the E/P ratio using DSC could be very useful as this technique is readily available and rapid, and as more classical techniques to determine this parameter, such as NMR and FTIR, show severe limitations for WGR samples, as discussed previously.

Using data reported by Batthacharee et al.[81] for rubber having an ethylene norbornene (ENB) composition of 5 w/w %, the commercial WGR samples should have ethylene proportions of 63 to 68 w/w %, in agreement with the conclusions from melt enthalpy comparison (66 %). Changes in T_g are within random fluctuations noted for standard samples, and therefore it is not possible, in this specific case, to ascertain whether changes in E/P ratio occur from one WGR sample to another using DSC. More noteworthy are changes in width of the glass transition, which can be quantified by noting the difference between onset and endpoint T_g, as reported in Table 2.6. In this case, most samples have widths of 7 to 9 ºC, whereas the sample having the largest particle size, and which was found to contain significant quantities of aluminum, WGR-D, exhibits a width of 19 ºC. This considerable increase in width is an indication that this sample is more heterogeneous in terms of EPDM composition and/or cross-link density.

Therefore, DSC shows promising potential as a semi-quantitative method to estimate:

1) Relative E/P ratios, by comparing glass transition, relative melting point and melt enthalpy, and

2) Sample homogeneity, by comparing glass transition width.

2.4 Conclusions

Various techniques were used to perform characterization of two different types of EPDM samples. The first type consists of standard EPDM samples prepared in our laboratory with varying cross-link densities and carbon black contents, as well as a sample contained both carbon black and glass. The content of these samples was known and controlled. The second type of samples consists of industrial WGR which were used to validate the usefulness on representative industrial samples. As their chemical composition was unknown, chemical analyses were performed by atomic absorption spectrometry (Si), ICP-OES (Al, Ca, Cd, Cr, Cu, Fe, Mg, Mn, Na, Ni, P, Ti, Zn) and elemental analysis (S). This information was used to better understand the results of thermogravimetric analysis, differential scanning calorimetry and solid-state proton NMR measurements.

NMR results were disappointing in the case of WGR as the presence of paramagnetic elements and possibly magnetic impurities causes important interferences and limited its usefulness, confirming the importance of testing the methods on real industrial samples.

Thermogravimetry is already used to measure carbon black and fillers (ash or residuals) for quality control of rubbers (ASTM D6370), and is also effective for WGR samples. More surprisingly, it was shown that it can be used to determine the cross-link density of EPDM through measurement of mass loss at 400 °C on samples from which small organic molecules had previously been extracted by Soxhlet. TGA-MS was used to explore what was happening at this temperature, and it was shown that degradation of cross-links occurs, resulting in emission of H_2S and SO_2. This technique can be used semi-quantitatively to compare vulcanized EPDM rubber samples of any shape, providing calibration curves for the appropriate E/P ratios have been established, changes in carbon black content do not affect results (except at no or very low carbon black content), and measurement of powdered

samples (such as WGR) is not problematic. This can provide a cost-effective and rapid method for quality control of WGR from vulcanized EPDM rubber.

Finally, DSC was shown to provide complementary information on the E/P ratio (relative melting point and melt enthalpy), although quantification was not performed in the present work. This observation could lead to its use for quality control of WGR, which are difficult to measure by infrared spectroscopy techniques (transmission and reflection) due to the presence of carbon black and other fillers, and for which this information cannot be retrieved easily by NMR due to peak broadening in the presence of paramagnetic species (Ca, Al) present in typical industrial samples.

2.5 Acknowledgements

The authors wish to acknowledge the financial support of the Natural Sciences and Engineering Research Council of Canada (NSERC). One of the authors (H. Liang) benefitted from a scholarship from the Chinese Scholarship Council, and thankfully acknowledges this support. Lion Copolymer Inc. is also thanked for providing EPDM prepolymers used in this work. The assistance of R. Plesu (TGA), P. Audet (solid-state NMR) and S. Groleau (GC ICP-OES) from the Department of chemistry, Université Laval, A. Macsiniuc (advice on sample preparation) and G. P. Assima (TGA-MS) from the Department of chemical engineering, Université Laval, is also gratefully acknowledged.

Chapter 3: Characterization of Recycled Styrene Butadiene Rubber Ground Tire Rubber: Combining X-Ray fluorescence, Differential Scanning Calorimetry and Dynamical Thermal Analysis for Quality Control

Huan Liang, Denis Rodrigue and Josée Brisson, Journal of Applied Polymer Science, published online 132, 42692 (2015). DOI: 10.1002/app.42692

Résumé

L’évaluation des principales techniques de caractérisation des caoutchoucs a été exécutée pour le caoutchouc butadiène-styrène (SBR) sur des échantillons de SBR standards ainsi que sur des échantillons de pneus de caoutchouc broyés recyclés (GTR) obtenus à partir d’une installation de recyclage de pneus industriels, et contenant un mélange de SBR et de caoutchouc naturel. Le but du travail était de fournir des informations supplémentaires pertinentes pour le contrôle de qualité dans le domaine du recyclage des caoutchoucs. Des valeurs de références pour les échantillons industriels ont été obtenues par la spectrométrie d'émission plasma à couplage inductif optique, par spectrométrie d’absorption atomique, par résonance magnétique nucléaire du proton en phase solide et par analyse (CHNS) élémentaire. Il a été démontré que la spectrométrie de fluorescence des rayons X est rapide et quantitative pour déterminer le contenu en zinc dans un contexte industriel. L'analyse thermogravimétrique, déjà utilisée pour déterminer la quantité de noir de carbone et de matériaux inorganiques dans des caoutchoucs et des GTR, est recommandé pour la détermination des rapports massiques de monomères pour le SBR ne contenant pas d’autres caoutchoucs, mais pas pour les GTR. Les mesures de transition vitreuse par calorimétrie différentielle à balayage (DSC) montrent que les changements de valeurs de température de transition vitreuse sont affectés par le ratio de monomère, et donc, la DSC peut être utilisée pour détecter des changements de composition en caoutchouc d’un lot à l’autre. Ces résultats montrent que la DSC et des techniques de caractérisation de spectroscopie de fluorescence des rayons X peuvent être utilisés pour caractériser les GTR et peuvent mener à des procédures de contrôle de qualité plus précises et rapides de ces échantillons complexes.

Abstract

Appraisal of the main rubber characterization techniques for styrene butadiene rubber (SBR) was performed on standard SBR samples as well as recycled ground tire rubber (GTR) from an industrial tire recycling facility, containing a blend of SBR and natural rubber. The aim of the work was to provide additional information relevant to quality control in the field of rubber recycling. Benchmark characterization of industrial samples by inductively coupled plasma optical emission spectrometry, atomic absorption spectrometry, solid-state proton nuclear magnetic resonance, and elemental (CHNS) analysis are reported. X-ray fluorescence spectrometry is shown to be rapid and quantitative for determining the zinc content in an industrial context. Thermogravimetric analysis, already used to determine carbon black and inorganic material content in rubbers and GTR, is recommended for determination of monomer weight ratios of SBR sources not containing other rubbers, but not for GTR. Differential scanning calorimetry (DSC) measurements of the glass-transition show that changes in monomer ratio affect glass-transition temperature values, and therefore, DSC can be used to detect changes in rubber composition from batch to batch. These results show that DSC and X-ray fluorescence spectroscopy characterization techniques can be used for GTR and may lead to more thorough and rapid quality control procedures of these complex samples.

3.1 Introduction

The increasing number of cars worldwide results in an increase in used tires. Their storage causes environmental and safety problems, while reprocessing and reuse of these tires in an economically viable way constitutes an important challenge.[33]

In 2003, it was estimated that around 290 million scrap tires were generated in the USA alone.[1] The tire sole accounts for about a half of each car tire, and is a blend of 10 to 40 % styrene butadiene rubber (SBR) with natural rubber (mainly composed of polyisoprene units). Depending on their use (all-season, all-terrain, high performance, snow, mud, SUV, truck, etc.) and manufacturer, various polymer compositions and additives are found in tires: sulfur is added for vulcanization, zinc oxide (ZnO) is added for activation, silica and calcium carbonates are used as fillers, etc.[5] In addition, reinforcement (steel bead wire, thermoplastic or natural polymer cord, etc.) are also imbedded in the rubber sole.

During the recycling process, tires are ground into a coarse powder, resulting in ground tire rubber (GTR). Magnets separate steel wires from the rubber, and both materials are recycled separately. Rubber powder is used to make rubber mats and other rubber-based articles, and can be incorporated in asphalt used for road pavement. Rubber powder can also be added to different materials to improve impact resistance and durability or for noise reduction.[89]

To be commercially viable, the GTR industry must deliver a product which meets quality standards, a task made difficult due to the wide range of tire composition and additives. Intrinsic characteristics of rubbers (no melt point, no solubility), batch-to-batch and within-batch variations also make quality control of GTR challenging.

Thermogravimetric analysis (TGA) is routinely used for compositional analysis and quantification of carbon black and ash content of GTR (ASTM D6370-99 and E1131-08). Crumb size and size distribution are measured by optical microscopy, although the latter is time-consuming and rarely reported. Cross-link density is measured by swelling experiments, although the small crumb size presents an additional challenge.[58] These methods provide partial characterization, but do not always correlate well with observed changes in crumb behavior during use. Determination of the monomer ratio which directly impacts on thermal and mechanical properties of rubbers is performed by pyrolysis-gas chromatography (ASTM

D3452), but cannot always distinguish between SBR samples with different monomer contents.[90] The refractive index method (ASTM D5775) proposed for compositional analysis of polymers is not useful for GTR due to the presence of carbon black and to the impossibility of making a homogeneous film.

It was decided, in this work, to use both standard SBR samples and real GTR samples from a recycling facility. The latter being ill characterized, benchmark values for elemental content and monomer ratio are first obtained using solid-state proton nuclear magnetic resonance (NMR). This technique has previously been used for ground rubber samples,[91-95] but is not amenable to routine quality-control measurements and, as shown in earlier work, can be difficult to implement for GTR due to the presence of magnetic impurities (metal residues).[96] Elemental content benchmark values are more straightforward to obtain, and a combination of readily available techniques (inductively coupled plasma optical emission spectrometry (ICP-OES), atomic absorption spectrometry (AAS), and elemental (CHNS) analysis) is used to provide a thorough characterization of samples, although these suffer from time-consuming sample preparation and are not ideal in the context of industrial rubber recycling quality control.

Thermogravimetric analysis (TGA) has been suggested as a means to obtain information on the butadiene/styrene (B/S) ratio of SBR. Shield and Ghebremeskel[97] showed that SBR content is related to shifts of the thermal degradation peaks, but these shifts can also be affected by the distribution of styrene in the copolymers (random or block) and by the diene microstructure. Castaldi and Kwon[69] performed TGA in air atmosphere and found an interesting phenomenon for neat SBR: a two-stage combustion was attributed to different oxidation rates of the butadiene backbone and styrene aromatic rings. This technique was therefore selected for further evaluation in the context of industrial quality control.

For elemental analysis, X-ray fluorescence (XRF) has recently been used to analyze various polymers. Fink *et al.*[98] and Mans *et al.*[99] investigated thermoplastics recycled from electronics enclosures (acrylonitrile butadiene styrene, polystyrene, styrene-butadiene, polyphenylene oxide and polyvinyl chloride) with this method, whereas Miskolczi *et al*.[100] Proposed its use for inorganic compositional analysis in compressed crumb rubber samples. Tertian and Claisse,[101] on the other hand, proposed a sample preparation method based on

compression with a cellulose binder, resulting in self-standing disks which can be kept as standard samples for further use. This method was also selected for further evaluation.

The present article therefore focuses on GTR characterization in terms of metal and atomic content by X-ray fluorescence and monomer composition by thermogravimetric analysis (TA) and differential scanning calorimetry (DSC).[73,102,103] Analyses reported include two types of samples. First, standard SBR samples of known composition were prepared in our laboratory and used to ascertain the potential and precision of each technique. Second, five tire sole GTR samples were obtained from a recycling facility and analyzed to provide samples more relevant to the real challenges faced in this field, and to determine to what extent the presence of numerous additives and heterogeneity from various types of tires affect characterization.

3.2 Experimental

3.2.1 Commercial GTR Samples GTR-A to GTR-E

Commercial SBR samples were provided by Recyclage Granutech Inc. (Plessisville, Qc., Canada). Samples were collected randomly from five different batches, designated by the abbreviations GTR-A to GTR-E. Selected samples all having an average particle size of 500 ± 10 μm were used. Cross-link density and particle size distributions were reported in a previous article.[58] Prior to measurements, all GTR samples were submitted to acetone extraction to remove low molecular weight molecules such as processing oils or organic additives.

3.2.2 Preparation of SBR Standard Rubber Samples (9CD to 40CD, 0CB to 100CB and 50CB+G)

In a 100 mL beaker with a magnetic bar, 2 g of a SBR pre-copolymer (PLF1502, containing a B/S monomer weight ratio of 76/24, kindly supplied by the Goodyear Tire & Rubber Co.) was dissolved in 20 mL toluene, heated to 60 °C to facilitate dissolution, and stirred until fully dissolved. In a 50 mL Erlenmeyer were introduced 10 mg tetramethylthiuram disulfide (TMDS), 40 mg stearic acid dissolved in 1 mL toluene, and 100 mg ZnO. This accelerator

solution was heated at 50 °C until complete dissolution was achieved, and was then added to the SBR solution, after which active carbon black (CC N991, Cancarb Limited Inc., Canada)

Table 3.1 Amounts Used for Standard SBR sample Preparation: Proportions of all Components

Component	Mass used (g)	Composition (phr)
SBR	2	100
Stearic acid	0.04	2
TMTD	0.01	0.5
ZnO	0.1	5
S_2Cl_2	0.04 to 0.2	2 to 10
Carbon black	0.00 to 1.4	0 to 70
Milled glass fibers	0.00 and 0.55	0 and 28

was added (from 0.60 to 1.40 g, corresponding to 30 to 70 parts per hundred of rubber or phr). Finally, an aliquot of the cross-linking agent corresponding to 0.05 to 2 phr of a 1.0 mL S_2Cl_2 solution in 10 mL toluene was added using a syringe. Carbon black (1.00 g) was added last, while stirring. The resulting mixture was poured rapidly into stainless steel molds previously sprayed with PEI 35838 ORAPI Northern-Cape silicon releasing agent (15 x 15 cm^2 plates having four 0.2 cm deep, 4 cm wide depressions). Solutions were allowed to dry in the molds for around two hours at room temperature in a hood. Once dry, films were removed from the mold, which was cleaned using ethyl acetate. Mold surfaces were then treated with the silicon releasing agent, and rubber samples were reinserted in the mold, covered with a silicon-treated plate, and placed for 30 minutes in a Carver press preheated to 180 °C.

Exact quantities of each component used during standard sample preparation are reported in Table 3.1-3.3, along with the abbreviations used in this work. Two types of standard samples

were prepared to evaluate the effect of different compositional changes. The first series is composed of standard samples containing 50 % carbon black and having the same B/S monomer ratio, but having varying cross-link densities. These are abbreviated YCD, where CD stands for cross-link density and Y is the numerical value of the sample cross-link density (ρ). A series of samples with varying proportions of carbon black was also prepared, with as constant as possible cross-link densities. These are abbreviated ZCB, where CB refers to the presence of carbon black and Z to the amount (w/w %) added to the sample with respect to SBR. In one of these samples, 50CB+G, '+G' indicates the addition of milled glass fibers (731ED, fiber diameter 10 μm, Owens Corning, USA). This sample was added to investigate

Table 3.2 Amount Used for Standard SBR Samples Preparation: Amount of Cross-link Agent S_2Cl_2 and Final Measured Cross-link Density for Samples with Constant Carbon Black Content but Varying Cross-link Density

Samples	Mass of S_2Cl_2 used (g)	Cross-link density (mol/cm^3)
CD-9	0.04	8.5
CD-11	0.08	11.2
CD-25	0.12	25.0
CD-29	0.16	29.4
CD-40	0.20	39.9

Table 3.3 Amount Used for Standard SBR Samples Preparation: Carbon Black and Milled Glass Fiber Amount Used in the Preparation of Samples with Constant Cross-link Density, within Experimental Error, But Varying Carbon Black Content (YCB)

Samples	Mass of carbon black used (g)	Mass of milled glass fibers used (g)	Composition of carbon black (phr)	Composition of milled glass fiber (phr)	Percentage of carbon black in samples (%)	Percentage of milled glass fiber in samples (%)
0CB	0	-	0	-	0	-
30CB	0.60	-	30	-	22	-
50CB	1	-	50	-	32	-
60CB	1.2	-	60	-	36	-
70CB	1.4	-	70	-	40	-
100CB	-	-	-	-	100	-
50CB+G	1	0.55	50	28	27	15

the effect of silica on various rubber measurements (glass transition, thermal resistance, NMR spectra, etc.), as preliminary observations showed the presence of silica in GTR. This is consistent with Michelin's proprietary silica blends used in tires to lower rolling resistance.

3.2.3 Cross-link Density Measurements

Cross-link density (ρ) of the rubber standards was measured by using ASTM D3616 swelling method, slightly modified to take into account sample size. For standard rubbers, samples (1 mm x 5 mm) were cut from rubber films, weighted accurately and submerged in toluene. These were allowed to swell for 72 hours at room temperature, protected from light. After 72 hours, excess solvent was removed using a pipette without touching the swollen gel pieces. Each gel piece was then lightly dabbed with absorbent paper and immediately weighted accurately. For commercial GTR samples, measurements were performed using a modified version of ASTM D6814 as described by Macsiniuc *et al.*[58].

3.2.4 Atomic Absorption Spectrometry (AAS)

Around 50 mg of each sample was placed in a porcelain crucible and calcined at 650 °C for 2 hours in a muffle oven, after which the temperature was raised to 700 °C and held overnight. Residues were quantitatively transferred to a plastic volumetric vial and dissolved in 1 mL hydrofluoric acid. Deionized water (HPLC grade, Milli-Q) was added to bring the volume to 50 mL. Five to 100 ppm standard solutions were prepared by dilution from an assurance grade standard silicon solution (10,000 mg/L in H_2O /4.0 % F^- purchased from Spex CertiPrep Inc.). A Perkin Elmer 3110 atomic absorption spectrometer was used with a nitrous oxide (35 mL/min)-acetylene (43 mL/min) flame at the 251.6 nm spectral line position, optimized according to the manufacturer's recommendations.

3.2.5 Inductively Coupled Plasma Optical Emission Spectrometry (ICP-OES).

Inductively coupled plasma optical emission spectrometry (ICP-OES) (Optima 3000, Perkin Elmer) was performed using a radio frequency power of 1300 W, and gas flows of 15 L/min for plasma, 0.5 L/min for the auxiliary gas, 0.8 L/min for the nebulizer, and 1.5 mL/min for the mobile phase. Sample calcination was performed as reported for AAS. Solutions were prepared by adding deionized water (HPLC grade, Milli-Q) and 10 mL nitric acid (ACS grade, Caledon Laboratories Ltd) to solubilize the resulting solid to a final volume of 100 mL.

3.2.6 CHNS Elemental Analysis

CHNS elemental analysis was performed on an organic elemental analyzer (Flash 2000, Thermo Scientific). Cystine, used as a standard sample, was put in a universal soft tin container (100pc, outside diameter = 5 mm, height = 8 mm, volume = 157 μL), which also served as a blank sample. Around 0.5 mg of each sample was encapsulated in the same type of container.

3.2.7 Differential Scanning Calorimetry (DSC)

Differential scanning calorimetry (DSC) was performed using a DSC823e (Mettler Toledo) apparatus with a liquid nitrogen cooling accessory. Approximately 15 mg of sample was encapsulated in an aluminum pan, and DSC measurements were performed by heating from

–100 °C to 100 °C at 20 °C/min under a nitrogen atmosphere, holding the sample at this temperature for 5 minutes and then cooling back to -100 °C at 20 °C/min. A second heating scan was then performed under the same conditions, and is the one reported in all cases.

3.2.8 Solid-state ^{1}H Nuclear Magnetic Resonance (NMR)

Solid-state ^{1}H NMR spectra of SBR samples were recorded on a 400 MHz solid-state NMR spectrometer (Bruker Biospin Ltd). Standard samples were cut into small pieces prior to introduction in sample tubes, whereas GTR samples were used as is. Each sample was packed in a 4 mm tube and spun at 8 kHz at the magic angle with scan time varying from 60 to 240s.

3.2.9 Thermogravimetric Analysis (TGA)

Thermogravimetric analysis (TGA) was performed using a TGA/SDTA 851e (Mettler Toledo) apparatus. Between 1 and 2 mg of sample was put in a ceramic pan, and measurements were performed by heating from 50 °C to 900 °C at 20 °C/min under air atmosphere.

3.2.10 Energy Dispersive X-Ray Fluorescence Spectrometry (XRF)

Energy dispersive X-ray fluorescence spectroscopy (XRF) was performed using a Minipal 4 benchtop X-ray fluorescence spectrometer (PAN Analytical) apparatus equipped with a rhodium anode tube, five tube filters, a helium purge capability and a silicon drift detector, running at a maximum of 30 kV and 1 mA. The calibration curve was obtained by measuring disks prepared using different quantities of sample GTR-A, dispersed in 0.5 g of cellulose, the final Zn concentration varying from 20 to 70 w/w %. The additional four GTR samples (GTR-B to GTR-E) were also dispersed in 0.5 g cellulose to yield samples with concentrations around 30 %, 55 % and 64 %, which were used to verify if the method was robust when GTR composition variations occur. All samples were placed in a Carver Press at 10,000 psi for 30 s to form self-standing disks having a diameter of 3 cm and a thickness of approximately 4.5 mm.

3.3 Results and Discussion

3.3.1 Chemical Analysis

Chemical analysis of GTR by inductively coupled plasma optical emission spectrometry (ICP-OES), atomic absorption spectrometry (AAS) and CHNS elemental analysis.

One of the first measurements undertaken in the present work aims at determining benchmark atomic composition for randomly selected industrial GTR samples, as these are then used to validate the methods used and to identify specific problems related to the presence of additives or to their granulometry. For this purpose, chemical analysis was performed using ICP-OES, AAS and CHNS elemental analysis. ICP-OES and AAS are useful to quantify metals and silica present, whereas CHNS analysis is used to determine the amount of sulfur. Results are reported in Table 3.4.

ICP-OES results show that the most abundant metal found in GTR samples is zinc, with concentrations varying from 1.97 to 2.23 w/w %. This is consistent with the use of ZnO as a catalyst/accelerator.[83] No correlation was found between Zn content and cross-link density, unfortunately but predictably, since ZnO is used as an accelerator and is not part of the cross-links themselves.

Iron is also found in small quantities, which is attributed to the presence of residues from the steel wires removed in the recycling facility. Sodium and calcium are also present in small quantities: these are added as salts such as $Na_2P_2O_7$ and $CaCO_3$ during tire fabrication. Other metals are not present above the detection limit of the method.

AAS is used to measure silicon, as silica is often incorporated in tires to decrease rolling resistance. A small, almost constant percentage of silicon (from 0.72 to 0.85 w/w % of SiO_2)

Table 3.4 Concentration (w/w %) of Metals in GTR as Determined by ICP-OES, of Si (expressed as SiO_2) by AAS and of S by CHNS Analysis

	Standard dev.	Detection Limit	GTR-A	GTR-B	GTR-C	GTR-D	GTR-E	Literature values
Residual mass[a]	1	-	8	7	6	8	5	-
Residual mass[b]	3	-	7	9	4	5	3	-
Al	0.02	0.04	0.00	0.00	0.00	0.00	0.00	0.21[104]
Ca	0.07	0.02	0.17	0.17	0.30	0.19	0.19	0.1[104]
Cd	-	0.01	0.00	0.00	0.00	0.00	0.00	-
Cr	-	0.01	0.00	0.00	0.00	0.00	0.00	-
Cu	-	0.01	0.00	0.00	0.00	0.00	0.00	-
Fe	-	0.01	0.16	0.30	0.05	0.25	0.00	0.28[104]
Mg	-	0.01	0.00	0.00	0.00	0.00	0.00	0.84[104]
Mn	-	0.01	0.00	0.00	0.00	0.00	0.00	-
Na	-	0.01	0.22	0.25	0.05	0.22	0.05	-
Ni	-	0.01	0.00	0.00	0.00	0.00	0.00	-
Zn	0.2	0.04	2.2	2.0	2.0	2.0	2.2	1.5[105]
$CaCO_3$, ZnO, Fe_2O_3, SiO_2	0.02	-	4.15	4.12	4.10	4.09	4.08	-
SiO_2	0.02	0.03	0.72	0.79	0.78	0.80	0.85	0.6[104]
S	0.1	0.001	1.2	1.7	1.3	1.6	1.5	1.1[105]

[a] As determined from calcinations prior to spectrometry measurements

[b] As determined from TGA analysis (see later section)

is present. CHNS analysis is finally used to determine the amount of sulfur, which is present in concentrations ranging from 1.2 to 1.7 w/w %. Sulfur forms cross-linking bonds created during vulcanization, so the possibility of gaining information on cross-link density from sulfur content was attractive. In a similar study, no correlation was found between cross-link density and sulfur content in EPDM-based GTR.[96] Likewise, it is not possible to quantitatively correlate cross-link density to the quantity of sulfur present in GTR samples in the present work, which may stem from the existence of more than one sulfur sources in the samples, as sulfur can also be present in carbon black. Another possible explanation is that individual cross-links are known to contain varying numbers of successive sulfur. The quantity of sulfur found was found to be relatively constant between 1.2 and 1.7 w/w %. The observed sulfur concentration is in agreement with results of Amari et al. who reported that typical SBR scrap tires were composed of 1.1 % of sulfur.[105] The sample having the highest cross-link density was the one with the lowest sulfur content, whereas if the sole source of sulfur was cross-links, and if the same number of sulfur atoms was found in each cross-link, this sample would have the lowest cross-link density. In order to compare with TGA results which are presented in the following section, Table II also includes the sum of calcium, iron, zinc and silicon expressed as their oxide forms ($CaCO_3$, Fe_2O_3, ZnO and SiO_2).

3.3.2 Energy Dispersive X-Ray Fluorescence Spectrometry (XRF)

XRF can be used for elemental analysis of elements with atomic number above 11. As it can be performed on solid samples, this technique is highly attractive for both qualitative and quantitative measurements in the industry, and it is used intensively by the mining industry instead of inductively coupled plasma mass spectrometry or atomic absorption spectrometry (AAS), which require labor-intensive and time-consuming sample digestion. XRF has been proposed as a fast and non-destructive tool to quantify rubber and GTR, [98,100, 101,106,107] but its use is not widespread, which may in part be related to variations caused by granulometry and sample surface in this technique. It has been used on vulcanized styrene copolymers,[108] recycled thermoplastics from electronic waste,[98] as well as waste ground rubber tire.[100] The latter study showed very interesting results, with differences between XRF and ICP-OES below 8 %. It was therefore decided to investigate this technique in the present work to verify if the results would be as good with different GTR sources.

Samples for XRF analysis were initially prepared as proposed by Miskolczi *et al.*[100] by hand pressing of the GTR powders. Initial trials with this technique resulted in brittle samples which could not be kept easily for further measurements or as control samples, and standard deviations were found to be very high. This was attributed to poor compactness and high heterogeneity, due to the granulometry of GTR. The use of a cellulose binder was tested next, following the work of Tertian on powdered samples.[101] This method also allows disk conservation for subsequent recalibration, which is useful for quality control. Standard SBR films were grinded and used to establish a calibration curve, but results were inconsistent with those of GTR samples, due to differences in powder granulometry, morphology and composition. Instead, a single GTR sample selected at random (GTR-A) was used to build a calibration curve by varying the mass of GTR used to form the disks.

A typical qualitative fluorescence diagram of such a sample, using GTR-A, is given in Figure 3.1, where it is compared with the spectrum of neat GTR (held in a sample cup with a polyethylene terephthalate film bottom). Dilution decreases peak intensity by a factor of approximately two, but each of the observable peaks remains clear and well defined. The most intense peaks correspond to zinc, iron and, to a lesser extent, bromine. Only the zinc peak presents an intensity large enough for quantitative analysis.

Figure 3.2 reports the calibration curve of the Zn Kα peak intensity as a function of Zn content (determined by ICP-OES) in cellulose-based disk specimens prepared by varying the quantity of GTR. The measureable upper concentration is limited by the quantity of GTR that can be included in a disk. A maximum of 70 w/w % GTR can be placed in a disk, which results in a linearity limit of 1.6 w/w % in the GTR powder. Higher Zn content in a disk leads to elastic specimens which are difficult to press into firm, self-standing. The calibration curve shows a good linear relationship between intensity and Zn content, especially considering the inherent inhomogeneity of GTR samples. Limit of detection and of quantification are 0.8 and 1.1 w/w % Zn in a GTR sample.

It must be noted that, in Figure 4.2, the disk concentration is used, and not the concentration in the initial GTR sample, as varying quantities of GTR-A were used to achieve this calibration curve. The use of this calibration curve must therefore be followed by a correction for the dilution factor.

The disk concentration obtained from the calibration curve, Zn_{DISK}, is first transformed into concentration in the GTR sample, Zn_{XRF}. This operation is straightforward, as following Equation 3.1:

$$Zn_{XRF} = Zn_{DISK} \times (m_{GTR} + m_{cellulose}) / m_{GTR} \quad (3.1)$$

where m_{GTR} and $m_{cellulose}$ are the masses of the GTR sample and cellulose in the disk, respectively.

In order to verify if a curve obtained with a single standard sample can be used to determine correctly the zinc content of GTR samples having different compositions, GTR-B to GTR-E were then measured using three different GTR disk concentrations, and resulting measurements are presented in Figure 3.2. These data points generally lie close to the calibration curve, although they are not distributed randomly but tend to lie above the curve, indicating a possible systematic error, which is however in the range of the estimated standard deviation.

Table 3.5 reports Zn concentrations calculated from the calibration curve of in Figure 3.2 (Zn_{XRF}) and compares these to the values obtained from ICP-OES. Detailed ICP-OES and XRF data are reported in Supplementary Material. In all cases, the error is smaller than the error estimated with a 95 % probability using Student's t-test. Relative errors obtained when compared to Zn_{ICP} ICP-OES measurements vary from 4 to 14 %, which shows that both methods are in good agreement.

The correlation observed in Figure 3.2, combined with the good fit of GTR samples using their ICP-OES determined zinc percentages, confirms that the use of a single standard to build the calibration curve is effective in eliminating matrix effects and allows determination of zinc content with absolute values.

It is concluded that X-ray fluorescence spectrometry is a non-destructive, fast and affordable technique for elemental determination of Zn in SBR-based GTR samples. Although this method shows a lower precision and higher detection limit than ICP-OES, due to its low maintenance, low cost, and low time requirement for sample preparation, it is a very attractive method for quality control in the industry.

a)

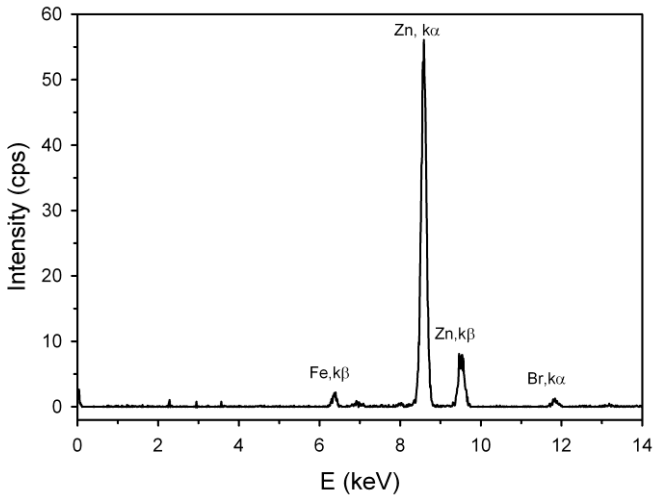

b)

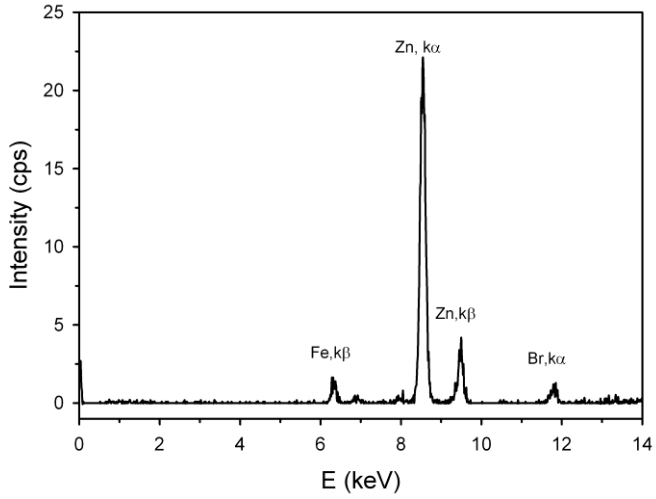

Fig. 3.1 X-Ray Fluorescence Spectra for a Representative GTR Sample (GTR-A) A) GTR Sample without Binder B) GTR-A Disk with Cellulose Binder (55 w/w % GTR)

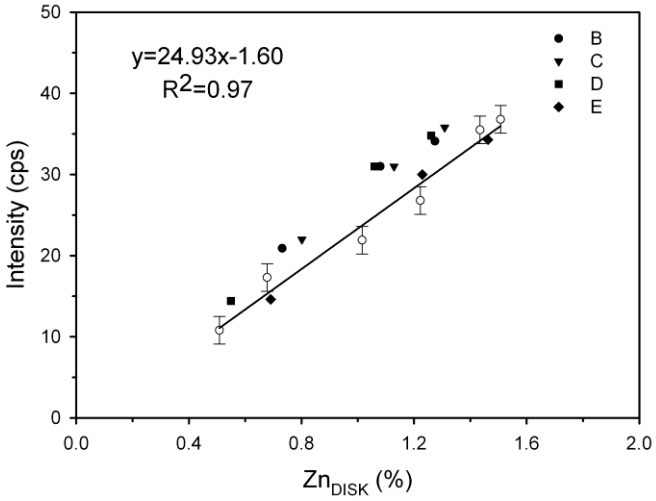

Fig. 3.2 Calibration Curve of Zn Using XRF (GTR-A Contents in Cellulose Disk Samples between 20 and 70 w/w %) as a Function of Zn Concentration in the Disk

The next aspect that will be discussed is the relative proportion of styrene and butadiene, as well as the possible presence of other polymers in the GTR samples. This will be investigated using NMR, TGA and DSC in the following section

Table 3.5 Zn Concentration as Determined from the XRF Calibration Curve and Compared with ICP-OES Results for GTR-B to E

GTR sample	Experimental XRF data			Zinc percentages as calculated by XRF					Comparison with ICP-OES results		
	mw (g)	mc (g)	I (cps)	Zn in disk ZnDISK (w/w %)	Zn in GTR ZnXRF (w/w %)	Average Zn in GTR ZnXRF (w/w %)	Standard deviation (w/w %)	Error with 95% confidence (± %)	ZnICP (%)	ZnICP - ZnXRF (w/w %)	Relative error (%)
	0.2957	0.5088	20.9	0.77	2.11						
GTR-B	0.6015	0.5070	31.0	1.18	2.17	2.10	0.07	0.18	1.99	0.11	5
	0.8985	0.5045	34.1	1.30	2.04						
	0.3234	0.4998	22.0	0.82	2.08						
GTR-C	0.6248	0.5040	31.0	1.18	2.13	2.12	0.03	0.08	2.04	0.08	4
	0.9073	0.5070	35.8	1.37	2.14						
	0.2115	0.5465	14.4	0.51	1.84						
GTR-D	0.5861	0.5035	31.0	1.18	2.19	2.04	0.18	0.45	1.97	0.07	4
	0.8962	0.5038	34.8	1.33	2.08						
	0.2454	0.5325	14.6	0.52	1.65						
GTR-E	0.6547	0.5117	30.0	1.14	2.03	1.88	0.20	0.5	2.19	0.31	14
	1.0245	0.5090	34.3	1.31	1.96						

3.3.3 Solid-State NMR Investigation of Monomer Ratio

Solid-state NMR spectroscopy is extremely powerful to investigate the chemical structure of insoluble material, but unfortunately, due to the high cost of the instrument and of its maintenance, solid-state NMR is not easily available to recycling facilities. Nevertheless, in the present work, it has been used to further characterize the samples. For standard SBR samples of known (B/S) monomer ratio, this will provide a confirmation that NMR-determined values are quantitative in the conditions used, whereas for industrial GTR samples of unknown composition, this will provide benchmark values of allylic (mainly butadiene from SBR and isoprene) versus aromatic (styrene), (B+I)/S, monomer ratios, as isoprene from natural rubber is also found in these samples.

Figure 3.3 reports NMR spectra of representative samples studied in this work. GTR samples have much higher peak width than SBR standard samples, which is attributed to the presence of residual paramagnetic iron in GTR samples,[96] causing an increase in T_2.[93] Due to this peak broadening, it is not possible to ascertain the relative proportions of different microstructural features for GTR samples. Three main peak regions can be seen in the spectra: a peak centered around 7.0 ppm, attributed to styrene aromatic ring protons, peaks between 5.0 to 5.2 ppm attributed to hydrogen atoms on butadiene double bonds that have not been opened by the vulcanization process, and finally, around 1.5-2.5 ppm, peaks associated to methyl and methylene groups. The main difference which can be noted between standard SBR and GTR spectra is the very low intensity of the styrene peak at 7.0 ppm for GTR samples (an enlargement of this peak region can be found in Supplementary material, Figure A2). This small intensity is in agreement with the use, in rubber tire soles, of a mixture of SBR and natural rubber, thus decreasing the styrene content. This, combined to peak broadening, results in the low intensity of the 7 ppm styrene peak for GTR samples.

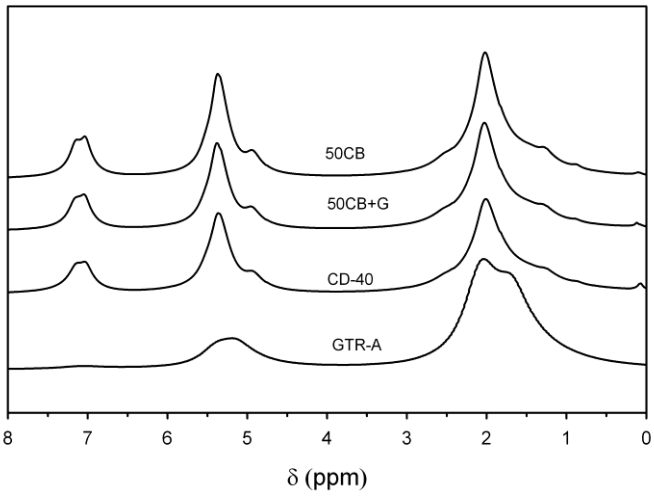

Fig. 3.3 Solid-state ^{1}H NMR Spectra of Representative Samples

In the 5 ppm region, two main peaks are observed: the main intensity peak at 5.2 ppm, which corresponds to -CH=CH- protons of 1,4 butadiene segments and a much smaller peak around 4.9 ppm which is attributed to CH_2=C- groups.[109] The relative intensity of this peak is much smaller as compared to the peaks in the 1-2 ppm region, indicating a lower quantity of double bonds, related to a smaller quantity of SBR due to blending with natural rubber and possibly other aliphatic rubbers.

Aliphatic protons are observed in the last region of NMR spectra. For SBR, the highest peak is observed at 2.1 ppm, attributed to aliphatic CH_2 groups, although smaller peaks appear from 0.9 to 2.7 ppm, corresponding to microstructural variations. On the other hand, in GTR samples, two peaks of similar intensities are clearly present at 1.8 and 2.1 ppm, assigned respectively to CH_3 and CH_2 aliphatic groups. Whereas CH_2 group can be associated to the presence of styrene, butadiene or other aliphatic rubbers, the peak at 1.8 ppm, attributed to methyl groups, is in agreement with the presence of an important amount of polyisoprene, of which natural rubber is composed. Relative intensities are similar to that observed in natural rubber, although the CH_2 peak is more prominent, as expected from the presence of SBR.[67,110]

Relative NMR peak intensities were used to ascertain the relative proportion of styrene. To do this, it was supposed that all polymers are composed of styrene and aliphatic rubbers (mainly butadiene and isoprene). The monomer ratio is calculated as following Equation 3.2:

$$(B+I)/S = \frac{5(I_5 + (I_2 - 3I_7/5))}{6I_7} \quad (3.2)$$

where I_5 the intensity of the peak at 5.0-5.2 ppm, corresponding to CH allyl hydrogen atoms of aliphatic rubbers; I_2 the intensity of the peaks between 1 and 3 ppm and centered around 2 ppm, which correspond to CH_3, CH_2 and CH groups of all rubbers present, and from which the styrene aliphatic proton are removed using the $3I_7/5$ term; I_7 is the intensity of the peak at 7 ppm, attributed to aromatic styrene protons. The 5/6 term is used to take into account the number of protons of each chemical group (5 for styrene, 6 for butadiene), which supposes that butadiene represents the largest proportion of aliphatic rubbers in the GTR samples and that it is only composed of 1,4 units. This evaluation is therefore semi-quantitative, and includes the following approximations:

1) Allylic protons which are transformed into aliphatic protons upon cross-linking are negligible as compared to those remaining,

2) Butadiene is composed only of 1,4 linkages, a reasonnable approximation for SBR prepared by emulsion polymerization which is known to contain less 1,2-linked units than solution SBR obtained by anionic polymerization,

3) Butadiene and isoprene both have the same number of protons per chemical unit, and the same distribution of allylic and aliphatic protons.

Results are reported in Table 3.6, and although this approach is semi-quantititative, a good fit is observed between the B/S weight ratio supplied by the manufacturer for the initial non-cross-linked SBR matrix (76/24) and the (B+I)/S value determined by NMR for the standard SBR samples, which is equivalent to B/S in the absence of isoprene in these samples, and which varies from 78/22 to 74/26, with an observed standard deviation of 2 %.

Proportions of aliphatic rubber and styrene (B+I)/S in GTR samples are also reported in Table 3.6, and these show values of 94/6 to 99/1, with a standard deviation of 3 %. Calculations

Table 3.6 Butadiene/Styrene (B/S) Proportion Calculations from NMR Data

Sample	(B+I)/S NMR	B/S data from manufacturer	Cross-link density ($x10^{-5}$ mol/cm^3) ± 1
GTR-A	99/1 ± 3	-	96
GTR-B	98/2 ± 3	-	13
GTR-C	95/5 ± 3	-	10
GTR-D	94/6 ± 3	-	9
GTR-E	94/6 ± 3	-	8
0CB	78/22 ± 2	76/24	13
30CB	74/26 ± 2	76/24	16
50CB	77/23 ± 2	76/24	25
60CB	78/22 ± 2	76/24	20
70CB	77/23 ± 2	76/24	23
50CB+G	77/23 ± 2	76/24	16

were also performed using a different approximation, by supposing that all aliphatic and allylic protons belonged to isoprene units instead of butadiene units, with little effect on the resulting percentages, due to the low intensity of the aromatic proton peak of styrene. The observed values correspond to the presence of only 2 w/w % styrene. This is lower that percentages found in pure SBR, which normally vary from 10 to 40 w/w % styrene, as expected since tire sole are composed of blends of SBR, natural rubber and polybutadiene.[33] Further, as discussed earlier, NMR results show that that large amounts of polyisoprene are

present. Polybutadiene, when present, will further decrease the (B+I)/S ratio, and the quantity present could not be determined in this case due to the above mentioned peak broadening.

Surprisingly, although samples were taken in five different lots, all GTR samples show the same (B+I)/S ratio, within the standard deviation of the method. NMR is therefore not precise enough, in the present case, to study changes in (B+I)/S ratio between these samples. More importantly, as all industrial samples showed similar values of (B+I)/S ratio, this indicates that monomer ratio may not be a critical parameter for GTR within a given recycling facility, depending on the tire source used. Nevertheless, using the NMR-determined benchmark (B+I)/S ratios, the possibility of using TGA for both carbon black and B/S or (B+I)/S ratio determination will be discussed next, as combining both characterizations in a single step could decrease the time needed for quality control.

3.3.4 Thermogravimetric Analysis

Thermogravimetric analysis (TGA) is used for routine carbon black and fillers (inorganics) present in rubbers, as described in ASTM D6370-99 and E1131-08. It has also been proposed for semi-quantitative estimation of cross-link density in EPDM GTR samples in a previous article[96]. Furthermore, as discussed in the introduction, Castaldi and Kwon[69] have previously observed a two-stage combustion attributed to different oxidation rates of butadiene and styrene in SBR. It was therefore decided to verify in the present work if this phenomenon could be used to investigate, quantitatively or semi-quantitatively, the monomer ratio in GTR samples.

In the present work, a series of SBR standard samples with varying proportions of carbon black and similar cross-link densities was prepared and investigated using TGA under air atmosphere. The corresponding degradation curves are shown in Figure 3.4A. The decomposition process is clearly divided in three stages, which start at 350, 450 and 550 °C, respectively. The number of degradation steps is different from that observed for EPDM samples discussed in a previous article,[96] for which two main degradation steps are observed: a first step at 400 °C, corresponding to the degradation of the rubber organic phase, and a second step, at 550 °C, corresponding to the oxidation of carbon residues formed in the first step, as well as carbon black initially present in samples, to carbon dioxide. Sulfur present in

A)

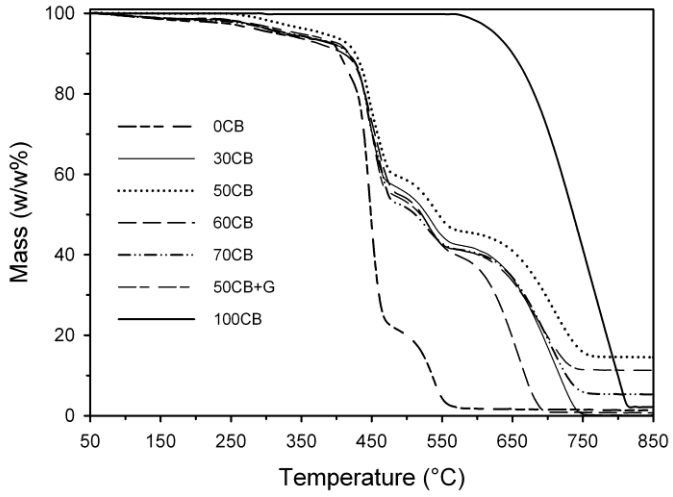

B)

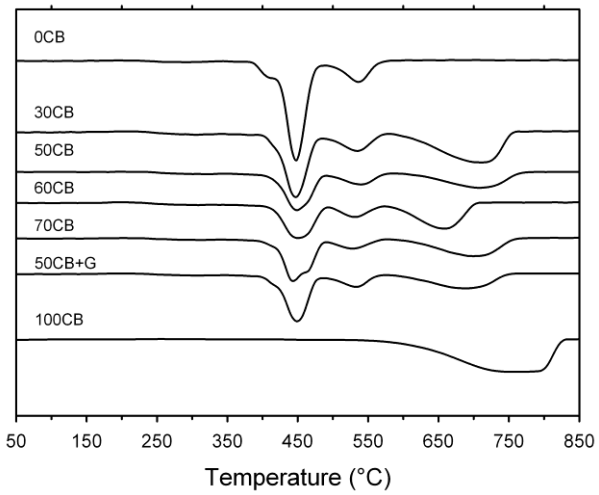

Fig. 3.4 TGA of Standard SBR Samples with Different Carbon Black Contents

A) Degradation Scans; B) 1st Derivatives of a Typical Scan.

cross-links has previously been shown to degrade near 400 °C, whereas sulfur present in carbon black degrades at higher temperatures (around 550 °C), both yielding SO_2.[96]

The occurrence of an additional weight loss step is normally associated with multiple mechanisms that are dominant at certain temperatures or reaction times.[111] This is typically observed for samples containing more than one type of compound, or when an important difference in thermal resistance exists between some of the compounds. In SBR, the first degradation step around 350-440 °C is attributed to butadiene units and possibly to aliphatic carbon atoms of styrene units. The second step, between 450 and 540 °C, is associated to the combustion of the remaining styrene benzene rings, which require a higher activation energy to oxidize.[69] The third step, starting around 550 °C, is similar for most rubbers and organic materials, and is related, as in the case of EPDM-based waste ground rubber, to the combustion of carbon to form carbon dioxide.[70,73] As reported in Figure 3.4A, degradation of the standard SBR samples containing no carbon black (sample 0CB) is mostly complete upon reaching a temperature of 600 °C, and the third degradation step can be used to determine directly the quantity of carbon black in the initial samples. Calculating the first derivatives, shown in Figure 3.4B, allows a straightforward and unambiguous evaluation of degradation temperatures in each step.

Above 750 °C, the curves do not reach zero due to remaining minerals such as ZnO. This residual mass is often designated as the ash content, or residual minerals. Mass percentages corresponding to the sum of the two first peaks for SBR, the second peak for carbon black and the last peak for residual minerals are reported in Table 3.6. These values are used to estimate the amount of carbon black and of residues. It must be noted that the sum of SBR, ZnO and SiO_2 percentages used to prepare the samples do not total 100 % due to the small quantity of stearic acid used, which is not taken into account in the calculation, and to S_2Cl_2, part of which evaporates and oxidizes to SO_2 during cross-linking. A good fit is observed, as

A)

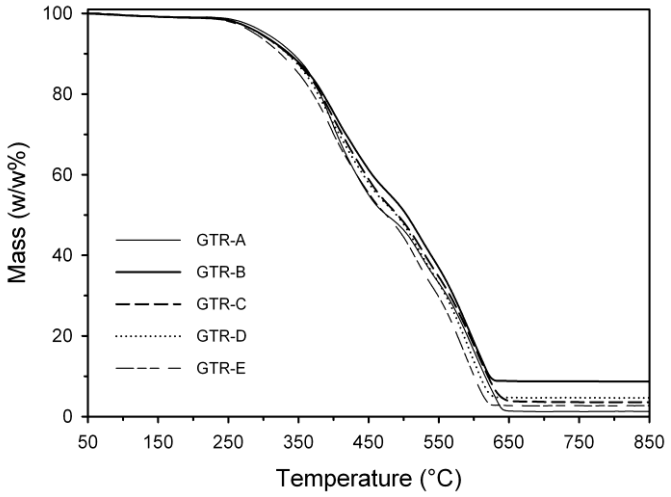

B)

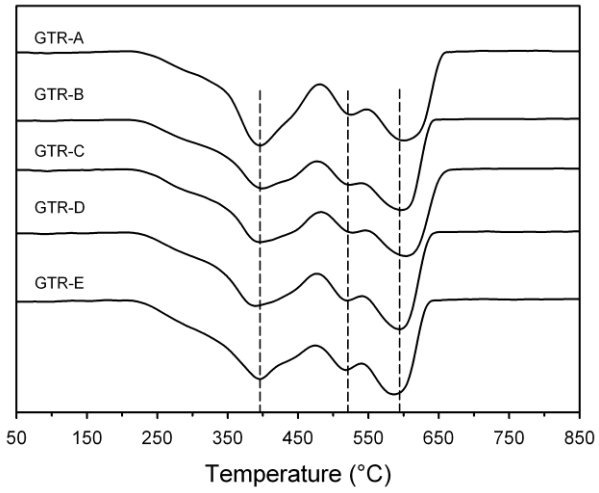

Fig. 3.5 TGA Temperature Scans for GTR Samples.

A) Degradation Curves B) 1st Derivatives

expected, between the percentage of carbon black used to prepare standard samples and third TGA mass loss. Residual mass percentages also fit, within experimental error, with the

quantity of inorganic substances (ZnO and SiO_2), used to prepare the standard samples, as these do not degrade in temperature range tested. This accounts for 2-5 w/w % of mass loss, with the exception of sample 50CB+G which contains milled glass, and therefore shows a much higher residual percentage of 18 w/w %.

It was attempted to determine the relative composition of styrene and butadiene by using the second peak to account for aromatic rings in styrene thermal degradation, thus allowing calculation of the weight percentage of styrene S as following Equation 3.3:

$$S\ (w/w\%) = \frac{2nd\ mass\ loss\ (w/w\%)}{77/104} \tag{3.3}$$

where the second mass loss is measured by thermogravimetry between 500 and 550 °C and is mainly attributed to the degradation of styrene units, and 77/104 corresponds to the molar mass ratio of the benzene ring in the styrene repeating unit.

The first peak, related to the degradation of aliphatic groups, is taken as the sum of aliphatic rubbers (butadiene, isoprene or other aliphatic rubber units) and of the aliphatic backbone of styrene, and is therefore used to approximate the quantity of aliphatic rubbers (B+I) w/w % as Equation 3.4:

$$(B+I)(w/w\%) = 1st\ mass\ loss\ (w/w\%) - \ S\,(w/w\%) \times \ 27/104 \tag{3.4}$$

where 27/104 corresponds to the mass ratio of aliphatic groups in the styrene unit. From these two percentages, the (B+I)/S weight ratio, which is equal to the B/S weight ratio for neat

Table 3.7 TGA Degradation Temperatures and Relative Mass Loss Percentages for Standard Samples

	Onset Tdegr 1 (°C)	1st mass loss [i] (w/w %)	1st mass loss [ii] (w/w %)	Onset Tdegr 2 (°C)	2nd mass loss [i] (w/w %)	2nd mass loss [ii] (w/w %)	1st + 2nd mass losses [i] (w/w %)	1st + 2nd mass losses [ii] (w/w %)	SBR used (w/w %)	Onset Tdegr 3 (°C)	3rd mass loss [a] (w/w %)	3rd mass loss [b] (w/w %)	Carbon black used (w/w %)	Residual mass (w/w %)	ZnO + glass used (w/w %)
0CB	346	79	80	491	19	18	98	98	95	-	-	-	-	2	5
30CB	348	64	65	509	16	10	80	75	74	601	15	20	22	5	4
50CB	369	52	52	484	13	11	65	63	65	610	31	33	32	4	3
60CB	358	45	46	496	15	11	60	57	61	571	38	41	36	2	3
70CB	362	47	47	489	11	9	58	56	57	576	37	39	40	5	3
50 CB +G	358	45	46	492	13	11	58	57	55	594	29	30	27	13	18

[a] Using temperatures determined by first derivatives

[b] Using fixed temperature ranges of 500, 550 and 750 °C

SBR, can be calculated and is compared in Table 3.7 to the value supplied by the manufacturer. All samples were prepared with the same prepolymer and therefore have the same B/S ratio. When using fixed temperatures for calculations, a higher B/S or (B+I)/S value for SBR standard samples is obtained from TGA as compared to the manufacturer value, indicating that TGA-determined values using fixed temperatures are not quantitative. On the other hand, for TGA values obtained at temperatures defined by the first derivative, values obtained are slightly higher than NMR-determined values, but correspond within two standard deviations to the supplier value, indicating that TGA can be used to quantify, to a precision of 4 %, the proportion of butadiene and styrene in the rubber chains of standard SBR samples. It can also be noted that the presence of carbon black does not affect these results.

TGA was also performed on the same series of commercial GTR samples for which NMR benchmark (B+I)/S values were measured, as reported in Figure 3.5A. GTR samples have first been submitted to a Soxhlet extraction, as it is known that, below 350 °C, a first mass loss appears in the degradation process of many industrial SBR samples, attributed to the volatilization of processing oil, excess curatives or other organic additives with low boiling-points.[70,74] This first degradation process is therefore absent from the TGA scans reported in the present study. For GTR samples, the same three degradation steps observed in standard SBR samples are present, but they are not as distinct, which may be due to variations in molecular weight, cross-link density and composition of tires used to prepare GTR powders. Three degradation steps can however be clearly distinguished on the first derivative curve in Figure 3.5B. As in the case of standard SBR samples, these curves are used to determine

Table 3.8 Calculation of Butadiene Percentage in SBR Rubber Molecules for Standard Samples also Containing Carbon Black, and for GTR Samples as Determined by NMR and TGA

Samples	Supplier value (w/w %)	TGA (w/w %)				NMR (w/w %)	
		Fixed temperatures (500, 550 and 750 °C)		Positions determined by first derivatives			
0CB		82		80		78	
30CB		82		78		74	
50CB		84		77		77	
60CB	76	80	83 ± 2[a]	76	79 ± 2[a]	78	77 ± 2[a]
70CB		86		81		77	
50CB+G		82		79		77	
GTR-A		82		79		99	
GTR-B		83		73		98	
GTR-C		80		75		95	
	-		81 ± 2[b]		75 ± 3[b]		96 ± 3[b]
GTR-D		79		72		94	
GTR-E		79		73		94	

[a] Average over all CB samples

[b] Average over all GTR samples

the quantity of carbon black, inorganic residuals and, tentatively, (B+I)/S content. Two methods are used to determine the B/S ratio: fixed temperature ranges and temperature ranges determined by first derivatives, which are indicated as dashed lines on Figure 3.4B.

Quantification of GTR samples is reported in Table 3.8. The main difference as compared to standard SBR samples is the higher residual mass, varying from 2.7 to 8.8 w/w % which fits, within experimental error, with the sum of residues as determined from calcination prior to ICP-EOS and AAS measurements, as reported in Table 3.4. These residues are mostly composed of ZnO, $CaCO_3$, SiO_2 and iron oxide (mainly Fe_2O_3).

As in the case of standard SBR samples, TGA is used to estimate the monomer weight ratio, expressed as (B+I)/S, which is reported in Table 3.8. For GTR samples, TGA-obtained values are underestimated by 15 to 21 % for the fixed temperature and first derivative-determined temperatures, respectively, as compared to benchmark NMR–determined values, whereas a standard deviation of 2 to 3 % is calculated from measurements performed on three to five different samples of each GTR. The TGA method clearly overestimates the quantity of styrene present. On one point both methods are in agreement: differences in (B+I)/S ratio between the various GTR samples studied are small.

These results clearly show that no quantitative evaluation can be made using TGA in the case of industrial GTR samples. This is attributed to the loss of definition in the TGA degradation pattern as seen in Figures 3.4 and 3.5: whereas each degradation step was well defined in standard SBR samples, an almost continuous degradation is observed for GTR, as mentioned earlier in this paper. This continuous degradation is related to GTR composition, as an important percentage of natural rubber is present, having a degradation temperature intermediate between those of butadiene and styrene, and therefore causing the observed transition widening. Furthermore, the quantity of styrene in GTR samples is close to the detection limit of this technique, thus contributing to make this method unsuitable for GTR samples. TGA determination of SBR content can therefore be useful for GTR samples made from SBR not mixed with other rubbers (from sources other than tires), but not from tire recycling sources.

In conclusion, for samples composed of SBR, thermogravimetric analysis can be used to determine the content of carbon black and of inorganic additives (as ash content), and can

also be used to estimate the monomer B/S ratio. Unfortunately, due to the limited amount of styrene and to the presence of natural rubber, estimations of the (B+I)/S monomer ratio cannot be made for GTR samples using TGA. The use of TGA to determine the B/S ratio of waste ground SBR from other sources is however proposed, as TGA is already used for determination of carbon black and of inorganic residues, and therefore this may improve quality control measurements without increasing measurement time.

3.3.5 Thermal Analysis by Differential Scanning Calorimetry

Thermal transitions have a direct effect on physical and mechanical properties of polymers, and are easily investigated using differential scanning calorimetry (DSC). The glass transition temperature (T_g) can be affected by many factors including crystallinity, cross-link density, efficiency of vulcanization, composition and microstructure, molecular weight and presence of additives.[112,113] For this reason, standard samples were prepared with controlled cross-link densities and carbon black content, using the same SBR rubber source and therefore having the same B/S monomer ratio.

Table 3.9 reports values for glass transition temperature T_g determined for onset, midpoint and endpoint for standard samples with varying cross-link density (DSC thermograms are available in Supplementary material). All values are very similar, and do not vary by more the experimental error of 1 to 2 °C. Thus, within the cross-link density range used in this work, which corresponds to the range of cross-links found for GTR samples, cross-links do not affect significantly the position of the T_g transition. For samples with different carbon black contents, likewise, variations are very small, of the order of the experimental error.

Table 3.9 DSC-Determined T_g Values and Swelling Measurement Cross-Link Density Results for Standard and GTR Samples

Sample	T_g			T_g width	Cross-link density
	Onset (°C)	Midpoint (°C)	Endpoint (°C)	Endpoint-Onset (°C)	($x10^{-5}$ mol/cm^3)
SBR standard samples – carbon black same concentration of sulfur					
0CB	-54	-49	-45	9	12.5
30CB	-55	-50	-46	9	16.1
50CB	-54	-49	-45	9	25.0
60CB	-54	-49	-45	9	20.2
70CB	-54	-50	-46	8	22.5
50CB+G	-53	-48	-44	9	15.7
SBR standard samples – 50 % carbon black, varying cross-link density					
CD-40	-53	-48	-43	10	39.9
CD -29	-54	-49	-45	9	29.4
CD -25	-54	-49	-45	9	25.0
CD -11	-55	-51	-48	7	11.2
CD -9	-54	-50	-47	7	8.5
GTR					
GTR-A	-61	-54	-48	13	95.8
GTR-B	-61	-54	-49	12	12.7
GTR-C	-61	-54	-50	11	9.6
GTR-D	-61	-54	-49	12	8.5
GTR-E	-61	-54	-49	12	8.2

This indicates that the effect of confinement due to the presence of carbon black, for up to 70 w/w %, on glass transition temperature T_g is negligible. It is concluded that changes in the glass transition temperature of GTR samples would be indicative of a change in GTR monomer composition, although these would be difficult to quantify, due to the rubber microstructure variations.

As compared to T_g values of standard SBR samples, all GTR samples have a T_g lower by 5 °C. Carbon black and cross-link density cannot account for this difference, which is therefore attributed to a difference in (B+I)/S monomer ratio.[112] This is in agreement with the lower quantity of styrene in GTR, as polystyrene has a higher glass transition temperature (95 to 128 °C) than polybutadiene (-103 to -55°C) or natural rubber (*cis*-polyisoprene, -73 to -69 °C).[114] Due to the complex blend of rubbers in GTR, it is not expected that T_g could provide a quantitative evaluation of rubber compositions, but any significant change in rubber composition could be detected by comparing T_g values. All GTR samples have the same T_g value, within experimental error, in agreement with NMR results that no significant change in (B+I)/S monomer ratio was noted for the GTR samples studied.

Although T_g position does not vary from one sample to another, T_g transition width does. For standard samples, the width varies from 7 °C for samples having the lowest cross-link density, to 10 °C for that having the highest cross-link density. GTR samples have slightly higher T_g widths as compared to standard samples, which is attributed to a higher composition heterogeneity. Interestingly, the sample with the highest width, GTR-A, is the one which has the highest cross-link density, thus confirming that the width can provide insights on cross-link density in the range studied. It should however not be used for quantification, as too many factors affect T_g, and as sample inhomogeneity may also lead to T_g width enlargement.

3.4 Conclusions

Investigation of the usefulness of XRF, DSC and TGA for quality control purposes (in addition to the well-established carbon black content determination by TGA) is reported in this article. A thorough investigation of commercial GTR samples and of standard SBR samples was first performed, to provide benchmark values.

XRF was used to quantify zinc in GRT samples. It is found essential to use a real GTR sample to provide a standard curve, due to matrix effects. Compressing the samples into pellets or disks in the presence of cellulose results in good repeatability. This rapid, simple and straightforward technique is therefore recommended in facilities where zinc quantification is an issue.

Thermogravimetry provides reliable semi-quantitative B/S ratios in neat SBR samples, but overestimates the (B+I)/S monomer ratio of GTR samples, which is attributed to the small amount of styrene units present and to the presence of other types of rubbers which degrade in temperature ranges intermediate to those of butadiene and styrene rubber units. It is unfortunately not recommended for this purpose in tire recycling facilities, although it can be recommended for recycled parts in which the only rubber present is SBR. Finally, DSC can be recommended as a complementary source of qualitative quality control, as large changes in (B+I)/S ratio can be identified through variations in the glass transition temperature.

The present work also shows that techniques which are quantitative or semi-quantitative in the case of neat SBR (such as B/S TGA determination) can be of more limited use for SBR-based GTR. Challenges remain in finding rapid techniques for estimation of the cross-link density, and in improving the quantification of the B/S ratio.

3.5 Acknowledgements

The authors wish to acknowledge the financial support of the Natural Sciences and Engineering Research Council of Canada (NSERC). One author (H. Liang) benefitted from a scholarship from the Chinese Scholarship Council, and thankfully acknowledges this support. Goodyear Tire & Rubber Co. and Recyclage Granutech Inc. (Plessisville, Qc., Canada) are also thanked for providing respectively the SBR prepolymers and waste ground rubber used in this work. The assistance of R. Plesu (TGA), P. Audet (solid-state NMR), S. Groleau (AAS and ICP-OES) and J.-M. Hardy (standard sample preparation), from the Department of chemistry, Université Laval, and A. Macsiniuc (advice on sample preparation) from the Department of chemical engineering, Université Laval, is also gratefully acknowledged.

Chapter 4: On the Use of the Thiol-ene Click Reaction to Modify the Surface of Ground Tire Rubber: Grafting of Polystyrene and Characterization of a Modified GTR/Polystyrene Blend

Huan Liang, Jacob Dion Gagné, Adrien Faye, Denis Rodrigue and Josée Brisson, in preparation

Résumé

La réaction chimique click thiol-ène a été utilisée pour greffer des chaînes de polystyrène sur la surface de poudrette de caoutchouc de pneus (GTR). Du polystyrène commercial ayant un bout de chaîne thiolé, PS-SH et ayant une masse molaire de_11 000 g/mol a été utilisé. De la poudrette de pneu industrielle (GTR) à base d'EPDM a été soumise à la réaction click en présence de polystyrène afin d'obtenir du GTR greffé par le PS. Plusieurs techniques de mesure de surface, dont la spectroscopie infrarouge à transformée de Fourier (FTIR) et la spectrométrie de rayons X photoélectronique (XPS) ont été utilisées pour détecter les changements à la surface des échantillons traités. Les caractérisations de surface montrent une augmentation des atomes de carbone aliphatiques et aromatiques par XPS et FTIR, confirmant que le greffage a bien eu lieu. Une augmentation importante du module de tension et de stockage est observée par analyse thermo-mécanique dynamique (DMTA) pour des composites préparées avec le GTR ayant des chaînes de PS greffées et du PS thermoplastique recyclé en comparaison des propriétés de composites GTR-PS sans traitement de surface._De plus, après la modification de surface, les échantillons montrent une résistance thermique légèrement plus grande, ce qui augmente les applications possibles.

Abstract

The thiol-ene click reaction was used to graft polystyrene chains onto the surface of ground tire rubber (GTR). Thiol-terminated commercial polystyrene with 11 000 g/mol molecular weight was used. Industrial ground tire rubber (GTR) was treated with thiol terminated polystyrene using the thiol-ene click reaction, resulting in PS-grafted GTR. Various surface measurement techniques, including Fourier transform infrared spectroscopy (FTIR) and X-ray photoelectron spectrometry (XPS) were used to detect surface changes of treated samples. The surface characterization results show an increase in aliphatic and aromatic carbon atoms both in XPS and FTIR, thus confirming that grafting has taken place. An important increase in tensile and storage moduli is observed from dynamic mechanical thermal analysis (DMTA) for PS-grafted GTR/PS composites as compared to GTR samples or GTR/PS composites. In addition, after surface modification, GTR samples show improved thermal resistance, which increases the possible range of applications.

4.1 Introduction

In the past decades, as is dramatically increasing the car consummation, post-use tires are also discarded in increasing amounts, which leads to severe environmental problems.[49,96] In order to facilitate their recycling, post-use tires are usually ground into powder, named ground tire rubber or GTR, and incorporated in various matrices to recycle them in large scale[115].

Recycling and reuse of tire rubber has become a hot topic in the industry worldwide. Various methods have been investigated to modify ground tire rubber, which can be separated into two classes, physical methods and chemical methods. The physical methods usually employ high energy (gamma)[116] or UV[40] irradiation, plasma[21] or ozone[20] to generate small polar groups on the surface of ground tire rubber powder, increasing the surface polarity to increase interactions with specific polymers such as poly (methyl methacrylate) (PMMA), poly (vinyl chloride) (PVC) or polyacrylamide (PAC). Ultrasonic treatments have also been proposed for devulcanization, leading to the deterioration of cross-links or to changes in composition of ground tire rubber, leading to changes in properties of ground tire rubber[117,118].

Chemical methods reported are more diverse. Colom et al. and Yehia et al. have proposed to chlorinate GTR for use as filler in polyvinyl chloride or high density polyethylene. [25,119] Some groups have used nitric acid and hydrogen peroxide to introduce functional groups onto the surface, then incorporated the resulting GTR to natural rubber and showed that good tensile properties were achieved. [27]

Use of polystyrene as a thermoplastic matrix has the advantage of killing two birds with one stone, as outlets for polystyrene are mainly in the food industry, for which recycled polystyrene is not acceptable. Addition of GTR could improve impact strength of recycled polystyrene, and the resulting material could have a wider range of possible applications, thus opening new markets for recycled polystyrene. However, to get good mechanical properties it is essential that interfacial adhesion occurs between the polystyrene matrix and GTR, and this requires modifications of the GTR or polystyrene. These have already been investigated as introduced following. The most popular way to graft polystyrene onto the ground tire rubber powder is free radical polymerization. In the presence of some initiators,

such as dibenzoyl peroxide (BPO), azobisisobutyronitrile (AIBN) or 2,2,6,6-tetramethylpiperidin-1-yl)oxyl (TEMPO), the styrene can be incorporated by graft polymerization on the surface of ground tire rubber powders. However, the unknown average molecular weight of grafted polystyrene led to uncertain effective chain entanglement in accordance to the research from Ferry[120].

With regard to the ground tire rubbers, they are usually vulcanized by sulfur in the presence of double bonds. Theoretically, it is not all double bonds which were consumed in the vulcanization due to the thiol-ene click reaction in the recent application of polymer and material synthesis were usually reported in the literatures. [121,122] As well, it is an alternative method in the aspect of the surface modification. [123,124] Wu and co-workers found an interesting approach facilitating thiol-ene surface modification with polymers deposited on the polystyrene substrates or polydimethylsiloxane. They used thiol terminated PEG without exact molecular weight to reacted with *ene* groups in the presence of DMPA, which is photo initiator. As a result, it showed that is a success selective surface modification with polyethylene glycol (PEG).[125]

Then thiol-ene click reaction was introduced to modify the ground tire rubbers with the known average molecular weight polystyrene thiol terminated. In this way, the desired molecular weight polystyrene can be grafted onto ground tire rubbers. After treatment, FTIR and X-ray photoelectron spectroscopy (XPS) were used to detect changes on the surface. Thermogravimetric analysis (TGA) and differential scanning calorimetry (DSC) were used to monitor the thermal resistance properties. Composites were prepared by blending with a polystyrene matrix, and mechanical properties, (elongation and storage moduli) were measured in comparison to the initial, non-treated GTR samples and to GTR-PS composites.

4.2 Experimental

4.2.1 Materials

Industrial EPDM-based GTR samples were supplied by Recyclage Granutech inc. (Plessisville, Qc., Canada). Thiol terminated polystyrene (11000 g/mol), 2,2-dimethoxy-2-phenylacetophenone (DMPA), were purchased from Sigma-Aldrich Corporation.

4.2.2 Thiol-ene click reaction

In a round bottom flask was inserted 0.5 g GTR and 30 mL toluene, then was added around 0.1 g DMPA and 0.1 g thiol terminated polystyrene then the resulting mixture was stirred. Dry nitrogen was used to purge the system. The system was next exposed to UV light (40 W, 365 nm) for 48 hours. Resulting treated GTR was filtered and washed three times with toluene during 1 hour to remove unattached polystyrene, then put under vacuum around 60 °C overnight. The resulting PS-grafted GTR is abbreviated GTR-g-PS.

4.2.3 Blends of GTR and recycled polystyrene

10 g polystyrene was dissolved in 35 mL toluene in a 250 mL beaker, then were added 10 g ground tire rubber powder under continuous stirring to achieve a homogeneous mixture. The solvent was left to evaporate in this way, and the resulting polystyrene/GTR mixture was deposited in a mold, which was covered with a lubricated aluminum foil (6 cm x 6 cm). The mold was moved to a heating plate and heated to 150 °C around 10 min. The 100 % GTR samples prepared at 200 °C. Samples were then removed from the mold and left to cool to the room temperature, and used for characterization and mechanical property measurements. These are abbreviated GTR/PSX or GTR-g-PS/PSX where X is the mass percentage of PS in the resulting composite.

4.2.4 Characterization

FTIR FTIR spectroscopy was carried out on a Thermo Nicolet Magna 850 Fourier transform spectrometer (Thermo Scientific) equipped with a MCT (mercury cadmium telluride) detector cooled with liquid nitrogen and a potassium bromide coated germanium beam splitter. A Golden-Gate^{TM} attenuated total reflection (ATR) module from Specac Ltd. was used to record attenuated total reflection spectra on a diamond crystal. The spectral region used covers the mid-infrared, from 750 to 4000 cm^{-1}. All spectra were recorded with 128 interferograms at a resolution of 4 cm^{-1}.

TGA Thermogravimetric analysis (TGA) was performed using a TGA/SDTA 851e (Mettler Toledo) apparatus equipped with a MT balance. One to two mg of samples were put in a ceramic pan, and measurements were performed by heating from 50 °C to 900 °C at 20 °C/min under nitrogen atmosphere.

XPS X-ray photoelectron spectra (XPS) were recorded on a XSAM800 XPS spectrometer (Kratos) with a monochromatized Al Kα X-ray source (1486.6 eV photons). Uncompacted powders were fixed on a glass plate through the use of double-sided adhesive tape. The X-ray spot size was 1000 and 300 μm for the acquisition of the survey and narrow scan regions, respectively. Binding energies were corrected to the carbon 1s peak located at 285.0 eV.

DMTA Dynamic Mechanical Thermal Analysis tests were performed by means of a RSA-III dynamic mechanical analyser (TA instruments) in the flexural and extension modes using a three-point free bending and tensile setup, respectively. Size of samples used was 6 mm wide, 30 mm long, and thickness varied from 0.7 to 1.1 mm. In the three-point free bending test, temperature was varied from 35 °C to 135 °C at a 10 °C/min heating rate. Tensile measurements were performed at room temperature with a 35 N cell, using a gauge length of 10 mm.

4.3 Results and Discussion

4.3.1 Thiol-ene click reaction

Various chain grafting techniques have been proposed in the literature.[126,127] However, grafting is usually performed by in-situ polymerization, and therefore, once the grafts are attached to the surface, it is very difficult to know their molecular weight or polydispersity. Changes in properties are observed, but difficult to relate to specific parameters such as chain entanglement, which depends on chain length. Therefore, in the present work, an already-prepared polymer was used to control this specific parameter, and grafted by a thiol-ene click reaction with double bonds present at the GTR surface. The molecular weight of the thiol terminated polystyrene can be characterized by SEC so that the average chain length and

polydispersity can be known. And mechanism for thiol-ene click reaction can be indicated as in the Figure 4.1.

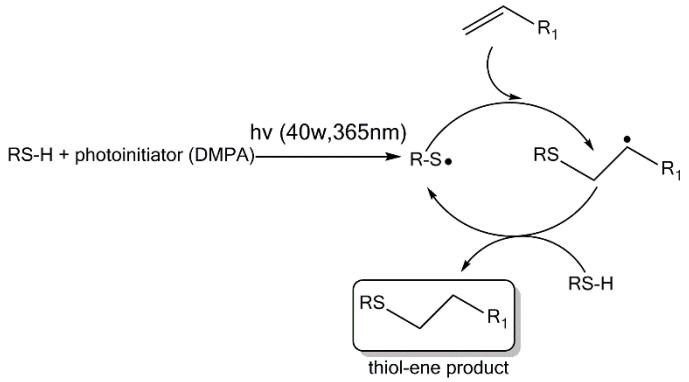

Fig. 4.1 Mechanism of the thiol-ene click reaction[128,129]

The mild conditions under which thiole-ene click reactions are performed (room temperature, safe photo-initiator and ultra-violet light result in a safe and easily operated grafting method.[121,122,130]

4.3.2 Characterization by ATR-FTIR

ATR-FTIR is a superb analytical tool for screening and profiling polymer samples. It can provide valuable quantitative analysis for polymer and plastic materials. Chemical bonds or functional groups can be identified by the experimental spectrum. By using the ATR setup, FTIR can also provide information which is specific to the sample surface.

In the present case, it has therefore been used to follow changes at the PS-grafted for initial and polystyrene grafted GTR samples. Figure 4.2 displays FTIR spectra of a typical non-

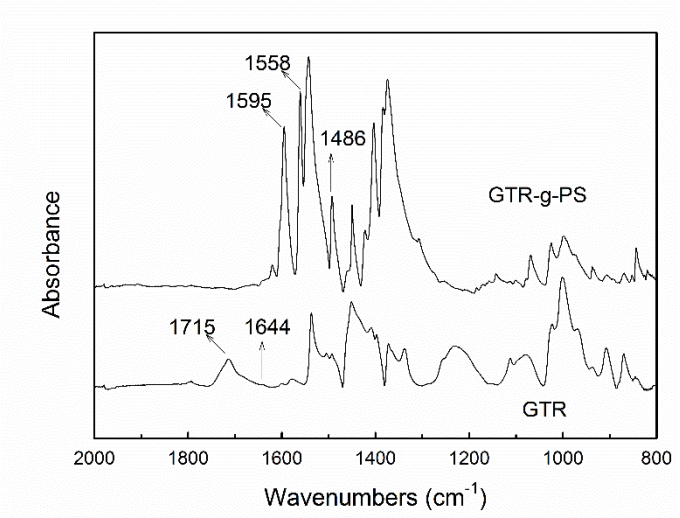

Fig. 4.2 FTIR spectra for GTR and polystyrene grafted GTR sample

modified initial GTR sample and of sample modified by grafting of a commercial polystyrene thiol. From Figure 4.2, it can be seen that the spectrum of the initial GTR sample is of poor quality, as testified by the abnormal peak shape observed. This is attributed to the presence of carbon black and glass fiber in the samples, as observed in previous papers[96,115]. However, after the grafting treatment, peak shape noticeably improves, which indicates that the contact between the diamond of the ATR apparatus and the rubber has changed, due to the presence of polystyrene chains at the GTR surface. Another evidence of the presence of PS chains is the appearance or increase in intensity of three peaks at 1486 cm^{-1}, 1558 cm^{-1} and 1595 cm^{-1} which are assigned to C=C stretch vibration of the aromatic ring. Meanwhile, a broad peak centered at 1715 cm^{-1} and a weak peak at 1644 cm^{-1} in the initial GTR powder, attributed to C=O or non-aromatic C=C bond stretching, disappeared from the grafted sample spectrum, again confirming that a new layer of polymer with different composition exists after grafting. Further, the intensity of non-aromatic C=C peaks can also decrease as the photochemical reaction consumes this groups when grafting of the polystyrene occurs through the thiol end group.

Although FTIR use for GTR is limited due to the poor quality of resulting spectra, in the case of grafting reactions, a significant improvement allows this technique to provide information on the chemical change at the GTR surface.

4.3.3 Thermogravimetric Analysis (TGA)

TGA detects the degradation of samples during heating, which can yield useful temperature range of materials, and also provides insights on their thermal degradation mechanism. Figure 4.3A and 4.3B report thermogravimetric curves and their first derivatives, as measured under nitrogen, for GTR and GTR-g-PS. For comparison purposes, degradation of pure thiol terminated polystyrene and of a GTR/PS composite sample have also been recorded.

An interesting observation can be made: for the initial GTR rubber powder, degradation first occurs around 370 °C, as shown in Figure 4.3A and 4.3B. The GTR sample is mostly composed of vulcanized ethylene propylene diene monomer and of carbon black or inorganics. This first degradation step is therefore attributed to the rubber phase of GTR. Once polystyrene is grafted onto the GTR, however, degradation at this temperature becomes very small and the peak disappears. This indicates that the presence of polystyrene inhibits this first degradation step, possibly due to the disappearance of reactive diene bonds after reaction with thiol-terminated polystyrene. The last degradation step occurs at the same temperature for all GTR samples, whether GTR and modified GTR rubber powder in the 650 °C to 750 °C temperature range, and was previously attributed to the decomposition of calcium carbonate,[96] which is present at a concentration of approximately 5 % in this type of GTR sample.

At the end of the degradation, the residual mass of GTR-g-PS and GTR have similar values. These are associated to the presence of carbon black and inorganic material in the initial GTR. The thiol terminated polystyrene decomposes completely, releasing small molecular weight gaseous species under these conditions. A small mass difference in mass loss can therefore be attributed to changes in relative proportions due to PS grafting, whereas relative proportions of EPDM to carbon black to inorganic material should not change. The small change in percentages is consistent with a small quantity of polystyrene added during grafting. As expected, adding 50 % PS to GTR decreases the residuals by a factor of a half.

A)

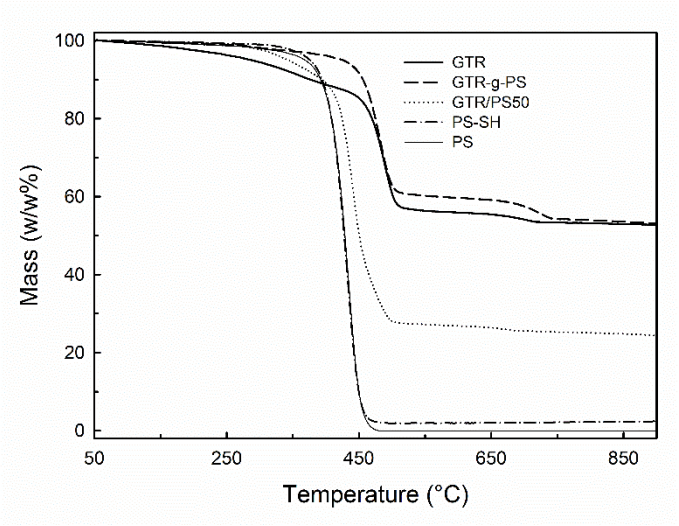

B)

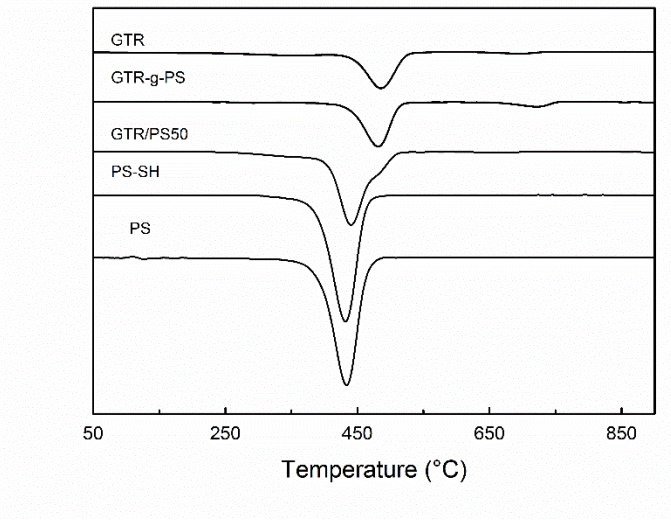

Fig. 4.3 Thermogravimetric mass loss, under nitrogen, of initial GTR and GTR-g-PS rubber powder A) Degradation curves B) Derivative of the degradation curves

A)

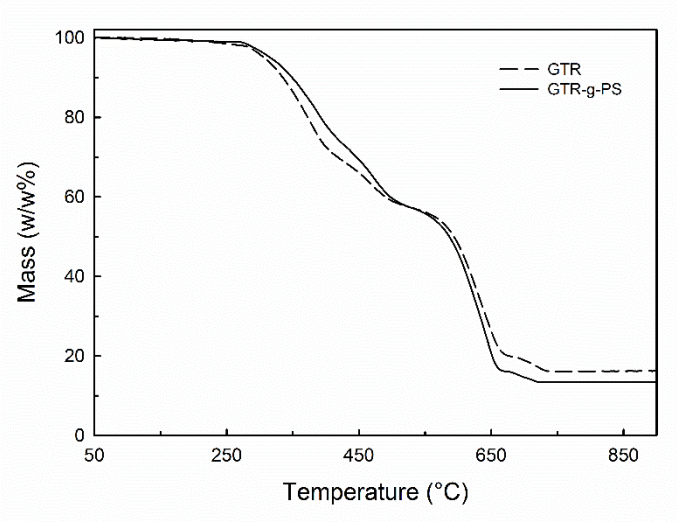

B)

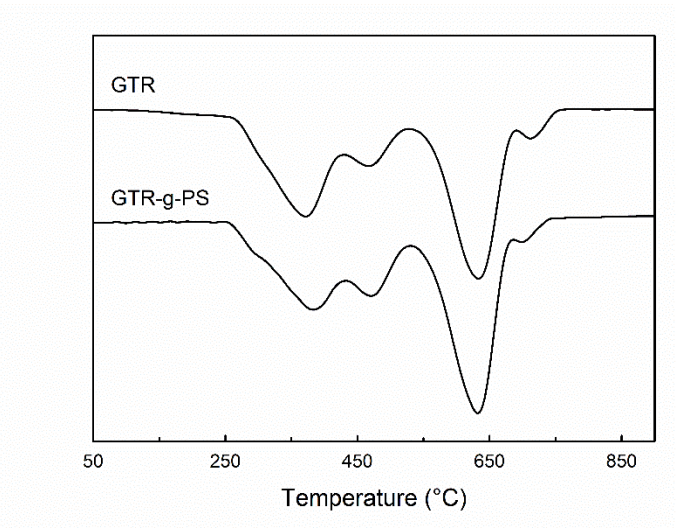

Fig. 4.4 Representative thermogravimetric mass loss, under air, of initial GTR and GTR-g-PS rubber powder A) Degradation curves B) Derivative of the degradation curves

Thermal degradation was also performed in air for GTR and GTR-g-PS, and is reported in Figure 4.4 The main difference between nitrogen and air degradation is the lower value of residuals in air, due to an additional oxidation step of carbon black to CO_2 around 640 °C. Final residual value therefore corresponds only to inorganic material present in GTR, mostly related to accelerators and fillers in EPDM. As for degradation under nitrogen, and as

expected, residual masses for GTR and GTR-g-PS are close, but in this case, the difference is more easily visualized. This is unusual, considering the small surface to bulk ratio in GTR this size, and is attributed to the relatively high molecular weight of grafted material, each grafted site increasing the mass of the sample by 11,000 g/mol. Mass of residuals form degradation in air is also reported in Table 4.1, along with standard deviation after three distinct measurements in each case. It must be noted that the standard deviation is relatively large, as expected from the intrinsic inhomogeneity of industrial GTR. Residuals from the grafted material show an even larger standard deviation, indicative of large variations in grafting degree from one part of the sample to another.

These values can be used for semi-quantitative evaluation of grafted percentages, since no changes in EPDM to carbon black to inorganic residuals is expected. In order to make sure this is the case, GTR samples used for this analysis were subjected to the same treatment as for grafting (three days in toluene under UV light, in the presence of DMAP), in the absence of the grafting material, as such a procedure can dissolve oils, small organic molecules or uncross-linked chains which are often present in GTR.

The percentage of polystyrene grafted onto the surface can then be obtained from the ratio of residuals following Equation (4.1):

$$100\%\,\mathrm{PS} = 100\% - \frac{\%residues_{\mathrm{GTR-g-PS}}}{\%residues_{GTR}} \tag{4.1}$$

Using this method, it can be estimated that 12 % PS is grafted onto GTR particles. Within experimental error, this matches the 1:10 ratio of PS-SH to GTR used during the reaction, indicating that most chains are either grafted or strongly physically attached to GTR.

Table 4.1 Residual masses after thermal degradation in air and amount of grafted polystyrene deduced from these values

	Residual mass (%)	Standard deviation (%)	Grafted Polystyrene (%)	Standard deviation (%)
GTR	16.3	0.9	12	3
GTR-g-PS	14.3	3		

Based on the analysis above, after grafting, the thermal stability of treated GTR shows a small improvement, and TGA measurements confirm that grafting has occurred, and was used for semi-quantitative estimation the percentage polystyrene grafted onto GTR.

4.3.4 X-ray Photoelectron Spectroscopy

X-ray photoelectron spectroscopy (XPS) was used to further investigate the variations in chemical composition on the GTR surface after the polystyrene grafting treatment. The surface composition analysis results obtained by XPS are summarized in Table 4.2 (including the manually transferred value from the atomic percent in XPS measurement to weight percent) and Figure 4.5.

Table 4.2 Surface elemental analysis of initial and modified GTR rubber powder by XPS

Elements	GTR		GTR-g-PS	
	(mol %)	(w/w %)	(mol %)	(w/w %)
C	80 ± 2	69 ± 2	87.9 ± 0.7	79.5 ± 0.6
O	13 ± 2	15 ± 2	9.4 ± 0.5	11.3 ± 0.6
Zn	0.58 ± 0.03	2.7 ± 0.1	0.90 ± 0.07	4.4 ± 0.3
Ca	0.7 ± 0.1	2.0 ± 0.3	1.1 ± 0.1	3.3 ± 0.3
Si	4.7 ± 0.3	9.5 ± 0.6	0.46 ± 0.08	1.0 ± 0.2
S	0.5 ± 0.1	1.2 ± 0.2	0.18 ± 0.01	0.43±0.02

From Table 4.2, it is seen that the total amount of carbon increases by around 10.4 %, which come from the grafting polystyrene. The oxygen and silicon content decrease by 4 % and the sulfur content by 0.7 %, while no significant change in calcium content can be observed. This is in agreement with the addition of polystyrene molecules at the fiber surface, thus decreasing, at the GTR surface, oxygen content related to metal oxides or the oxidation of the rubber itself. SI and S atom ratio also decrease for this reason, whereas precision is not sufficient to ascertain the changes in calcium. However, due to the low homogeneity at the GTR surface, no attempt was made to correlate these change to a thickness of polystyrene at the GTR surface.

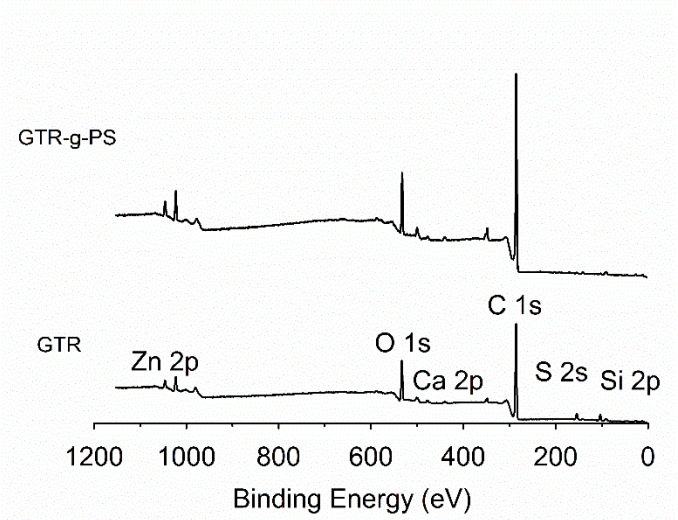

Fig 4.5 XPS spectroscopy of initial and modified GTR rubber powder

It is also interesting to note that Zn and Ca are not present in the same concentration as previously determined by ICP-OES analysis[96], which gave a value of approximately 5 % whereas values of 0.58 – 1.1 % are observed by XPS. XPS is a surface analysis method, and investigates samples at a 5-10 nm. This difference therefore indicated that the surface of GTR is poor in zinc in calcium as compared to the bulk.

Figures 4.6A and 4.6B report surface changes in GTR rubber powder before and after treatment through the investigation of C1s core electrons. For the initial GTR samples, a main peak is observed at 285 eV (C1), corresponding to carbon atoms bound only to other carbon atoms, whereas a smaller peak at 287 eV can be assigned to carbon atoms bonded to either sulfur or oxygen atoms, possibly from cross-links or from rubber oxidation during GTR production[131,132]. After PS grafting, the main carbon peak shifts to a slightly higher position at around 283.5 to 285 eV for the initial GTR rubber powder, and appears to increase slightly in width.

A)

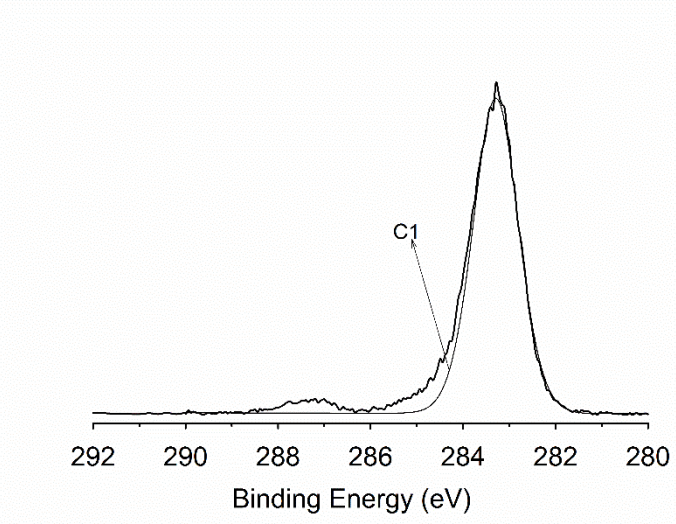

B)

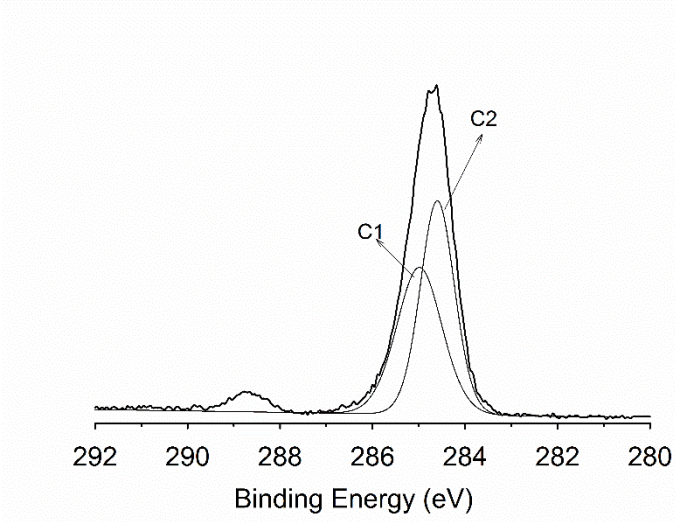

Fig. 4.6 C1s core spectra of A) GTR and B) GTR-g-PS

Spectral decomposition shows that to two different types of C peaks occur this case. The lower energy peak named C2 in Figure 4.6 and appearing at 284.6 eV for the grafted GTR sample is attributed to polystyrene ring carbons[133], thus confirming that polystyrene has indeed been grafted onto the surface. The observed C1/C2 ratio of is close to that expected for pure polystyrene, which would be 0.33, thus confirming an important polystyrene presence at the GTR surface. A very small peak near 291 eV, barely above the background noise, may also be the styrene π- π^* satellite. One last observation can be made: the C-S /C-O peak at 287.5 eV disappears and is replaced by a peak at 288.5 eV, in the carbonyl region. Disappearance of the C-S/C-O peak could be related to surface coverage, and addition of C-S bonds between the PS and the GTR would not compensate for this, considering the small proportion of C-S bonds at compared to added C-C bonds added per grafted polystyrene chain (one C-S per 1000 C-C bonds, approximately, considering the molar weight of PS used), but the appearance of the C=O peak is more surprising. It could be due to partial oxidation of the polymer surface by traces of oxygen in the UV grafting process.

In summary, XPS results confirm that the GTR surface has been covered with appreciable amounts of polystyrene.

4.3.5 Dynamic mechanical thermal analysis (DMTA)

In order to test the efficiency of the grafting treatment in improving GTR-matrix contact, composites were prepared with PS. Solution blending was performed in toluene, this solvent having been selected for its relatively low toxicity and its good Flory-Huggins polymer-solvent interaction parameter.[134] Dynamic mechanical thermal analysis (DMTA) was used to investigate the mechanical properties of the resulting materials.

GTR/PS composites were first prepared at various concentrations and their storage moduli are reported in Figure 4.7. In all cases, the initial storage modulus decreases with increasing temperature, which is attributed to an increase in segment mobility. [135] For PS and PS-based composites, an abrupt decrease in storage modulus around 90 °C can be associated to the glass transition temperature of the PS matrix. In the whole temperature range, samples prepared with pure GTR, in the absence of a thermoplastic matrix, show low storage moduli as compared to the value from the GTR/PS composites. This is due to the poor contact between GTR particles, which causes much of the energy to be dispersed in non-elastic

deformation of the samples, such as particle displacements. Introduction of a PS matrix combined with the solvent treatment allows the storage modulus to rise, up to a 70 % composition, after which the value decreases to that of pure GTR samples, as shown in Figure 4.7. Larger polystyrene quantities in the composites will lead to the increase in rigidity and therefore of storage modulus. [136]

From this data, and from comparison with literature data[54,135], a 50 % GTR blending ratio was selected for investigation in the present work. As shown in Figure 4.7, the grafted GTR allowed a 100 % increase in storage modulus, as compared to a composite with the same composition but prepared using untreated GTR. The ratio of storage moduli with and without grafted GTR allows to follow more easily changes at different temperatures, and is reported in Figure 4.8. This ratio is close to 2 (corresponding to the 100 % increase already mentioned) up to a temperature of approximately 75 °C. This is before the glass transition temperature of polystyrene, which occurs from 90 to 110 °C according to DSC measurements and from 90 to 122 °C according to the position of tangent delta in DMTA. Slightly before the beginning of the glass transition, from 75 to 90 °C, this ratio further rises up to a value of 7. In this temperature range, the storage modulus is much more sensitive to the strength of the interface, and therefore these measurements confirm that grafting considerably improves the quality of the PS thermoplastic matrix – GTR interface. After 90 °C, the ratio slowly decreases, but remains higher than 2. These observations are strong indications that the interface has been improved by the used of treated GTR particles, causing an important increase in storage modulus. Elastic moduli values are also reported in Table 4.3, along with their standard deviation for three samples, for three representative temperatures, 65 °C (well below Tg, when the matrix is in the glassy state), 80 °C (transition range) and 95 °C (above Tg, when the matrix is in the rubbery state). These values confirm that the observed improvement is statistically significant.

Improvement in interface results in better local connection between the GTR particles and the surrounding tough polystyrene matrix, and should therefore also result in an increase in Young's modulus. Figure 4.9 shows Young's modulus of composite samples, as obtained from DMTA in the tensile mode. Increasing the GTR concentration in GTR/PS composites

results in a decrease in Young's modulus, due to the increase in the rubbery phase concentration in a rigid phase. [54,135,137]

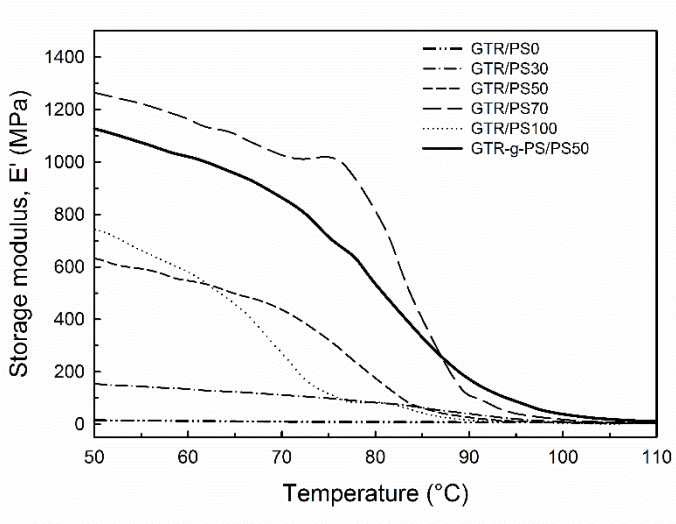

Fig. 4.7 Variation of storage modulus (E') as a function of temperature

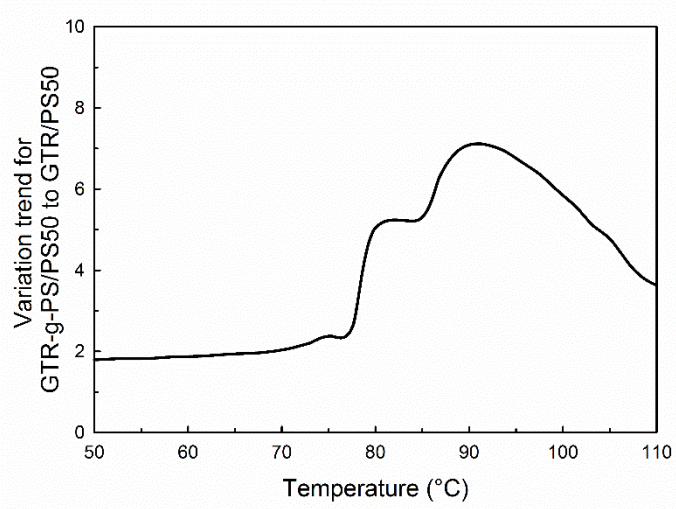

Fig. 4.8 Variation trend for storage modulus (E') as a function of temperature for GTR-g-PS/PS50 over by GTR/PS50

Table 4.3 Storage moduli of the samples at different temperature

	65 °C	80 °C	95 °C
	MPa	MPa	MPa
GTR/PS100	523 ± 39	89 ± 4	7 ± 2
GTR/PS70	1190 ± 120	102 ± 19	6 ± 1
GTR/PS50	535 ± 75	177 ± 21	14 ± 2
GTR/PS30	122 ± 15	80 ± 6	19 ± 4
GTR/PS0	11 ± 3	8 ± 2	7 ± 2
GTR-g-PS/PS50	944 ± 63	450 ± 30	85 ± 7

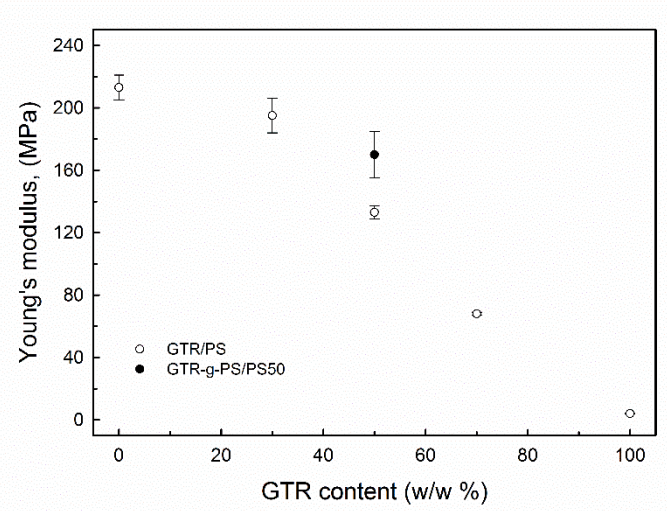

Fig. 4.9 Young's modulus of GTR and GTR-g- PS as a function of GT content

However, as expected, for the composite prepared with GTR-g-PS, Young's modulus also increases. The increase is of approximately 25 % compared to the GTR/PS having the same composition. This is attributed to the grafted polystyrene chains on the GTR surface, which improve adhesion between GTR and chains in the polystyrene matrix due to the chemical similarity of the grafted chains. These are expected to entangle with matrix chains, thus assuring a good stress transfer. This explains the observed increase in Young's modulus.[138,139]

DMTA measurements therefore provide useful information for the different ratio of GTR/PS and GTR-g-PS/PS composite samples. Glass transition temperature can be obtained, but more importantly, storage modulus increases below the Tg and even more so in the vicinity of this transition, as well as increase in Young's moduli indicate that GTR-matrix interface is strengthened by the grafting treatment performed at the GTR surface.

4.4 CONCLUSIONS

EPDM GTR rubber powders were modified through a thiol-ene click reaction that successfully grafted polystyrene onto the surface of GTR rubber powder. Various techniques were used to verify the grafting, such as FTIR, TGA, XPS and DMTA. In FTIR, spectral quality improved for grafted samples, and C=O and C=C bands at 1715 and 1644 cm^{-1} decreased in intensity or disappeared in grafted GTR, whereas aromatic ring bands at 1486 cm^{-1}, 1558 cm^{-1} and 1595 cm^{-1} appeared with strong intensity. XPS results confirm this observation, with increases in carbon content and, more specifically, in aromatic carbon atoms. Form XPS, it is estimated that carbon content increases by approximately 10.4 %. Additionally, the C1s core spectrum changes upon grafting, and peak widening is attributed to the addition of aromatic carbon atoms from PS upon grafting. These data confirm that polystyrene is grafted onto the GTR surface, although an exact quantification is difficult due to inhomogeneities in crumb size and geometrical form.

TGA results also show that grafting slightly increases thermal stability, which is tentatively attributed to the disappearance of reactive double bonds near or at the GTR surface. The difference in residuals under air atmosphere indicates that grafted GTR comprises a larger amount of degradable carbon chains in comparison to initial GTR, which confirms that

polystyrene chains were grafted onto GTR. These values were used in a semi-quantitative evaluation of the quantity of polystyrene grafted onto the surface, which yielded a value of 12 ± 3 % PS. Residuals variations also indicate that GTR composition in inhomogeneous, as expected by the industrial source, but also that it is even more so after grafting, and therefore that the grafting process itself is inhomogeneous.

DMTA measurement show good improvement for the GTR-g-PS/PS blends when compared to the initial GTR/PS blends, storage modulus increases by a factor of 2 near room temperature up to a factor of 7 in the temperature range close to Tg, in which the interface contributes more markedly. Further, Young's moduli increase by a factor of 25 %. These observations indicate that the grafting chains at the GTR surface improves the interface between GTR and the thermoplastic PS matrix, and enables efficient stress transfer between PS and the GTR rubber particles.

In summary, use of the thiol-ene click reaction for grafting polystyrene onto GTR surface was demonstrated, and the use of long PS chains grafted at the surface allowed improvement in the interface of PS/GTR composites, which is attributed to chain entanglement between grafted an matrix and polystyrene chains. Stability of GTR was also slightly improved by this process.

4.5 ACKNOWLEDGEMENTS

The authors wish to acknowledge the financial support of the Natural Sciences and Engineering Research Council of Canada (NSERC). One author (H. Liang) benefitted from a scholarship from the Chinese Scholarship Council, and thankfully acknowledges this support. Recyclage Granutech Inc. (Plessisville, Qc., Canada) is also thanked for providing the ground tire rubber in this work. The assistance of Y. Giroux (for DMTA analysis) from the Department of chemical engineering, Université Laval, is also gratefully acknowledged.

Chapter 5: Conclusions and Recommendations

5.1 General conclusions

So far, the recycling of end of life tires is still a great challenge, as well as their use in blends with thermoplastics. Increasing concern and interest in this field is based on environmental regulations. In the past decades, several studies have been published to reuse the impact of used tire on the population and to increase recycling of tires.

In this project, two type of commercial recycled rubbers, EPDM and SBR, were investigated by various techniques. Quality control methods were investigated, and preliminary tests were performed to modify GTR for blending with polystyrene, another polymer for which post-use recycling applications which are economically viable are needed. Finally, some achievements were gained and listed as the following.

Previously, in the laboratory, we have used TGA, DSC, NMR, FTIR, ICP-OES, AAS and CHNS analytical methods to characterize the commercial recycled GTR rubber powder from two different compositions (EPDM-based and SBR-based), so that we can understand the composition of these rubber materials in more details. In accordance to the characterization results of commercial recycled GTR rubber powders, we prepared standard samples of pure EPDM and SBR copolymers blended with carbon black, cross-link agents, glass fibers and accelerator in varying proportions. We then used these standard samples to verify to what extent the various techniques used could provide information on the ground tire rubber powder. This work has improved knowledge of possible technique for industrial quality control, although there are still some unsolved problems in this field.

Surface modification was performed using the following steps. A photochemical reaction was employed to modify the surface of commercial recycled GTR rubber powders, by grafting thiol-terminated polystyrene. The polystyrene was grafted onto the GTR rubber surface through formation of a C-S bond. FTIR and XPS were used to detect surface variations of composition upon grafting these chains. This work is considered preliminary, and has opened various possibilities for future investigations. The results will be discussed later in this conclusion.

Finally, the polystyrene-modified GTR rubber powder was mixed with recycled polystyrene. Resulting composites were characterized by dynamic mechanical thermal analysis (DMTA) to determine the mechanical properties, and compared to values for the initial GTR compressed samples and for composites prepared with non-grafted GTR. In this way, it is possible to determine how this treatment change mechanical properties, which is an indirect means to investigate the changes in interface interactions due to chain grafting.

In the first article (chapter 2), various techniques were employed to perform characterization of two types of EPDM samples. The first type, standard samples, was prepared in the laboratory, and consisted in EPDM samples with varying cross-link degree and carbon black quantities, as well as a sample contained both carbon black and glass. These samples were used as controls, as their exact composition was known. Commercial recycled EPDM ground rubber samples were also used to verify if the techniques which were found useful for standard samples did not have unforeseen problems due to the presence of various additives in the tires. Then they can validate the usefulness on representative industrial samples. Their detailed composition being unknown, this was first established by a series of chemical analysis including AAS (Si), ICP-OES (metals) and CHNS (S). These will provide information to better understand the results from NMR, TGA and DSC.

Next, the NMR results unfortunately exhibited broad peaks due to interference from presence of para-magnetic metals (Ca or Al), and were therefore not useful for cross-link determination, but were used for monomer compositional investigation.

Thermogravimetric analysis is normally used to determine quantities of carbon black and fillers (designated as ash or residuals) according to the ASTM D6370 method, and was used to complete the analysis of commercial recycled rubber samples. Meanwhile, a surprising phenomenon, qualitatively reported in the literature attracted our attention in this technique. At the beginning of degradation, around 400 °C, the mass loss varies with cross-linking density for ground tire rubber. Thermogravimetric analysis coupled with mass spectrometry showed that this is due to sulfur containing gas emission, in the form of sulfur dioxide (SO_2) indicating that the cross-linking bridges are destroyed at this temperature to form SO_2, before the polymer has a chance to emit carbon dioxides (CO_2) or other gases due to degradation. This observation is specific to EPDM. Quantitative evaluation of this phenomenon results is

in linear relationship. However, for the different types of samples (standard samples with different monomer ratios and ground tire rubber powders), different slopes were obtained, which was attributed to the competitive occurrence of different degradation variables. This shows that TGA can be used for cross-linking density evaluation of EPDM samples, but only if the EPDM is of a similar composition or source.

Finally, the melting transition of commercial recycled EPDM samples was investigated using DSC and it was found that these were related to the ethylene/propylene ratio of rubber phase. This technique can therefore be useful for analysis of industrial GTR samples for which FTIR measurements are difficult (due to the presence of carbon black and glass fibers) whereas NMR is too expensive for recycling companies and suffers from peak broadening due to the presence of paramagnetic metals).

In the second article (chapter 3), SBR-based GTR quality control methods were reinvestigated. First, in this second article, we have put specific attention to zinc quality control, and XRF spectroscopy was introduced for this purpose. It was observed that, when using pure samples, repeatability was poor, and in order to decrease the effect of particle geometry, a cellulose binder agent was added. To prepare a standard curve, a series of the same GTR sample was prepared as pellets with different GTR contents. After measurement, the results give a linear quantitative curve which can be used to quantify zinc content for other SBR-based GTR samples. This method is rapid, show a good repeatability and is convenient in the industries.

Quantification of the butadiene/styrene ratio was shown to be reliably determined by TGA in neat SBR samples, but not in the case of GTR SBR samples, due to the presence of other rubbers (natural rubber and perhaps some contaminants) that degrade in a similar temperature range as styrene or butadiene, so that this influences the analytical results.

Finally, DSC may be used for the (butadiene plus isoprene)/styrene ratio determination through determination of changes in the glass transition temperatures, which is also a quality control method in the industry.

In the third article (chapter 4), GTR rubber powder was subjected to surface modification. A photochemical reaction was performed on existing double bonds at the GTR surface by a thiol-ene reaction with thiol terminated polystyrene. The FTIR and XPS techniques were

used to detect the surface variations. FTIR results showed that the intensity of C=O (1715 cm^{-1}) and C=C (1644 cm^{-1}) bonds changed in modified samples. Meanwhile, after the polystyrene grafting treatment, the intensity of aromatic carbon valence bands at 1486 cm^{-1}, 1558 cm^{-1} and 1595 cm^{-1} indicated that polystyrene was grafted onto the GTR rubber powder surface. These results indicate that the grafting was successful.

The TGA curve in nitrogen atmosphere indicated that thermal resistance for polystyrene grafted GTR was slightly increased, which is attributed to consummation of relative double bonds near or on the surface. The difference in TGA residuals under air atmosphere for initial GTR and grafted GTR samples revealed that polystyrene was successfully grafted onto the GTR surface, and were used for semi-quantitative evaluation of the amount of polystyrene on the surface. A value of 12 ± 3 % was obtained. Variations of residuals from one sample to another show that PS-treated GTR is even more inhomogeneous that the original non-treated GTR.

DMTA results show good improvement for the GTR-g-PS /PS composites in comparison to GTR/PS composites. The storage modulus increases at least by a factor of 2 in the whole temperature range studies, which spans from room temperature to above Tg. The highest increase factor of 7 is obtained close to Tg, and is further proof of the improvement in interface interaction between the treated GTR surface and a recycled polystyrene matrix. Further, Young's modulus increases by a factor of 25 %. From these results, it is proposed that grafted polystyrene chains form entanglements with PS chains of the thermoplastic matrix, which enables efficient stress transfer between PS and the GTR rubber particles.

Based on the analysis above, the characterization methods for quality control of ground tire rubber in industries and an efficient modification method have been proposed. However, much work remains on this subject.

5.2 Recommendations for prospective works

From the general conclusions above, some work is still required in the future to improve characterization of GTR and to better understand how surface treatments will help to improve properties of GTR-based blends with thermoplastics.

In the case of quality control, for the GTR EPDM samples, it would be interesting to explore in more details the quantification of the ethylene/propylene by DSC. In the present work, relying on work from the literature, is was supposed this would not be quantitative, but this would be interesting to verify. In order to do this, a wider variety of EPDM with varying ethylene/propylene ratio, cross-link density and additives would be essential.

The X-ray fluorescence technique could also extended to GTR EPDM rubber powders, following the same approach as described for SBR powders in chapter 3. This method can quantify metals or other heavy atoms such as bromine (Br) inside the GTR particles. It would be interesting to verify if the use of a single sample with different concentrations also works for GTR EPDM or for batches of GTR from unknown sources.

With regard to the GTR SBR samples, a rapid, time-saving and economic method for cross-link density determination is still required to improve quality control. A possible route could be to use dynamical thermal analysis, in which various relaxation processes can be determined, including the glass transition temperature. Although Tg was not found to be proportional to cross-link density in DSC measurement alone in this work, the possibility that other transitions should be explored. Additionally, Raman spectroscopy may provide information of C-S or S-S bonds in the GTR samples, which form the cross-links. The intensity of C-S bonds may be related to the cross-linking density. In the presence of carbon black in the GTR rubber powder, preliminary measurements have shown that the laser beam degrades the GTR surface, but fast measurements or changes it the intensity of the laser beam may be adjusted to minimize this effect.

Modifications of the GTR surface for improving mechanical properties is certainly the area in which the most promising and the greatest challenges remain. The present work represents a very preliminary study of this specific GTR recycling problem. Work which could be performed include studies with other thiol-terminated thermoplastic polymers, such as polypropylene. A wider range of mechanical properties, including tensile tests and impact tests, should also be performed.

With regard to the modification, the determination of the number of double bonds on the surface of GTR samples is a remaining challenge, and could provide information on the ratio of reacted dienes at the surface. Some strategies could be attempted to determine the numbers

of double bonds. First, the GTR samples can be submitted to iodine or bromine, which would react with the double bonds of GTR rubber powders, and XPS would be used to quantify the changes in intensity for iodine or bromine at the surface, as compared to an atomic species which does not vary much, such as zinc, before and after additional reaction. XRF could also be used to detect the changes in iodine and bromine, but in the bulk of the samples and not only at the surface. Second, another indirect titration method can be tried in this case, which is the same used to determine the insaturation number in fatty acids. An iodine solution, in excess, is used as a reactant to double bonds, then the excess is back-titrated with sodium thiosulfate. It may however be impossible to do this, depending on the quantity of double bonds at the surface of a specific GTR.

In the photochemical reaction, the thiol terminated polystyrene was used for the surface modification. In the experiment, the small mass of thiol terminated polystyrene was used because of the high price of this commercial product, around $200/g, which increases the cost and is not economic for large-scale modification in the industry. In order to reduce the reactant cost, a different means of synthesizing the polystyrene is sought. Some preliminary tests have been performed with a reversible addition-fragmentation chain transfer polymerization to synthesize thiol terminated polystyrene.

This is a very interesting and economic way to synthesize polystyrene with a thiol end group, because the reaction is initiated thermally, without initiators such as AIBN or BPO, which are dangerous and harmful to the environment. In this method, dibenzyl trithiocarbonate (DBTC) is used as the chain transfer agent. It is a commercial product, and changes in the mass of DBTC can be used to control chain length, which can be used to optimize the length needed for optimum interfacial contacts between GTR and a polymer matrix, as well as the stress transfer when the samples are strained. In order to verify the presence of the SH end group, MALDI-TOF MS could be used in this case.

Other polymers with thiol termination could be synthesized in the photochemical reaction. Atom transfer radical polymerization and living anionic polymerization can be used to produce various thiol-terminated polymers, such as methyl methacrylate for ATRP and butadiene for anionic polymerization.

At present, in the preliminary experiments, the only recycled thermoplastic used was polystyrene, and it was blended with GTR EPDM rubber powder, but not with GTR SBR, which should be more compatible with PS, as SBR is styrene-butadiene copolymer. Experiments could also be performed by varying the thermoplastic matric and the GTR source.

References

1. United States Environmental Protection Agency. Wastes − Resource Conservation – Common Wastes & Materials − Scrap Tires, Available at: http://www.epa.gov/osw/conserve/materials/tires/basic.htm (accessed January 2014).
2. Shulman, V. L.; Tyre Recycling, Rapra Technology Limited: Shawbury, 2004; p 7.
3. Evans, A.; Evans, R., The Composition of a Tyre: Typical Components, The Waste & Resources Action Programme:Banbury, 2006; p 2.
4. Chung, W. J.; Griebel, J. J.; Kim, E. T.; Yoon, H.; Simmonds, A. G.; Ji, H. J.; Dirlam, P. T.; Glass, R. S.; Wie, J. J.; Nguyen, N. A.; Guralnick, B. W.; Park, J.; Somogyi, Á.; Theato, P.; Mackay, M. E.; Sung, Y.-E.; Char, K.; Pyun, J., Nat. Chem. 5, 518, 2013.
5. Ghosh, P.; Katare, S.; Patkar, P.; Caruthers, J. M.; Venkatasubramanian, V., Rubber Chem. Technol. 76, 592, 2003.
6. Sonnier, R.; Taguet, A.; Rouif, S. in Functional Polymer Blends: Synthesis, Properties, and Performance, Mittal, V. editor, CRC Press Taylor & Francis Group: Florida, 2012; p 286.
7. White, J. R.; De, S. K.; Rubber Technologist's Handbook, Rapra Technology Limited: Shawbury, 2001; p 131.
8. Tantala, M. W.; Lepore, J. A.; Zandi, I. Proceedings 12th International Conference on Solid Waste Technology and Management, Philadelphia, PA, 1996.
9. Stanojević, D. D.; Rajković, M. B.; Tošković, D. V., Hem. Ind. 65, 727, 2011.
10. Ad Hoc Civil Engineering Committee, Design Guidelines to Minimize Internal Heating of Tire Shred Fills, 1997, Available at http://www.rma.org/design-guidelines-to-minimize-internal-heating-of-tire-shred-fills/, accessed in 2015.
11. Humphrey, D. N. In The Tire Industry Conference, Hilton Head, SC, 1999; p 16.
12. Kim, H.-S.; Geiger, A.; Amirkhanian, S. N.; Park, T.-S.; Kim, K.-W. In The 6th International Conference on Road and Airfield Pavement Technology, Sapporo, Japan, 2008; p 7.
13. Mashaan, N. S.; Ali, A. H.; Karim, M. R.; Abdelaziz, M., Int. J. Phys. Sci. 6, 684, 2011.
14. Mashaan, N. S.; Ali, A. H.; Karim, M. R.; Abdelaziz, M., Int. J. Phys. Sci. 6, 2189, 2011.
15. Karacasu, M.; Okur, V.; Er, A., Sci. World. J. 2015,1, 2015.
16. Juma, M.; Korenová, Z.; Markoš, J.; Annus, J.; Jelemenský, L., Pet.Coal 48,15, 2006.
17. Scatolim Rombaldo, F. C.; Luz Lisbôa, C. A.; Alvarez Méndez, O. M.; dos Reis

Coutinho, A., Mater. Res. 11,359, 2008.
18. Osayi, J. I.; Iyuke, S.; Ogbeide, S. E., J. Catal. 2014, 9, 2014.
19. Mahallati, P.; Rodrigue, D., Int. Polym. Proc. 29, 280, 2014.
20. Fan, P.; Lu, C., J. Polym. Environ. 19, 943, 2011.
21. Grythe, K. F.; Hansen, F. K., Langmuir 22, 6109, 2006.
22. Tyczkowski, J.; Krawczyk, I.; Wożniak, B., Surf. Coat. Technol. 174–175, 849, 2003.
23. Shanmugharaj, A. M.; Kim, J. K.; Ryu, S. H., Appl. Surf. Sci. 252, 5714, 2006.
24. Burillo, G.; Clough, R. L.; Czvikovszky, T.; Guven, O.; Le Moel, A.; Liu, W. W.; Singh, A.; Yang, J. T.; Zaharescu, T., Radiat. Phys. Chemical. 64, 41, 2002.
25. Naskar, A. K.; Bhowmick, A. K.; De, S. K., J. Appl. Polym. Sci. 84, 622, 2002.
26. Colom, X.; Carrillo, F.; Cañavate, J., Composites Part A 38, 44, 2007.
27. Yehia, A. A.; Mull, M. A.; Ismail, M. N.; Hefny, Y. A.; Abdel-Bary, E. M., J. Appl. Polym. Sci. 93, 30, 2004.
28. Aggour, Y. A.; Al-Shihri, A. S.; Bazzet, M. R., Open J. Polym. Chem. 3, 48, 2013.
29. Abdel-Bary, E. M.; Dessouki, A. M.; El-Nesr, E. M.; Hassan, M. M., Polym. Plast. Technol. Eng. 36, 241, 1997.
30. Tolstov, A.; Grigoryeva, O.; Fainleib, A.; Danilenko, I.; Spanoudaki, A.; Pissis, P.; Grenet, J., Macromol. Symp. 254, 226, 2007.
31. Naskar, A. K.; De, S. K.; Bhowmick, A. K., J. Appl. Polym. Sci. 84, 370, 2002.
32. Coiai, S.; Passaglia, E.; Ciardelli, F.; Tirelli, D.; Peruzzotti, F.; Resmini, E., Macromol. Symp. 234, 193, 2006.
33. Karger-Kocsis, J.; Mészáros, L.; Bárány, T., J. Mater. Sci. 48, 1, 2013.
34. Zhang, J.; Chen, H.; Ke, C.; Zhou, Y.; Lu, H.; Wang, D., Polym. Bull. 68, 789, 2012.
35. Miwa, Y.; Yamamoto, K.; Sakaguchi, M.; Shimada, S., Macromolecules 32, 8234, 1999.
36. Miwa, Y.; Yamamoto, K.; Sakaguchi, M.; Shimada, S., Macromolecules 34, 2089, 2001.
37. Prakanrat, S.; Phinyocheep, P.; Daniel, P., Appl. Spectrosc. 63, 233, 2009.
38. Yu, Z. S.; Li, Y.; Wang, Y. R., Express Polym. Lett. 5, 911, 2011.
39. Yu, J. J.; Ryu, S. H., J. Appl. Polym. Sci. 73, 1733, 1999.
40. Shanmugharaj, A. M.; Kim, J. K.; Ryu, S. H., Polym. Test. 24, 739, 2005.

41. Du, M.; Guo, B.; Jia, D., J. Polym. Res. 12, 473, 2005.
42. Allmér, K.; Hult, A.; Rånby, B., J. Polym. Sci., Part A: Polym. Chem. 27, 1641, 1989.
43. Tazuke, S.; Matoba, T.; Kimura, H.; Okada, T. In ACS Symposium Series 121, Washington, DC, 1980, p 217.
44. Yao, Z. P.; Rånby, B., J. Appl. Polym. Sci. 40, 1647, 1990.
45. Fuhrmann, I.; Karger-Kocsis, J., Plast. Rubber Compos. 28, 500, 1999.
46. Fuhrmann, I.; Karger-Kocsis, J., J. Appl. Polym. Sci. 89, 1622, 2003.
47. Sonnier, R.; Leroy, E.; Clerc, L.; Bergeret, A.; Lopez-Cuesta, J. M., Polym. Bull. 26, 274, 2007.
48. Scaffaro, R.; Dintcheva, N. T.; Nocilla, M. A.; La Mantia, F. P., Polym. Degrad. Stabil;. 90, 281, 2005.
49. Shanmugharaj, A. M.; Kim, J. K.; Ryu, S. H., J. Appl. Polym. Sci. 104, 2237, 2007.
50. Lee, S. H.; Zhang, Z. X.; Xu, D.; Chung, D.; OH, G. J.; Kim, J. K., Polym. Eng. Sci. 49, 168, 2009.
51. OH, J. S.; Isayev, A. I., Rubber Chem. Technol. 75, 617, 2002.
52. Kampouris, E. M.; Papaspyrides, C. D.; Lekakou, C. N., Polym. Eng. Sci. 28, 534, 1988.
53. Montagna, L. S.; Santana, R. M. C., Plast. Rubber Compos. 41, 256, 2012.
54. Veilleux, J.; Rodrigue, D. In MACROMEX 2014 Third US-Mexico Meeting "Advances in Polymer Science" and XXVII SPM National Congress, Nuevo Vallarta, Mexico, 2014.
55. Frenkel, J., Rubber Chem. Technol. 13, 264, 1940.
56. Flory, P. J., J. Chem. Phys. 10, 51, 1942.
57. Flory, P. J.; Rehner, J., J. Chem. Phys. 11, 521, 1943.
58. Macsiniuc, A.; Rochette, A.; Rodrigue, D., Prog. Rubber, Plast. Recycl. Technol. 28, 43, 2012.
59. Matzen, D.; Straube, E., Colloid Polym. Sci. 270, 1, 1992.
60. Zhao, F.; Bi, W.; Zhao, S., J. Macromol. Sci. Part B Phys. 50, 1460, 2011.
61. Fry, C. G.; Lind, A. C., Macromolecules 21, 1292, 1988.
62. Zimmer, G.; Guthausen, A.; Blümich, B., Solid State Nucl. Magn. Reson. 12, 183, 1998.
63. Aluas, M.; Filip, C., Solid State Nucl. Magn. Reson. 27, 165, 2005.

64. Litvinov, V. M., Macromolecules 39, 8727, 2006.
65. Pistor, V.; Scuracchio, C. H.; Oliveira, P. J.; Fiorio, R.; Zattera, A. J., Polym. Eng. Sci. 51, 697, 2011.
66. Kovaľaková, M.; Fričová, O.; Hronský, V.; Olčák, D.; Mandula, J.; Salaiová, B.; Holubka, M., Chem. Listy, 105, S350, 2011.
67. Zhang, A.; Chao, L., Eur. Polym. J. 39, 1291, 2003.
68. Ver-Strate, G.; Wilchinsky, Z. W., J. Polym. Sci., Part B: Polym. Phys. 9, 127, 1971.
69. Castaldi, M. J.; Kwon, E. In 13th North American Waste to Energy Conference, Orlando, FL, 2005; p 19.
70. Sircar, A. K., Rubber Chem. Technol. 65, 503, 1992.
71. Cui, H.; Yang, J. L.; Liu, Z. Y., Thermochim. Acta 333, 173, 1999.
72. Formela, K.; Haponiuk, J., Iran Polym. J. 23, 185, 2014.
73. Arockiasamy, A.; Toghiani, H.; Oglesby, D.; Horstemeyer, M. F.; Bouvard, J. L.; King, R., J. Therm. Anal. Calorim. 111, 535, 2013.
74. Fernández-Berridi, M. J.; González, N.; Mugica, A.; Bernicot, C., Thermochim. Acta 444, 65, 2006.
75. Choi, G.-G.; Jung, S.-H.; Oh, S.-J.; Kim, J.-S., Fuel Process. Technol. 123, 57, 2014.
76. Ucar, S.; Karagoz, S.; Ozkan, A. R.; Yanik, J., Fuel 84, 1884, 2005.
77. De Marco Rodriguez, I.; Laresgoiti, M. F.; Cabrero, M. A.; Torres, A.; Chomón, M. J.; Caballero, B., Fuel Process. Technol. 72, 9, 2001.
78. Miguel, G. S.; Aguado, J.; Serrano, D. P.; Escola, J. M., Appl. Catal., B 64, 209, 2006.
79. Averko, Y.; Pegoraro, M.; Penati, A., Eur. Polym. J. 10, 693, 1974.
80. Hofman, W. In Rubber Handbook Technology; Hanser Publishers: Munich, 1988.
81. Bhattacharjee, S.; Bender, H.; Padliya, D., Rubber Chem. Technol. 76, 1057, 2003.
82. Heideman, G.; Noordermeer, J. W. M.; Datta, R. N.; Van Baarle, B., Kautschuk Gummi Kunst. 58, 30, 2005.
83. Hertz, D. L., Elastomerics 116, 1721, 1984.
84. Zeyen, R. L., Rubber World 199, 14, 1988.
85. Pistor, V.; Ornaghi, F. G.; Fiorio, R.; Zattera, A. J., Thermochim. Acta 510, 93, 2010.
86. Crespi, G.; Valvassori, A.; Zamboni, V.; Flisi, U., Chim. Ind. (Milan) 55, 130,

1973.

87. Steinhoff, W. In High Performance Elastomers: 2000 Conference Proceedings, Rapra. Technology Ltd., Shawbury, United Kingdom, 2000; pp 5.4.

88. Rao, T.; "Effect of Crosslink Density and N660 Carbon Black on Tearing Behaviors of Natural Rubber Vulcanizates," Master's Thesis, University of Akron, 2012.

89. Fang, Y.; Zhan, M.; Wang, Y., Mater. Des. 22, 123, 2001.

90. Obrecht, W.; Lambert, J.-P.; Happ, M.; Oppenheimer-Stix, C.; Dunn, J.; Krüger, R. In Ullmann's Encyclopedia of Industrial Chemistry, 7th ed, Wiley-VCH: Weinheim, 2010; p 623.

91. Sardashti, M.; Gislason, J. J.; Lai, X.; Stewart, C. A.; O'Donnell, D. J., Appl. Spectrosc. 55, 467, 2001.

92. Luo, H.; Klüppel, M.; Schneider, H., Macromolecules 37, 8000, 2004.

93. Arantes, T. M.; Leão, K. V.; Tavares, M. I. B.; Ferreira, A. G.; Longo, E.; Camargo, E. R., Polym. Test. 28, 490, 2009.

94. Kawahara, S.; Chaikumpollert, O.; Sakurai, S.; Yamamoto, Y.; Akabori, K., Polymer 50, 1626, 2009.

95. Nakazono, T.; Matsumoto, A., J. Appl. Polym. Sci. 118, 2314, 2010.

96. Liang, H.; Hardy, J.-M.; Rodrigue, D.; Brisson, J., Rubber Chem. Technol. 87, 538, 2014.

97. Shield, S. R.; Ghebremeskel, G. N., Rubber World 223, 25, 2000.

98. Fink, H.; Panne, U.; Theisen, M.; Niessner, R.; Probst, T.; Lin, X., Fresenius, J., Anal. Chem. 368, 235, 2000.

99. Mans, C.; Hanning, S.; Simons, C.; Wegner, A.; Janβen, A.; Kreyenschmidt, M., Spectrochim. Acta Part B 62, 116, 2007.

100. Miskolczi, N.; Nagy, R.; Bartha, L.; Halmos, P.; Fazekas, B., Microchem. J. 88, 14 2008.

101. Tertian;, R.; Claisse, F., Principles of Quantitative X-ray Fluorescence Analysis; Heyden & Son: London, 1982; p 317.

102. Radhakrishnan, C. K.; Sujith, A.; Unnikrishnan, G., J. Therm. Anal. Calorim. 90, 191, 2007.

103. Noriman, N. Z.; Ismail, H.; Rashid, A. A., Polym. Test. 29, 200, 2010.

104. Cunliffe, A. M.; Williams, P. T., Environ. Technol. 19, 1177, 1998.

105. Amari, T.; Themelis, N. J.; Wernick, I. K., Resources Policy 25, 179, 1999.
106. Metz, U.; Hoffmann, P.; Weinbruch, S.; Ortner, H., Mikrochim. Acta 117, 95, 1994.
107. Mans, C.; Simons, C.; Hanning, S.; Janßen, A.; Alber, D.; Radtke, M.; Reinholz, U.; Bühler, A.; Kreyenschmidt, M., X-Ray Spectrom. 38, 52, 2009.
108. Mellawati, J.; Sumarti, M.; Menry, Y.; Surtipanti, S.; Kump, P., Appl. Radiat. Isot. 54, 881, 2001.
109. Choi, S.-S.; Kim, Y.; Kwon, H.-M., RSC Adv. 4, 31113, 2014.
110. Kovaľaková, M.; Fričová, O.; Hronský, V.; Olčák, D.; Mandula, J.; Salaiová, B., Road Mater. Pavement 14, 946, 2013.
111. Jimenez, A.; Lopez, J.; Torre, L.; Kenny, J. M., J. Appl. Polym. Sci. 73, 1069, 1999.
112. Kraus, G.; Childers, C. W.; Gruver, J. T., J. Appl. Polym. Sci. 11, 1581, 1967.
113. Chapman, A. V.; Tinker, A. J.; Brickendonbury, H., J. Elast. Plast. 56, 533, 2003.
114. Andrews, R. J.; Grulke, E.A., Glass Transition Temperatures of Polymers. Wiley Database of Polymer Properties; Wiley: Hoboken, 2003; Chapter 5. Available at http://onlinelibrary.wiley.com/doi/10.1002/0471532053.bra039/full
115. Liang, H.; Rodrigue, D.; Brisson, J., J. Appl. Polym. Sci. 132, 42692, 2015.
116. Herrera-Sosa, E. S.; Martínez-Barrera, G.; Barrera-Díaz, C.; Cruz-Zaragoza, E., Adv. Mater. Sci. Eng. 2014, 1, 2014.
117. Scuracchio, C. H.; Waki, D. A.; da Silva, M. L. C. P., J. Therm. Anal. Calorim. 87, 893, 2007.
118. Kim, J. K.; Lee, S. H.; Hwang, S. H., J. Appl. Polym. Sci**.** 90, 2503, 2003.
119. Colom, X.; Cañavate, J.; Carrillo, F.; Velasco, J. I.; Pagès, P.; Mujal, R.; Nogués, F., Eur. Polym. J. 42, 2369,2006.
120. Ferry, J. D., Viscoelastic Properties of Polymers; John Wiley & Sons, New York, 374p., 1980.
121. Hoyle, C. E.; Bowman, C. N., Angew. Chem. Int. Edit. 49, 1540, 2010.
122. Lowe, A. B., Polym. Chem. 5, 4820, 2014.
123. Hensarling, R. M.; Patton, D. L., In Thiol-x Chemistries in Polymer and Materials Science, Lowe, A.; Bowman, C. editors ; RSC Pub.: Cambriage, pp. 259-285, 2013.
124. Liang, X.; Shen, A.; Guo, Z., In Thiol-x Chemistries in Polymer and Materials Science, Lowe, A.; Bowman, C. editors ; RSC Pub.: Cambridge, pp. 286-303, 2013.
125. Wu, J.-T.; Huang, C.-H.; Liang, W.-C.; Wu, Y.-L.; Yu, J.; Chen, H.-Y., Macromol. Rapid Commun. 33, 922, 2012.
126. Liu, Y.; Cavicchi, K. A., Macromol. Chem. Phys. 210, 1647, 2009.
127. Feng, L.; Cavicchi, K. A.; Katzenmeyer, B. C.; Wesdemiotis, C., J. Polym. Sci., Part A: Polym. Chem. 49, 5100, 2011.
128. Hoyle, C. E.; Lowe, A. B.; Bowman, C. N., Chem. Soc. Rev. 39, 1335, 2010.
129. Cole, M. A.; Jankousky, K. C.; Bowman, C. N., Poly. Chem. 4, 1167, 2013.

130. Nair, D. P.; Podgórski, M.; Chatani, S.; Gong, T.; Xi, W.; Fenoli, C. R.; Bowman, C. N., Chem. Mater. 26, 724, 2014.
131. Lukáš, J.; Tyáčková, V., J. Membr. Sci. 58, 49, 1991.
132. XPS database. Accessed online : http://techdb.podzone.net/xpsstate-e/ on August 18, 2015.
133. Zhang, X. X.; Zhu, X. Q.; Liang, M.; Lu, C. H., J. Appl. Polym. Sci. 114, 1118, 2009.
134. Sobhy, M. S.; Mahdy, M. M. M.; El-Fayoumi, M. A. K.; Abdel-Bary, E. M., Polym. Test. 16, 349, 1997.
135. Asaletha, R.; Kumaran, M. G.; Thomas, S., Eur. Polym. J. 35, 253, 1999.
136. Thomas, S.; Joseph, K.; Malhotra, S. K.; Goda, K.; Sreekala, M. S., Polymer Composites, Macro- and Microcomposites; Wiley-VCH: Weinheim, Germany, 244 p, 2012.
137. Danesi, S.; Porter, R. S., Polymer 19, 448, 1978.
138. Barentsen, W. M.; Heikens, D., Polymer 14, 579, 1973.
139. Ibrahim, B.; Kadum, K. M., Int. J. Eng. Technol. 12, 19, 2012.

Appendix

Chapter 2: SUPPLEMENTARY DATA

Thermal and thermogravimetric analysis of EPDM samples.

Table A.1 Mass used, in grams, of each component for standard samples prepared and measured in this work.

	EPDM	Stearic acid	TMTD	ZnO	S_2Cl_2	Carbon black	Milled glass fibers
0CB	2	0.04	0.01	0.1	0.12	0	0
30CB	2	0.04	0.01	0.1	0.12	0.6	0
50CB	2	0.04	0.01	0.1	0.12	1	0
60CB	2	0.04	0.01	0.1	0.12	1.2	0
70CB	2	0.04	0.01	0.1	0.12	1.4	0
100CB	0	0	0	0	0	1	0
50 CB+G	2	0.04	0.01	0.1	0.12	1	0.55
CD53-2	2	0.04	0.01	0.1	0.04	0	0
CD53-6	2	0.04	0.01	0.1	0.08	0	0
CD53-9	2	0.04	0.01	0.1	0.12	0	0

CD53-14	2	0.04	0.01	0.1	0.16	0	0
CD71-1	2	0.04	0.01	0.1	0.04	0	0
CD71-4	2	0.04	0.01	0.1	0.08	0	0
CD71-7	2	0.04	0.01	0.1	0.12	0	0
CD71-8	2	0.04	0.01	0.1	0.16	0	0
CD71-11	2	0.04	0.01	0.1	0.2	0	0

Table A.2 Zinc concentrations obtained for GTR samples using the calibration curve. Each measurement corresponds to a different disk. Comparison is made with results from ICP-OES. (Note: the different number (GTR-B1, B2) represent different Zn concentration in disk specimens)

	Zn concentration in disk specimen (w/w %)		
	XRF	ICP-OES	Difference
GTR-B1	0.73	0.72	0.01
GTR-B2	1.08	1.11	0.03
GTR-B3	1.27	1.24	0.03
GTR-C1	0.63	0.64	0.01
GTR-C2	1.13	1.11	0.02
GTR-C3	1.31	1.29	0.02
GTR-D1	0.55	0.47	0.08
GTR-D2	1.06	1.11	0.05
GTR-D3	1.26	1.23	0.03
GTR-E1	0.66	0.58	0.08
GTR-E2	1.23	1.07	0.16
GTR-E3	1.47	1.24	0.23

Table A.3 Statistical analysis of various measurements made on GTR-A for XRF measurement (GTR-E).

No.	Intensity (cps)	Standard deviation	Average intensity (cps)	Standard error
1	24.5			
	25.2	0.35	24.8	
	24.8			
	25.3			
2	25.4	0.06	25.3	0.69
	25.3			
	24.0			
3	23.7	0.25	24.0	
	24.2			

Table A.4 TGA Degradation Temperatures and Relative Mass Loss Percentages for GTR SBR Samples.

Sample	Onset $T_{degr\ 1}$ (°C)	1st mass loss [a] (w/w %)	1st mass loss [b] (w/w %)	Onset $T_{degr\ 2}$ (°C)	2nd mass loss [a] (w/w %)	2nd mass loss [b] (w/w %)	Onset $T_{degr\ 3}$ (°C)	3rd mass loss [a] (w/w %)	3rd mass loss [b] (w/w %)	Residual mass (w/w %)
GTR-A	272	50	54	487	14	12	542	29	27	7
GTR-B	247	44	50	477	17	10	546	30	31	9
GTR-C	241	50	52	480	16	13	552	30	31	4
GTR-D	244	48	52	477	18	14	546	30	30	4
GTR-E	240	48	49	457	16	13	544	30	32	6

[a] Using temperatures determined by first derivatives

[b] Using fixed temperature ranges of 500, 550 and 750 °C

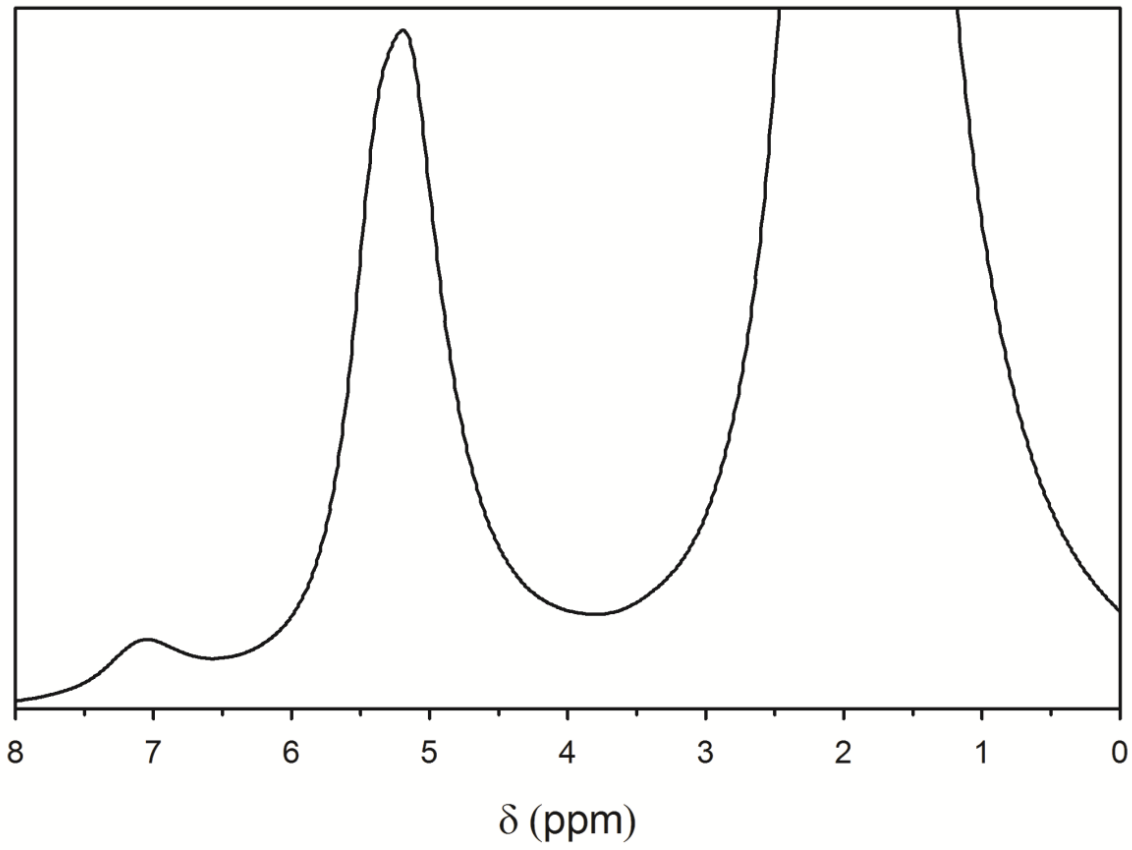

Fig. A.1 NMR spectrum of WGR-A: close-up view showing the peak at 7 ppm

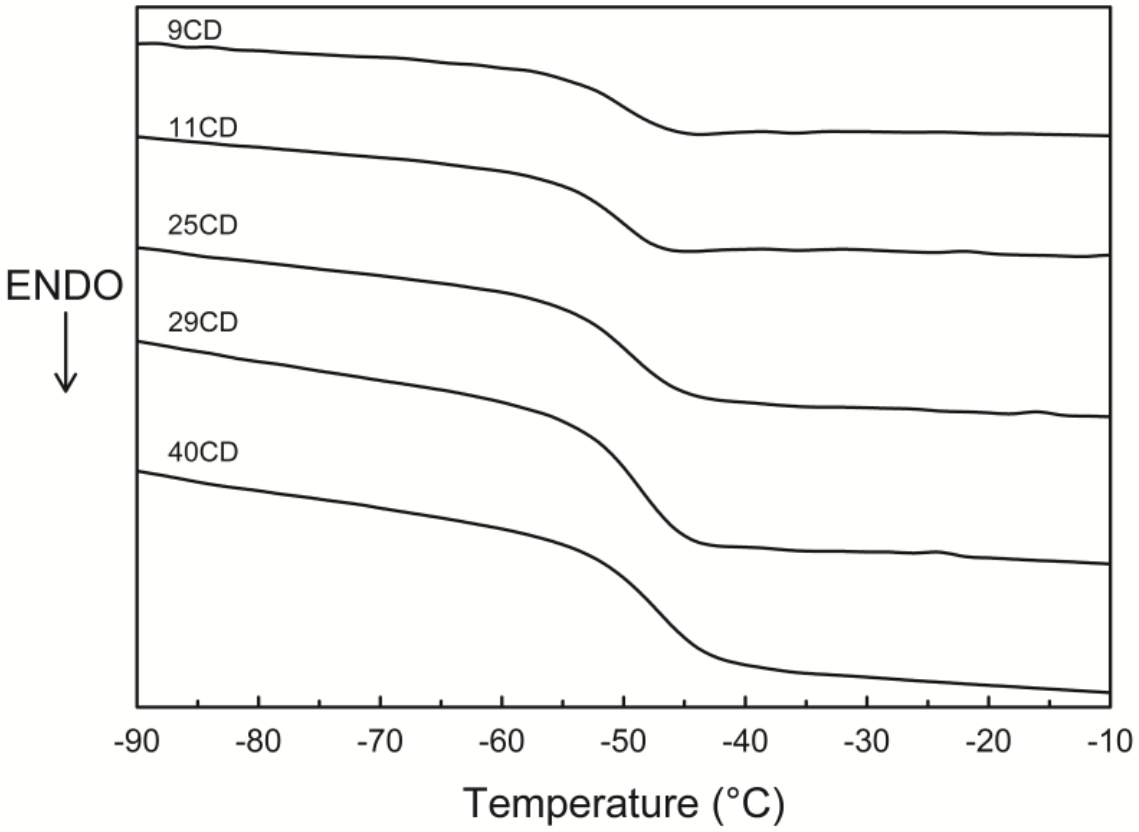

Fig. A.2 DSC Thermograms for Standard SBR Samples with varying Cross-Link Density.

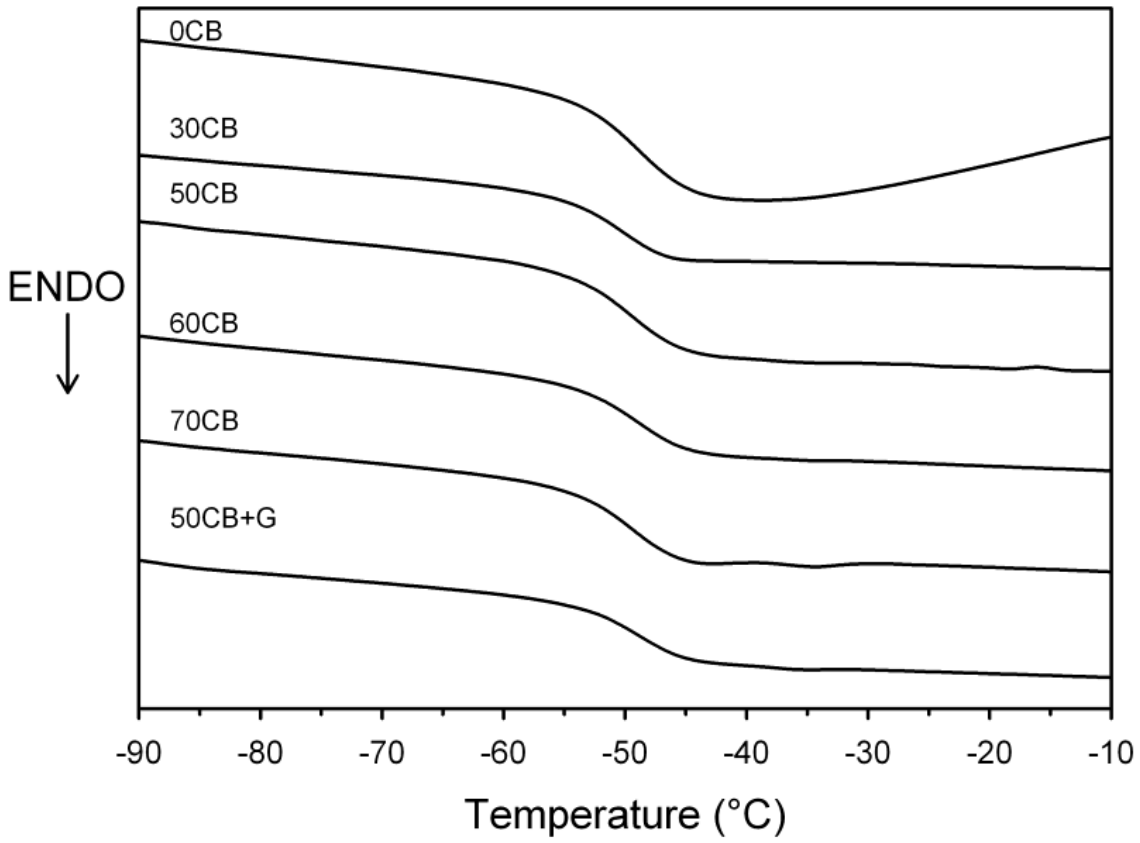

Fig. A.3 DSC Thermograms for Standard SBR Samples with with varying Carbon Black Content.

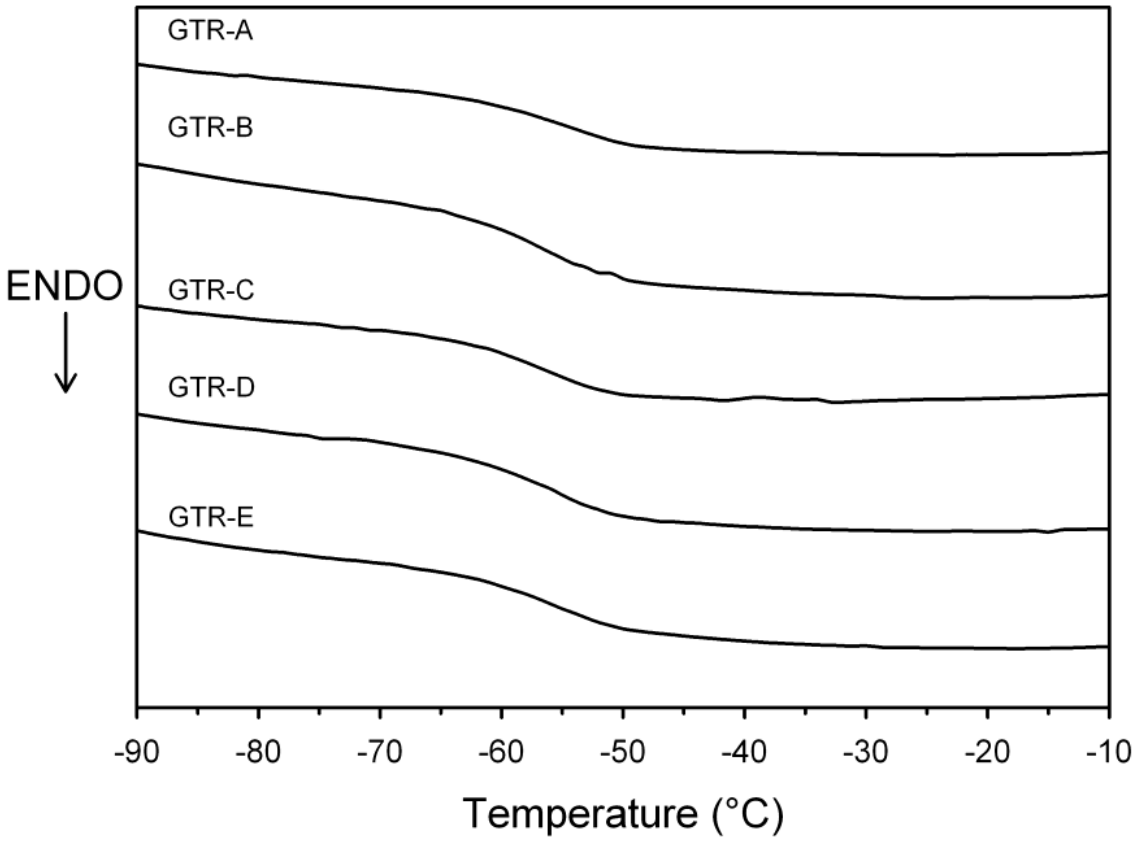

Fig. A. 4 DSC Thermograms for GTR Samples.